Aus dem Institut für Neuropathologie
(Zentrum für Neuropathologie und Prionforschung, ZNP)
Ludwig-Maximilians-Universität München
Direktor: Prof. Dr. med. Dr. h. c. Hans Kretzschmar FRCPath

Und dem Laser-Forschungslabor
Klinikum der Universität München
Wissenschaftlicher Leiter: Dr. rer. biol. hum. Ronald Sroka

Fluorescence spectroscopic measurements of absolute and relative photosensitizer concentrations in tissue for the optimization of photodynamic therapy

Dissertation
zum Erwerb des Doktorgrades der Humanbiologie
an der Medizinischen Fakultät der
Ludwig-Maximilians-Universität zu München

vorgelegt von
Gesa Kniebühler
aus
Hannover
2014

Mit Genehmigung der Medizinischen Fakultät
der Ludwig-Maximilians-Universität München

Berichterstatter:	Prof. Dr. med. Jochen Herms
Mitberichterstatter:	Prof. Dr. med. Friedrich-Wilhelm Kreth Prof. Dr. rer. nat. Kirsten Lauber
Mitbetreuung durch den promovierten Mitarbeiter:	Dr. rer. biol. hum. Herbert Stepp
Dekan:	Prof. Dr. med. Dr. h. c. M. Reiser, FACR, FRCR
Tag der mündlichen Prüfung:	22.01.2014

For my family

Table of contents

Abstract

Photodynamic therapy (PDT) is a minimally invasive therapy form for the treatment of malignant tumors, but also for other tissue changes, e.g. for acne. To perform PDT, a photosensitizer is activated by light, which induces cell death by the interaction with oxygen or by the direct formation of radicals of those cells which took up the photosensitizer. The outcome of the treatment is influenced mainly by the concentration of oxygen and of the photosensitizer in the target tissue, its triplet state quantum yield, the light dose applied and the time interval between application of the photosensitizer and treatment, the so-called drug light interval (DLI). These parameters have to be adjusted in such a way that ideally, all tumor cells are destroyed but the normal tissue stays intact.

In the present thesis, protoporphyrin IX (PpIX) and temoporfin concentrations are evaluated in different tissue types after these photosensitizers have been applied for the treatment of malignant glioma (PpIX) and cholangiocarcinoma (temoporfin). Analyzed is the dependency of the applied photosensitizer dose and the initial photosensitizer concentration in the target tissue on treatment outcome. In addition, pharmacokinetics that were obtained through concentration measurements are linked to the DLI. Aim of the investigation is to determine the relative and absolute photosensitizer concentrations in order to be able to optimize PDT in the future.

The first part of this thesis concentrates on the investigation of PpIX accumulation in the different tumor parts (vital solid tumor tissue, infiltrating parts, necrotic tissue) and in glioma of different grades of malignancy (WHO grade III & IV). Tissue samples were evaluated that had been gathered during fluorescence guided resections (FGR), performed with 5-aminolevulinic acid (5-ALA), a precursor of PpIX, at the approved dose of 20 mg/kg body weight (Gliolan®, medac GmbH, Wedel, Germany). Apart from the gain of knowledge on the accumulation of PpIX in the different tumor parts and grades of malignancy, the aim of this study was to determine whether the approved dose of 5-ALA is also effective in case of PDT.

Analyzed were tissue samples of 22 patients. On the basis of histological grading, tissue samples were divided into vital, infiltrating and necrotic grade IV, grade III as well as non-neoplastic biopsies. The mean concentration of vital grade IV tumor tissue, 5.8 ± 4.8 µmol/l (n=8), differs significantly from the mean of grade III tumors, 0.2 ± 0.4 µmol/l (n=4). Infiltrating and necrotic tissue biopsies resulted in concentrations of 1.0 ± 1.0 µmol/l (n=4) and 0.5 ± 0.5 µmol/l (n=4). Literature on the absolute PpIX concentration in human skin and human Barrett's esophagus indicates that tissue damage is induced at a concentration of about 1 - 2 µmol/l and 2 - 9 µmol/l, respectively. Thus it can be assumed that a PDT for vital grade IV tumors is effective, while grade III tumors do not seem to be a responsive target. To draw a precise conclusion on infiltrating parts, an analysis on a cellular basis needs to be performed. The method used in this thesis however, is not suitable for a cellular PpIX concentration analysis.

The second part of this thesis concentrates on the dependence of the outcome of interstitial PDT (iPDT) of malignant glioma on the initial photosensitizer concentration and the photobleaching effect. Aim of the study was to further understand their correlation.

In a pilot study, iPDT was performed on five patients with non-resectable glioblastoma multiforme (GBM) after administration of 20 or 30 mg/kg b. w. 5-ALA (Gliolan®, medac GmbH, Wedel, Germany). In each patient, the *in vivo* fluorescence in tissue was measured before and after radiation in order to determine the photobleaching effect by comparison. In addition, stereotactic biopsies were taken before radiation, which were partly used for histological assessment and partly for determining the absolute photosensitizer concentration *ex vivo*. The PDT effectiveness was determined on day 1 after iPDT via magnetic resonance imaging (MRI). The initial PpIX fluorescence intensity, the photobleaching effect, the histologic findings and the MRI images were correlated and all parameters compared with the follow-up. It could be demonstrated

that high initial PpIX concentrations (1.4 - 3.0 µmol/l) and strong photobleaching in three patients were accompanied by a good treatment result and long survival time (29, 30 and 36 months). The biopsies of the remaining two patients showed low PpIX concentrations (0 - 0.6 µmol/l). Accordingly, before iPDT, no or only low fluorescence could be measured *in vivo*. In agreement with the fluorescence data, good treatment results failed to appear, the patients died of the tumor after 3 and 9 months. These results indicate that, in order for a treatment to be effective, a minimum photosensitizer concentration needs to be present in tissue. In addition, an approach towards an applicable implicit dosimetry model for iPDT was taken by demonstrating an easy and safe implementation of *in vivo* fluorescence measurements. Through this implementation, an early prognosis of iPDT outcome seems possible.

The third part of this thesis concentrates on the effectiveness of PDT for cholangiocarcinoma (CC) at low dose of meso-tetrahydroxyphenyl chlorine (mTHPC, Foscan®, Biolitec pharma Ltd., Dublin, Ireland). Literature shows that for treatment of CC, the combination of stenting and PDT performed with the photosensitizer porfimer sodium (Photofrin®) enhances the survival time by a mean of 265 days. However, side effects such as the photosensitivity of the patients, requiring shielding from direct sunlight for up to three months, and the risk of perforations of the organ walls through PDT demonstrate a restriction in PDT as palliative treatment for CC. The aim of this study was to investigate PDT of CC performed with Foscan® at a low dose, in order to introduce a treatment with the same outcome, while lowering the side effects.

In this study, 14 PDTs were performed in 13, not specially selected, consecutive patients. Foscan®, which was approved in Europe in 2001 for the palliative treatment of head and neck cancer at a dose of 0.15 mg/kg b. w., a fluence of 20 J/cm^2 and a DLI of 96 h, was administered to the patients at a mean dose of 0.44 ± 0.007 mg/kg b. w. (3 mg/patient), 50 J/cm and a DLI between 20 - 72 h. In 5 of the13 patients the relative fluorescence intensity was determined directly before PDT on the tumor and normal surrounding tissue. In another 4 of the 13 patients, normalized fluorescence kinetics were measured in the oral cavity, to gain data for optimizing the DLI. After analysis of the data, the DLI was adjusted from the initial 20 to 67 - 72 h. As indicator for a successful treatment, the survival time of the PDT patients was evaluated with the Kaplan-Meier method. At the time of evaluation, the median survival time was 13 months. At the same time 8 of the 13 patients were still alive. Skin irritations or severe complications such as organ wall perforations could not be observed during the patients' hospital stay and were not reported later on. The results of the 14 PDTs with Foscan® at a low dose which were performed in this study show the same treatment outcomes compared to Photofrin® PDT – while lowering the side effects and complications. In addition a treatment protocol was introduced, forming the base for studies with a greater patient collective.

Zusammenfassung

Die photodynamische Therapie (PDT) dient der minimalinvasiven Behandlung von malignen Tumoren, aber auch anderer Gewebeveränderungen wie z. B. der Akne. Bei der PDT wird ein Photosensibilisator mittels Licht aktiviert, der durch die Wechselwirkung mit Sauerstoff bzw. durch die direkte Erzeugung von Radikalen zum Tod der Zellen führt, die den Farbstoff aufgenommen haben. Beeinflusst wird das Therapieergebnis hauptsächlich durch den Sauerstoffgehalt und die Konzentration des Photosensibilisators im Zielgewebe, die Quantenausbeute seines Triplettzustands, die Dosierung des eingestrahlten Lichts und das Intervall zwischen Applikation des Photosensibilisators und der Behandlung, dem sogenannten Drug Light Interval (DLI). Diese Parameter müssen derart aufeinander abgestimmt sein, dass möglichst alle Tumorzellen aber kein Normalgewebe zerstört werden.

In der vorliegenden Dissertation werden Konzentrationen von Protoporphyrin IX (PpIX) und Temoporfin in verschiedenen Gewebearten untersucht, nachdem diese Photosensibilisatoren zur Behandlung von malignen Gliomen (PpIX) und Cholangiokarzinomen (Temoporfin) appliziert wurden. Analysiert wird die Abhängigkeit des Behandlungsergebnisses von der applizierten Dosis und der initialen Photosensibilisatorkonzentration im Zielgewebe. Zusätzlich werden durch Konzentrationsmessungen erhaltene Pharmakokinetiken zum DLI in Bezug gesetzt. Ziel der Untersuchungen ist es, die PDT durch Bestimmung der relativen und absoluten Konzentrationen des Photosensibilisators in Gewebe für zukünftige Behandlungen zu optimieren.

Der erste Teil dieser Arbeit konzentriert sich auf Studien zur PpIX-Anreicherung in verschiedenen Tumorbereichen (vitales solides Tumorgewebe, Infiltrationszone, nekrotisches Gewebe) und in Gliomen unterschiedlichen Malignitätsgrades (WHO Grad III & IV). Es wurden Gewebeproben untersucht, die während fluoreszenzgestützter Resektionen (FGR) entnommen wurden. Durchgeführt wurden die FGR mit 5-Aminolävulin Säure (5-ALA), einem Vorläufer von PpIX, in der zugelassenen Dosis von 20 mg/kg Körpergewicht (Gliolan®, medac GmbH, Wedel, Deutschland). Neben der Untersuchung der Anreicherung von PpIX in verschiedenen Tumorbereichen und in Tumoren verschiedenen Malignitätsgrades war das Ziel der Studie zu erforschen, ob die für die FGR zugelassene Dosis von 5-ALA ebenfalls für die PDT effektiv ist.

Analysiert wurden Gewebestücke von 22 Patienten. Auf der Basis des histologischen Befundes wurden die Gewebeproben in vitale, infiltrierende und nekrotische Grad IV-, Grad III-, sowie nicht-neoplastische Biopsien unterteilt. Die mittlere PpIX-Konzentration in vitalem Grad-IV-Tumorgewebe unterscheidet sich mit $5{,}8 \pm 4{,}8$ µmol/l (n=8) signifikant von derjenigen der Grad-III-Tumore mit $0{,}2 \pm 0{,}4$ µmol/l (n=4). Für infiltrierend wachsende bzw. nekrotische Gewebeproben wurde die Konzentration von $1{,}0 \pm 1{,}0$ µmol/l (n=4) und $0{,}5 \pm 0{,}5$ µmol/l (n=4) ermittelt. Literaturdaten zur absoluten PpIX-Konzentration in humaner Haut und humanem Barrett-Ösophagus geben eine notwendige Konzentration von ca. 1 - 2 µmol/l bzw. 2 - 9 µmol/l an, um eine Gewebereaktion hervorzurufen. Somit ist davon auszugehen, dass eine PDT für vitale Grad-IV-Tumoren effektiv ist, während die PDT für Grad-III-Tumore nicht geeignet erscheint. Um genauere Aussagen über die infiltrierenden Bereiche treffen zu können, müsste eine Untersuchung auf zellulärer Ebene erfolgen. Die in dieser Arbeit verwendete Methode der PpIX-Konzentrationsbestimmung ist dafür jedoch nicht geeignet.

Der zweite Teil dieser Arbeit beschäftigt sich mit der Untersuchung der PDT-Wirkung auf maligne Gliome in Abhängigkeit von der initialen Photosensibilisatorkonzentration und der Photobleichung. Ziel der Studie war es, diesen Zusammenhang genauer zu verstehen.

In einer klinischen Pilotstudie wurden interstitielle PDTs (iPDT) an fünf Patienten mit nichtresektablen Glioblastomen multiforme (GBM) nach Gabe von 20 oder 30 mg/kg Körpergewicht 5-ALA (Gliolan®, medac GmbH, Wedel, Deutschland) durchgeführt. Bei allen Patienten wurde jeweils vor und nach der Bestrahlung die In-vivo-PpIX-Fluoreszenz des Gewebes gemessen, um

durch den Vergleich die Photobleichung des Photosensibilisators zu bestimmen. Zusätzlich wurden vor der Bestrahlung stereotaktische Biopsien entnommen, von denen ein Teil histologisch ausgewertet, und bei einem anderen Teil die absolute Photosensibilisatorkonzentration *ex vivo* bestimmt wurde. Die PDT-Wirkung wurde am Tag 1 nach iPDT mittels Magnetresonanztomographie (MRT) untersucht. Die initiale PpIX-Fluoreszenzintensität, die histologischen Befunde und die MRT-Aufnahmen wurden korreliert und alle Parameter mit dem Follow-up verglichen. Es konnte gezeigt werden, dass hohe initiale PpIX-Konzentrationen (1,4 - 3,0 µmol/l) und starke Photobleichung bei drei Patienten mit einem guten Behandlungsresultat und langer Überlebensdauer (29, 30 und 36 Monate) einhergingen. Die Biopsien bei zwei weiteren Patienten wiesen geringe PpIX-Konzentrationen (0 - 0,6 µmol/l) auf. Entsprechend konnte vor der iPDT im Gewebe keine bzw. eine sehr geringe In-vivo-Fluoreszenz gemessen werden. Übereinstimmend mit den Fluoreszenzmessungen blieben gute Behandlungsresultate aus, die Patienten verstarben nach 3 und 9 Monaten an ihrer Tumorerkrankung. Diese Ergebnisse deuten darauf hin, dass für eine erfolgreiche PDT eine Mindestkonzentration an Photosensibilisator im Gewebe vorhanden sein muss. Außerdem wurde ein Schritt in Richtung eines anwendbaren impliziten Dosimetriemodells für die iPDT gemacht, indem eine einfache und sichere Implementierung zur In-vivo-Messung von Fluoreszenz gezeigt wurde. Durch diese Implementierung scheint eine frühe Prognose der iPDT-Wirkung möglich zu sein.

Der dritte Teil dieser Arbeit beschäftigt sich mit der Effektivität der PDT des Cholangiokarzinoms (CC) unter Verwendung von niedrig-dosiertem Meso-Tetra-(Hydroxyphenyl-)Chlorin (mTHPC, Foscan®, Biolitec pharma Ltd., Dublin, Irland). Literaturdaten zeigen, dass bei Behandlung von CCs eine Kombination aus Implantierung von Stents und einer PDT mit dem Photosensibilisator Porfimer-Natrium (Photofrin®) die Überlebenszeit im Mittel um 265 Tage verlängert. Allerdings stellen Nebenwirkungen wie die Photosensibilisierung, die eine Abschirmung von direkter Sonnenstrahlung für bis zu drei Monate erfordert, und das Risiko der Perforationen von Organwänden durch die PDT Einschränkungen dieses Verfahrens in der palliativen Behandlung dieser Erkrankung dar. Ziel dieser Studie war es, die PDT von CCs mit niedrig-dosiertem Foscan® zu erforschen, um eine Behandlung mit der Effektivität einer Photofrin®-PDT bei geringeren Nebenwirkungen aufzuzeigen.

In dieser Studie wurden 14 PDTs an 13 nicht selektionierten, aufeinanderfolgenden Patienten durchgeführt. Foscan®, das in Europa seit 2001 für die palliative PDT-Behandlung von Kopf-Hals-Karzinomen mit einer Dosis von 0,15 mg/kg Körpergewicht bei 20 J/cm^2 und einem DLI von 96 Stunden zugelassen ist, wurde mit einer mittleren Dosis von 0,044 ± 0,007 mg/kg Körpergewicht (3 mg/Patient), 50 J/cm und einem DLI zwischen 20 - 72 Stunden durchgeführt. Bei 5 der 13 Patienten wurde die relative Fluoreszenzintensität unmittelbar vor PDT-Behandlung am Tumor und im umgebenden Normalgewebe bestimmt. Bei weiteren 4 der 13 Patienten wurden normierte Fluoreszenzkinetiken in der Mundschleimhaut gemessen, um Daten für die Optimierung des DLI zu erhalten. Nach Analyse der Daten wurde das DLI von anfangs 20 auf 67 - 72 Stunden erhöht. Zur Bestimmung des Erfolgs der PDT wurde die Überlebensdauer der PDT-Patienten nach der Kaplan-Meier-Methode ausgewertet. Zum Zeitpunkt der Auswertung lag die Überlebenszeit im Median bei 13 Monaten. Zum selben Zeitpunkt lebten noch 8 der 13 Patienten. Hautirritationen oder schwerwiegendere Komplikationen wie Perforationen der Organwände konnten während des Krankenhausaufenthalts nicht beobachtet werden und wurden auch in der Folgezeit nicht berichtet. Die Ergebnisse der in dieser Studie durchgeführten 14 PDTs mit reduzierter Foscan®-Dosis zeigen die gleiche Wirkung wie eine Photofrin®-PDT – bei gleichzeitig reduzierten Nebenwirkungen und Komplikationen. Zusätzlich wurde ein Behandlungsprotokoll entwickelt, auf dessen Basis Folgestudien an einem größeren Patientenkollektiv erfolgen können.

1 Introduction

The present doctoral thesis is a cumulative thesis and consists of three original manuscripts [1-3]. The common aim of the manuscripts is to investigate the feasibility of photodynamic therapy and to monitor treatment parameters for therapy optimization. To reach this goal, photosensitizer concentration measurements were performed *in vivo* and *ex vivo*. *In vivo* measurements were conducted with optical fiber probes whereas for *ex vivo* measurements, an extraction procedure was implemented and fluorescence was measured with a fluorescence spectrometer. Thus, the present thesis is an interdisciplinary work, combining physical and chemical methods for better understanding the clinical outcome of photodynamic therapy.

Measurements were performed on two different cancer types, human malignant glioma and cholangiocarcinoma, demonstrating the possibility to transfer the results to different organs. The detailed approach and the results of these studies are published in the above mentioned manuscripts, while background information is given in the following paragraphs of this introduction.

1.1 Photodynamic diagnosis, fluorescence guided resection and photodynamic therapy

Substances which render tissue photosensitive have been known for centuries. They have been used for treatment of diseases, e.g. vitiligo, which uses the sun as a source of light for irradiation [4]. However, the photodynamic diagnosis (PDD) and therapy (PDT) performed nowadays were first established in 1898 when Oscar Raab, student of Hermann von Tappeiner (1847 – 1927), noticed the toxic effect on paramecia exposed to acridine when irradiated with light [5]. After this discovery, experiments with different substances on enzymes followed [6] and first therapies were performed by von Tappeiner et al. in 1903 - 1905 [7, 8]. However, PDD, PDT and related procedures such as interstitial PDT (iPDT) and fluorescence guided resection (FGR) are still subject of today's investigations.

1.1.1 Photodynamic diagnosis

Photodynamic diagnosis (PDD) is a powerful tool for the intraoperative detection of premalignant lesions and tumors. It relies on the tumor-selective uptake of a fluorescing photosensitizer or its precursor. Before treatment, the photosensitizer or precursor is administered to the patient either topically, orally or intravenously. After allowing some time for accumulation in the malignant tissue, the region of interest is irradiated by light within the absorption band of the photosensitizer. Most photosensitizers are based on porphyrin or chlorin molecular structures and, thus, show similar spectral behavior, e.g. they commonly absorb strongly in the blue spectral range (400 - 495 nm). Fluorescence light always experiences a spectral shift to longer wavelengths and is, therefore, mostly emitted in the red spectral range (620 - 750 nm), which consequently simplifies the detection of the fluorescence signal. If the fluorescence light is detected through a long-pass filter which blocks the blue excitation light not entirely, the tumor will appear in red and the surrounding normal tissue in blue color, yielding good visual contrast during the examination. Such typical "PDD images" are obtained, for instance, for bladder cancer detection [9] or for fluorescence guided resection of malignant glioma [10].

1.1.2 Fluorescence guided resection

During fluorescence guided resection (FGR), the tumor-specific fluorescence is exploited to decide on tissue removal. After administering the photosensitizer systemically, the surgeon can resect the tumor layer by layer and is instantly informed through the fluorescence image, whether there is any residual tumor tissue left. Since the extent of resection influences the local recur-

rences, FGR is of particular interest during resection at tumor borders, where in common surgery it is often hard to distinguish between tumor and normal tissue.

Both, the highly specific photosensitizer accumulation and the dependence of recurrences on the degree of resection apply to malignant glioma, especially to glioblastoma multiforme (GBM) [10-12]. At the same time, the risk of inducing neurological deficits when resecting glioma too aggressively is of particular importance [13]. Thus, FGR is a great treatment option for this kind of tumor, compared with standard white light surgery. As shown in a phase III study, the rate of residual bulk tumor tissue can be reduced applying FGR, and the time to recurrence can be increased compared to standard therapy. However, overall survival could not be improved [14]. One difficulty arises for instance when treating infiltrating tumors. For infiltrating tumors the tumor cell density decreases at the borders, as does the fluorescence signal. In consequence, the measured signal in infiltrating zones is lower than in, e.g., proliferating parts, and might even not be detectable at all. Yet, the photosensitizer concentration in the tumor cells of the infiltrating zone itself might be the same as for tumor cells in the proliferating part. Hence further investigations to enhance FGR are necessary, particularly with regard to detecting fluorescence *in vivo* more sensitively.

1.1.3 Photodynamic therapy

Commonly photodynamic therapy (PDT) is used to treat malignant tumors in many different organs minimally invasively [15], but it can also be applied to non-oncological diseases, such as acne and warts [16, 17].

Like PDD and FGR, PDT is performed in two steps. In the first step, the photosensitizer is administered, and in the second step, it is activated by irradiation with light within its absorption band. After excitation from the ground state into the first excited singlet state, as illustrated in the Jablonski diagram in Figure 1, the electrons can either undergo relaxation directly into the ground state via internal conversion or via emission of a fluorescence photon. Alternatively, they can be transferred into a triplet state via inter-system crossing. As the relaxation from the triplet state to the ground state – via internal conversion or phosphorescence – is a slow process, there is a significant probability for energy transfer to other molecules. Through this energy transfer, reactive oxygen species or singlet oxygen may be produced, which in turn induce the cytotoxic reaction in PDT, referred to as type I and type II reactions, respectively [18]. Since the PDT effect is initiated by the electrons in the triplet state, a high triplet quantum yield is desirable for photosensitizers used during PDT.

Singlet oxygen diffuses only about 0.01 - 0.02 µm in tissue [8], and consequently oxidized molecules are induced close to the location of the photosensitizer. The details of the cell death mechanism thus depend strongly on the intracellular distribution of the photosensitizer. Most photosensitizers accumulate in the cell membrane or membranes of organelles, for instance the Golgi apparatus, lysosomes, endoplasmic reticulum or mitochondria [19]. In consequence, the cells die either via necrosis due to cell membrane damage or vessel collapse, or via apoptosis induced by damage of organelle membranes [20].

Regardless of the cell death mechanism, PDT is primarily a local therapy. The radical formation takes place in proximity of the selectively accumulated photosensitizer and is restricted to the irradiated tissue volume. This is caused by the limited penetration depth of light into tissue of about 1 mm to 1 cm in the visible spectral range. However, the limited penetration depth of light in tissue can also be a restriction for PDT of tumors in deeper tissue regions. Therefore, light in the red spectral range is preferentially used for irradiation as it typically propagates deeper into the tissue, although a lower absorption coefficient of most photosensitizers has to be accepted in this spectral range. Consequently, the therapeutic penetration depth, referred to as the distance between radiation entrance into tissue and depth of the resulting necrosis, is larger for red compared to blue excitation light.

In addition to the local effect, PDT also induces an immune response, which is described further in [21, 22].

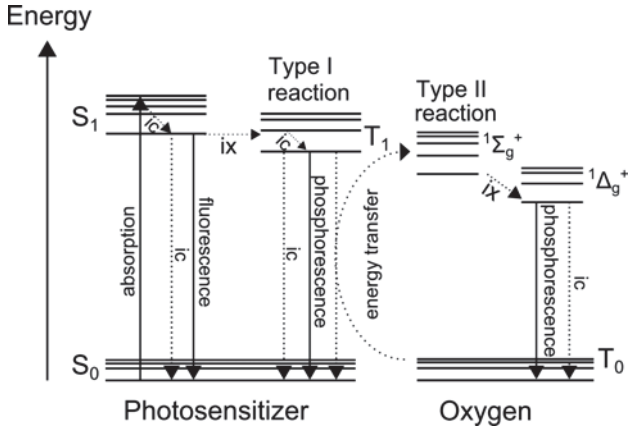

Figure 1. Jablonski diagram of PDT reaction

Another main feature of PDT, apart from the possibility of local treatment and the immuno-PDT, is the possibility to repetitively treat patients. As mentioned before, most photosensitizers accumulate in the cell membranes. Only very few accumulate in the nucleus [4, 23], for which reason the DNA stays intact. In contrast, in radiotherapy as a standard treatment, healthy tissue surrounding the tumor is unavoidably exposed to the irradiation. As a result the DNA of normal cells can be affected and radiotherapy can only be performed until a threshold dose is reached. This threshold dose is attempted to be minimized by applying multileaf collimators and by irradiating from many different angles. Chemotherapy as another standard treatment can result in resistance of tumor cells and is also, when administered systemically, not highly selective. It affects all rapidly dividing cells, resulting, for instance, in bone marrow suppression. PDT, however, can be minimally toxic for the surrounding normal tissue when the correct photosensitizer is used and light is applied locally. Ideally, photosensitizers only accumulate in tumor cells, and healthy cells are not treated at all as the light alone does not cause any tissue damage. However, such an ideal photosensitizer has not been found yet and, in addition, endogenous photosensitizers can be excited at the wavelength of the applied photosensitizer, resulting in treatment of healthy cells. In order to conduct PDT, light needs to be delivered to the target tissue. Different approaches of light delivery exist, depending on the treatment site. In case of treatment of skin diseases, light is applied without the use of sophisticated optical devices, while lesions in hollow organs can be irradiated via fibers introduced through the working channel of an endoscope. Therefore, PDT of cholangiocarcinoma, for example, can be performed during the commonly performed endoscopic retrograde cholangiopancreatography (ERCP) for replacement of stents. If PDT is not only performed on a superficial lesion but in a larger volume, light can be applied through diffusors connected to light transmitting fibers which are inserted into the tissue itself. This treatment is called interstitial PDT (iPDT) [24, 25].

The outcome of PDT, however, depends on the same parameters for all treatment approaches. Important parameters are the photosensitizer concentration, the applied light dose, the oxygen concentration in the target tissue and the drug-light interval (DLI), defined as the time between photosensitizer application and irradiation. This thesis concentrates on the photosensitizer concentration and the DLI.

When regarding the photosensitizer concentration, it has to be kept in mind that the efficacy of the photosensitizer does not depend on the concentration alone, but also on its photophysical parameters, i.e. its extinction coefficient and triplet quantum yield. If the photosensitizer concentration at the treatment site is known, the light dose can be adjusted accordingly. A lower singlet oxygen induction because of a lower photosensitizer concentration can be compensated by a higher light dose and vice versa. Nonetheless, if no photosensitizer is present, singlet oxygen

cannot be induced, for which reason a threshold photosensitizer concentration for effective PDT must be present. The same is true for molecular oxygen in the target tissue, which is required for the formation of singlet oxygen. Measurements of oxygen concentrations are also a subject of current investigations [26], but they are not addressed in the present thesis.

In the third study of this thesis, the DLI is assessed. The DLI strongly depends on the specific photosensitizer, its application form and its pharmacokinetics in the human body. Commonly, photosensitizer pharmacokinetics differ in plasma, normal and tumor tissue. Therefore, the contrast of fluorescence light emission between normal and tumor tissue varies with time, which is called transient selectivity. In addition, the point in time for maximal photosensitizer concentration in a tumor does not necessarily correlate with the point of maximal contrast. The DLI can thus be chosen based upon different assumptions. It can either be the time interval between drug administration and highest fluorescence contrast between the tumor site and the surrounding normal tissue, greatest photosensitizer accumulation in plasma or greatest photosensitizer accumulation in the tumor tissue [27-29]. Ideally, the point in time of maximal photosensitizer concentration in the tumor is chosen to maximize the PDT effect. However, if the contrast between tumor and normal tissue is not high at that time, a different point in time with a better contrast might be preferable. Naturally, the choice between a good contrast and high photosensitizer concentration also depends on the targeted organ. In case of brain malignancies, for example, harming normal tissue during treatment may result in stronger side effects than during bladder or skin treatments. Accordingly, a higher contrast rather than a maximal photosensitizer concentration would be preferable for brain malignancies. Nevertheless, when administering a low photosensitizer dose, treatment at maximal photosensitizer concentration might be favorable over a good contrast. The time differences between time of greatest contrast and time of highest photosensitizer concentration may amount to several hours or even days. Regardless of the strategy according to which the DLI is chosen, DLIs of commonly used photosensitizers range from a few hours, as in the case of 5-aminolevulinic acid (5-ALA) induced protoporphyrin IX (PpIX), up to several days, for instance in case of temoporfin [19]. In order to determine these times, pharmacokinetics can be assessed by monitoring the relative fluorescence intensity at the same tissue site. This is possible because in this case, the fluorescence intensity strongly depends on the photosensitizer concentration, due to only small variations in time of the optical parameters, i.e. absorption and scattering. However, when trying to derive absolute photosensitizer concentrations from the fluorescence measurements, the varying optical parameters have to be considered, as described in section 1.3.

1.2 Photosensitizers

A variety of classes of photosensitizers exists. For each class, different drugs are commercially available, showing different pharmacological, chemical and photophysical behavior. Which photosensitizer is suited best depends on the targeted organ. Nevertheless, for all photosensitizers, high target selectivity, high absorbance at long wavelengths, fast pharmacokinetics and especially high reactivity are desired. A high reactivity is achieved by a high triplet state quantum yield and a high life time.

Hence most photosensitizers are alike in their basic structure, possessing an aromatic ring which causes the fluorescence when the photosensitizer is excited. The main differences between photosensitizers arise from the central metal ion in the main aromatic ring and the chemical composition of the side chains. These side chains also determine the intrinsic characteristics of a photosensitizer, e.g. their lipophilicity – in other words, whether a photosensitizer can penetrate a cell membrane easily. Consequently, it also determines the intracellular localization. Another significant influence on the localization is given by the route of administration of the photosensitizer. Some photosensitizers can be applied topically or systemically, but in most cases one application route is preferable. By applying it directly to the treatment region, e.g. topically when treating skin lesions, an inherent selectivity is given. But also by choosing a drug light interval

with a high contrast between tumor and normal tissue, as described above, the selectivity can be enhanced.

In the studies of this thesis, 5-ALA-induced PpIX was applied for treatment of malignant glioma while meso-tetrahydroxyphenyl chlorine (mTHPC, Foscan®) with the generic name temoporfin was used for PDT of cholangiocarcinoma. However, purified hematoporphyrin derivative (HPD, Photofrin®) is commonly used for PDT of cholangiocarcinoma instead of mTHPC, for which reason all three are described in more detail in the following paragraphs.

1.2.1 Protoporphyrin IX

Protoporphyrin IX (PpIX) is part of the heme biosynthesis pathway, in which 5-ALA is formed into porphobilinogen and uroporphyrinogen III before protoporphyrinogen IX and finally PpIX is synthesized [30]. In a last step, a ferrous ion (Fe^{++}) is inserted into the porphyrin ring by the enzyme ferrochelatase to form heme. The chemical structures of 5-ALA and PpIX are shown in Figure 2a and 2b. Since almost all cells of the human body synthesize heme, PpIX is also present within these cells and not only in tumor cells. Nevertheless, when exogenous 5-ALA is administered before treatment, it can be observed that PpIX accumulates selectively in tumor cells. The main reason is believed to be a reduced activity of ferrochelatase [31, 32] and, for some tumors, a more active porphobilinogen deaminase, which catalyses the formation of uroporphyrinogen from porphobilinogen [33]. In addition, the selectivity is increased by the hydrophilic characteristics of 5-ALA, for which it cannot penetrate healthy skin or membranes easily. Tumorous skin and tissue layers, however, show an increased permeability, which permits 5-ALA to pass into deeper tissue layers [34]. Nevertheless, the penetration depth of 5-ALA remains limited, why deeper lying or thicker lesions are difficult to treat. In order to elude this problem, different lipophilic derivatives of 5-ALA have been examined [35, 36].

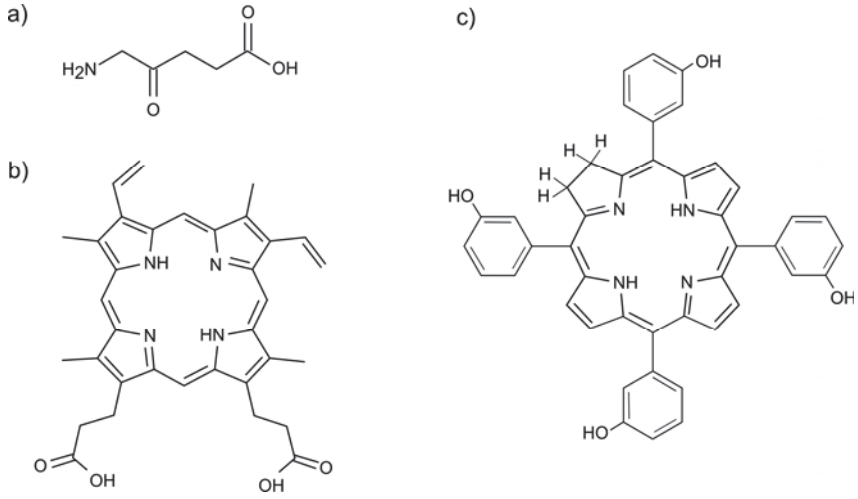

Figure 2. Chemical structures of a) 5-aminolevulinic acid, b) protoporphyrin IX and c) temoporfin

Also, apart from the limited penetration depth of 5-ALA itself, the limited penetration depth of the excitation light restricts the achievable treatment depth. PpIX has one main absorption band at 412 nm, the Soret band, and four smaller vibrational Q-bands at around 508 nm, 541 nm, 580 nm and 635 nm in tissue. For typical "PDD images", the absorption band at 412 nm is used, yielding high contrast albeit limited penetration depth. Also, for some treatments, the limited optical penetration depth is desirable, e.g. PDT of actinic keratosis is performed with blue light, in order to intentionally keep the therapeutic penetration depth minimal [37]. Most often, however, the absorption band at 635 nm is exploited for PDT.

A great advantage in using PpIX for PDT is its rapid pharmacokinetics. The concentration of PpIX in tumor peaks at about 1 - 6 h after administration of ALA, depending on the lesion, and

the patients are photosensitive only for about 24 h [30, 38]. Thus, the risk of side effects such as skin burns is low and patients can be exposed to light shortly after treatment, which is a great advantage for the patient, especially when PDT is used for palliative treatment. For skin lesions, PDT with PpIX can even be performed in an outpatient setting.

Clinically approved indications for ALA or its derivatives are PDT for actinic keratosis and basal cell carcinoma (BCC), as well as PDD for bladder cancer and FGR for malignant glioma. Also, experimental clinical applications of ALA and its derivatives have been reported for PDT of bladder and PDD and iPDT of prostate cancer [39-41], as well as for PDT and iPDT of brain tumors [25]. In case of skin cancer, ALA can be applied in form of an ointment. In case of bladder cancer, ALA is instilled intravesically or, for deeper lying lesions, administered systemically. When performing FGR, PDT or iPDT of brain tumors, ALA is delivered orally in a drinking solution. Although it is administered systemically for treatment of malignant glioma, PpIX accumulates highly selectively in the tumor volume. A main reason for this selectivity is the blood brain barrier. ALA cannot penetrate the intact blood brain barrier, but in brain tumors there are fewer tight junction molecules, i.e. claudins and occludins, for which reason the barrier is more permeable for ALA [42, 43]. In the first and second study of this thesis, 5-ALA (Gliolan®, medac GmbH, Wedel, Germany) was used, as precursor of PpIX, for treatment of malignant glioma at the approved dose of 20 mg/kg b. w.

1.2.2 Porfimer sodium

Porfimer sodium, approved in 1993 in Canada, was the first photosensitizer to be approved for PDT (Photofrin®, Axcan Pharma Inc., Mont-Saint-Hilaire, Canada). It is the purified part of hematoporphyrin derivative (HpD) and consists of up to eight porphyrin rings, although its exact composition has still not been determined. Due to the Soret band and Q-bands of the porphyrin ring structure, it can be excited, just like other porphyrin-based photosensitizers, at a number of wavelengths between 400 and 650 nm [44]. However, for PDT, the absorption band at 630 nm is commonly used because it favors the optical penetration depth over the absorption probability.

Porfimer sodium is commonly administered intravenously and has been shown to be selective and effective in several tumor models [45]. Today, it is still frequently used for PDT, especially for treatment of cholangiocarcinoma, although it has also been shown that at the commonly administered dose of 2 mg/kg b. w., it is not very selective, and the absorbance at the red spectral range is low [19]. Yet, when staying out of strong sunlight, only light erythema are reported in addition to side effects specific to the treated organ. After PDT of cholangiocarcinoma, to name one example, mild constipation, coughing, nausea, pain and swelling at injection site, mood changes, fever and tachycardia may occur [46].

Compared to 5-ALA, porfimer sodium has a long DLI of 40 - 50 h. Another drawback is the pronounced and long-lasting photosensitization of skin for 4 - 12 weeks [8], restricting the patients' quality of life immensely because they have to shield from direct sunlight during this time. However, compared to 5-ALA it is suitable, for instance, for treatment of cholangiocarcinoma because of its higher penetration depth.

1.2.3 Temoporfin

Meso-tetrahydroxyphenyl chlorin (mTHPC, temoporfin) is a single pure chlorine compound and a potent photosensitizer. Its chemical structure is shown in Figure 2c. The phototoxicity of temoporfin exceeds the phototoxicity of porfimer sodium by about a factor of 100 - 200 [19, 47]. In addition, temoporfin is excited at 652 nm, where the penetration of light into tissue is significantly higher than at 630 - 635 nm. The therapeutic penetration depth of temoporfin, including light penetration depth and diffusion constant, has been reported to be up to 9 mm [48] for PDT of cholangiocarcinoma, while the therapeutic penetration depths of PpIX and porfimer sodium have been reported to be only 2 and 4 - 6 mm, respectively [46, 49].

Temoporfin is approved for head and neck PDT with the trade name Foscan® (Biolitec pharma Ltd., Dublin, Ireland). It is commonly applied intravenously, together with a lipid emulsion to induce a better distribution. In human plasma, the concentration decreases with half-lives reported to be about 40 and 45 h [50, 51], whereas the concentration in tissue is lower than in the vascular system at first. Then it rises above it before it decreases again. For squamous-cell carcinoma at three different stages, it could be shown that the concentration peak measured in the tumor tissue appears before the peak in normal tissue (about 30 - 70 h versus 60 - 90 h) [52]. As is true for other photosensitizers as well, its localization and its contrast in tissue depend on time. Therefore, the balance between either vascular or tissue damage can be adjusted by choosing the appropriate DLI, as has been proven in clinical treatment [29, 53]. The determination of the ideal DLI, however, is still a subject of present research. The DLI for the clinically approved indications is 96 h (at 0.15 mg/kg b. w. i.v.), accordingly, direct tissue damage is induced during PDT. In literature, one study can be found in which temoporfin is applied for PDT of cholangiocarcinoma at a dose of 0.15 mg/kg b. w. However, side effects such as cholangitis and haemobilia had to be reported, which resulted in one death [54]. In the third manuscript of this thesis, temoporfin was used at low doses (0.032 - 0.063 mg/kg b. w.) in order to reduce side effects. Doses were chosen on the basis of a study performed by Betz et al. The study describes how, in case of basal cell carcinoma PDT, good results were achieved in a similar dose range (0.03 - 0.05 mg/kg b. w.) with DLIs ranging from as low as 1 - 48 h [55]. Based on this publication, a DLI of 20 h was chosen for the study of this thesis. The contrast at such a short DLI is still low, but because of the low dose, a low contrast was assumed to be sufficient to avoid damage to the surrounding normal tissue. However, after five patients had been treated, no contrast could be determined at all. At the same time, pharmacokinetics measurements conducted on oral tissue indicated maximal photosensitizer concentrations at 60 - 120 h after drug application. For both reasons, the DLI was changed for the following patients to 67 - 72 h. Although the chosen DLI for temoporfin is longer than the DLI for porfimer sodium, the complete duration of systemic photosensitization is less than two weeks and thus considerably shorter [29].

1.3 Photosensitizer concentration measurements

The photosensitizer uptake is strongly patient dependent. Thus, the concentration in tissue cannot be determined by regarding the applied dose alone. In addition, to optimize treatment, the concentration has to be measured, ideally *in vivo* before and during treatment. Many approaches to determine the absolute concentration are based on fluorescence measurements. However, the optical properties, i.e. absorption and scattering, have an important impact on the measured fluorescence spectra, preventing a direct correlation of measured fluorescence intensity to photosensitizer concentration. An exception would be an infinitesimal small single bare fiber, explained below, which, however, would not be suitable for collecting enough fluorescence photons for a sufficient signal to noise ratio. Therefore, the optical properties of tissue have to be considered to be able to correct the measured fluorescence spectra to obtain the so-called intrinsic fluorescence spectrum, which matches a fluorescence spectrum measured in a clear solution, i.e. measured without interference of scattering or absorption. Consequently, it can be calibrated to indicate the absolute photosensitizer concentration value. Direct and indirect approaches of determining optical properties [56] *ex vivo* as well as *in vivo* and accordingly the intrinsic fluorescence spectra have been investigated for more than 20 years, but are still subject of current research. In all three studies of the present thesis, relative and absolute photosensitizer concentrations were measured *in vivo* and *ex vivo*, respectively.

For the first study of this thesis, the absolute photosensitizer concentration was measured *ex vivo* with a fluorescence spectrometer after extraction of the photosensitizer from tumor biopsies. Other determination methods of the photosensitizer concentration are based on optical fiber setups, with the intention of being usable *in vivo*, for instance through endoscopes. In order to compensate for the interference of variable optical tissue parameters, they either include remission

measurements and correction algorithms [57-59], or use fiber geometries with a low sensitivity to the optical parameters of the tissue. The simplest approach is to use a single optical bare fiber for measurements [60, 61]. When the mean free path of the excitation and fluorescence light is large compared to the fiber diameter, the influences of the optical parameters of the tissue on the fluorescence measurements are low. A comparison of four different approaches has been performed and published by the author of this thesis [62]. Based on these results, a single optical fiber measurement approach was chosen for the *in vivo* fluorescence measurements in the second publication of this thesis. Though other, more complicated, probe geometries deliver better results, using a single optical fiber as a probe simplifies the set-up enormously, while still allowing to receive useful data. The raw fluorescence spectra were, accordingly, correlated to the photosensitizer concentration present in tissue.

1.4 Photobleaching as dosimetry model

Photobleaching has to be taken into account when determining the photosensitizer concentration. While the photosensitizer is irradiated, it can be inactivated due to conformational changes called photobleaching, which result in a permanent decrease in fluorescence intensity. These molecular changes arise when the excited photosensitizer reacts with the surrounding media, mainly by oxidization. Therefore, photobleaching depends on the irradiation light dose and the present oxygen concentration [63]. Due to this dependence on the oxygen concentration, it is not possible to increase photobleaching and, consequently, the PDT effect, by simply increasing the light intensity. The light intensity needs to be chosen in relation to the oxygen present in tissue and the diffusion constant. Therefore, when tissue containing a photosensitizer is exposed to light in an uncontrolled way prior to measuring the fluorescence, the initial photosensitizer concentration can no longer be derived reliably. However, when irradiation is controlled, photobleaching can also be used for PDT dosimetry.

Dosimetry models in PDT try to evaluate the tissue damage induced during PDT from different parameters. In order to monitor and individualize treatment, different dosimetry models can be applied. As mentioned above, the outcome of PDT depends on different parameters, i.e. photosensitizer concentration, oxygen concentration, light dose and the DLI. If each parameter is monitored separately, the dosimetry model is called an explicit model. Another monitoring approach is the direct dosimetry model, for which the concentration of singlet oxygen that is responsible for cellular damage is directly measured. A third approach, called implicit dosimetry model, is to monitor the bleaching kinetics as an indicator for the PDT-induced singlet-oxygen production. This dosimetry model is based on the assumption that PDT induced singlet oxygen causes not only tissue damage but the photodegradation of the photosensitizer as well. In that case, the bleaching kinetics implicitly contains information on the relative PDT dose [64]. Although these different dosimetry models are proposed and researched, there is still no gold standard for monitoring and realizing patient dependent treatment.

In the second study of this thesis, an approach towards an implicit dosimetry model based on photobleaching was investigated in a pilot study of iPDT. The relative fluorescence intensity was measured before and after iPDT of GBMs with the same set-up used for treatment. After the fluorescence intensities before and after treatment were compared, the relative bleaching rate could be determined, gaining information about the treatment itself. Moreover, the results of the pilot study suggest that the measurement of the fluorescence kinetics is suitable as an early treatment prognosis, as was also speculated by Pogue et al. [65]. Fluorescence measurements could be employed easily and were shown to be safe.

Naturally, for realizing a true implicit dosimetry model, the initial absolute photosensitizer concentration needs to be known. In that case, the PDT effect could be predicted even more precisely, and patient specific treatment would be possible. This encourages further investigations to determine the absolute photosensitizer concentration *in vivo*.

1.5 Glioma

The age standardized incidence rate in 2008 for primary tumors of the central nervous system (ICD-10 Code C70 - C72) in the developed part of the world amounts to 6.0 for men and 4.4 for women per 100,000 [66]. In Germany, the incidence was even higher with 7.7 and 5.3 per 100,000 [67]. About 30% of all primary tumors of the central nervous system are categorized as glioma, while, when focusing on malignant brain tumors, glioma make up even 80% [68]. Named are glioma after their origin – they arise from the glial cells – and categorized by their location, cell type and grade. Commonly, grading is conducted via the WHO classification scheme based on histopathology, dividing gliomas into grade I - IV. Treatment procedures are chosen based on the grades. Therefore, sampling remains indispensable [69], although diagnosis of tumors of the central nervous system is commonly achieved by MRI [70-72]. Biopsies can either be taken via a stereotactic approach or during the resection surgery.

In the WHO classification, gliomas which are not infiltrating and proliferating slowly are classified as grade I, having a high probability of a cure after resection, whereas grade IV tumors are the most lethal tumors. Grade IV tumors are related to a fast progress of the disease, before and after treatment. Often, necrotic tissue is found in the central part. Unfortunately, the most common gliomas in adults are grade IV glioblastoma multiforme (GBM) as demonstrated with data taken during 2005 - 2009 in the USA, which make up 15.8% of all primary tumors of the brain and central nervous system and even 54% of all gliomas [73]. Data from 1992 - 1997 in the USA show the highest yearly incidence of all gliomas for glioblastoma multiforme with 2.96 per 100,000 compared to the next highest incidence of 0.49 per 100,000 for grade III anaplastic astrocytoma, yielding a 5-year survival expectancy of less than 3% [74]. Even the two-year survival expectancy of GBMs was as low as 8% and the one-year survival resulted to 28%. This hardly changed over the years, given a 5-year survival rate of 5% for data acquired in the USA from 2004 - 2007 [68].
In order to make a prognosis on survival time, however, the location of the tumor and, of course, the patient's general condition and age have to be taken into account in addition to the grading. Nevertheless, published data from the USA state 5-year survival rates of about 90 - 100% for grade I [74], 50 - 80% for grade II and 30 - 80% for grade III gliomas [68], depending on the exact tumor type.

Currently, glioma patients are commonly treated by open tumor resection and fractionated radiotherapy with concomitant and adjuvant temozolomide. Especially for patients with methylated promoter O(6)-methylguanine-DNA methyltransferase (MGMT), the survival time was increased with the introduction of temozolomide [75]. Thus, the promoter status is in addition to the already mentioned location of the tumor and the condition and age of the patient, an important factor to predict survival time. The decision on the exact treatment procedure, however, is usually personalized and decided on case by case [76].

An additional, promising but still experimental, treatment is PDT. PDT of glioma was not yet applied as stand-alone therapy, but as adjuvant therapy together with resection by postsurgical irradiation of the resection cavity, or as iPDT treatment of selected tumors (e.g. small in size, no infiltration of the corpus callosum, no infiltration of the ventricle) in case a resection is not possible. Theoretically, not only small glioma can be treated with iPDT, but the limited penetration depth of light in tissue requires a high density of fibers, which limits the feasibility.

As described in chapter 1.3.3, ideally the PDT and also the iPDT is a minimal invasive treatment form. However, major complications could result from iPDT of glioma, depending on the volume and the location of the tumor, as well as the photosensitizer used.

In the first study [1] of this thesis, basic research was conducted on the concentration of PpIX in suspected grade IV tumors. For this study, tissue samples were acquired during FGR performed after administration of 5-ALA. PpIX concentrations were highest in vital grade IV tumors with 5.8 ± 4.8 µmol/l measured for 8 patients. The concentration was significantly higher compared to grade III tumors (0.2 ± 0.4 µmol/l), which were determined in another four patients.

What is more, a high variation in the amount of photosensitizer within a single grade IV tumor could be determined. For infiltrating zones as well as necrotic tissue, PpIX levels were much lower than in the solid tumor. Therefore, it needs to be investigated further whether PDT is applicable for infiltrating tumors and tumors containing necrotic tissue.

Another potential improvement in glioma diagnosis that could be derived from the results of this study is the guidance of stereotactic biopsy sampling. A fiber probe measuring the absolute PpIX concentration could indicate whether the probe tip is in normal tissue, the infiltrating zone, necrotic tissue or the vital part of the tumor. Thus, surgeons could identify the location from which to take a relevant tissue sample. During an interdisciplinary project in which the author took part, potential fiber probe and endoscope set-ups were evaluated and a method to exploit the fluorescence of a second fluorophore to detect vessels was developed and published [62, 77, 78]. However, further research in this area is necessary to verify its reliability.

The contribution of Gesa Kniebühler to this study was to determine the PpIX concentration and to perform the analysis of the spectra, together with Ann Johansson. Determining the PpIX concentration included the extraction of PpIX and measurements of fluorescence with a fluorescence spectrometer.

The second manuscript of this thesis comprises results of investigations on the use of PpIX for iPDT [2], parts of which were also presented at the Photonics Europe conference [79]. Aim of the study was to investigate the dependence of the PpIX concentration on the treatment outcome. Through *in vivo* fiber based measurements of the fluorescence intensity before and after PDT, *ex vivo* absolute concentration measurements and MRI it could be shown that the treatment outcome depends on the PpIX concentration in the tumor. Moreover, it seems possible to easily implement a safe method to determine the presence and bleaching of photosensitizer and therefore achieve an early treatment outcome prognosis.

The contribution of Gesa Kniebühler to this study was to determine the PpIX concentration of the biopsies. This involved performing the extraction procedure and the measurements of the PpIX fluorescence with a fluorescence spectrometer.

1.6 Cholangiocarcinoma

Cholangiocarcinomas (CCs) are malignant tumors of the bile duct. About one third of CCs are localized within the liver and about two third arise within the perihilar region, involving the common bile duct and/or the hepatic ducts.

The yearly incidence rate of CCs in the western world is about 3 - 5 per 100,000 [80]. Since they are highly lethal, refraining from treatment results in a median survival time of only about three months. Therefore, investigations on improving treatments are of great importance. Together with carcinomas of the gallbladder, CCs account for 2% of all malignant tumors [81]. The only curative treatment for patients with CCs is the complete resection (R0) [82]. However, a complete resection is, at time of diagnosis, possible for only about one third of the patients [83]. A reason for this and, consequently, the high mortality rate is that at the time of diagnosis, CCs are often in an advanced state. This means that the tumor can either be too large, or metastases can be present already. Lymph node metastases are present in about 30 -50% of cases at time of diagnosis, while distant metastases occur in less than 20% of patients. Metastases of CCs have been found in lymph nodes, liver, lung, skin and bones as well as in the peritoneum [84, 85]. As a result, the five-year survival time for the most common (60%) hilar CC has been reported to be only about 30% for patients who underwent R0 resection, and 0% for patients with partial (R2) or no resection [86, 87].

In order to enable a decision about a treatment procedure, perihilar CCs are often classified further according to the pattern of the involvement of the hepatic duct bifurcation. First intro-

duced by Bismuth and Corlette, the advanced classification scheme is shown in Figure 3 [88-90]. If the bifurcation is affected (hilar CC), the tumor is considered a Klatskin tumor, which is the case for Bismuth type II - IV. Since the stages are defined depending on the tumor location, they consequently indicate to a great part the possibility of resection of the tumor. Hence, the expected survival time may also be estimated based on the Bismuth type. For Bismuth type IV, however, a complete resection is not possible. Although staging of CCs via the Bismuth classification is common practice, Zervos et al. [91] could not find a significant correlation between stage and survival time for any of the different staging systems. Thus, they suggest that an aggressive resection should be performed for any stage of CC.

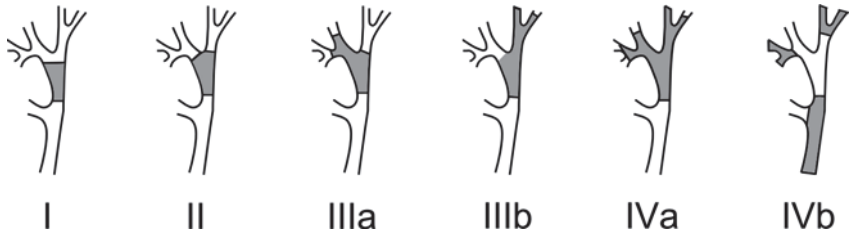

Figure 3. Bismuth classification of CCs. Grey parts indicate tumor location

A different approach is a palliative treatment, especially because of the estimated low survival times for extended resections with positive margins left and a rate of death after surgery of 10% [86, 92]. Common treatments for non-resectable CCs are biliary endoprosthesis, chemotherapy and radiation therapy. In the last few years, photodynamic therapy (PDT) also gained in importance. While the implantation of stents results in a median survival time of six months after diagnosis, stenting can easily be combined with PDT, which results in a median survival of 12 months for retrospective studies [93]. In a meta-analysis of six prospective studies [94], the median survival for stenting alone could be prolonged by 265 days on average. Photofrin® is commonly used for PDT of CCs. However, when using Photofrin®, patients remain photosensitive and require shielding from sunlight for up to three months. This is a great disadvantage, especially in view of the treatment being palliative. What is more, there have been reports of complications such as organ wall perforations. In order to maintain a good clinical outcome while reducing the side effects and, most importantly, shortening the period of photosensitivity, the use of temoporfin (Foscan®) at a low dose has been investigated in the third manuscript [3] of the present thesis. For this study, 13 patients with CCs of all Bismuth types, for which a complete resection was no longer possible, were treated in 14 PDT sessions and the survival time until publication was analyzed. Apart from performing the treatment and evaluating the outcome, fluorescence measurements were performed to find the optimal DLI and suggest an optimized treatment protocol.

The contribution of Gesa Kniebühler to this study was to perform the contrast fluorescence measurements during ERCP as well as the fluorescence kinetics measurements together with Thomas Pongratz. She also evaluated the data and wrote the manuscript.

1.7 References

[1] Johansson A, Faber F, Kniebühler G, Stepp H, et al. Protoporphyrin IX fluorescence and photobleaching during interstitial photodynamic therapy of malignant gliomas for early treatment prognosis. Lasers in Surgery and Medicine 2013.

[2] Johansson A, Palte G, Schnell O, Tonn J-C, et al. 5-Aminolevulinic acid-induced protoporphyrin IX levels in tissue of human malignant brain tumors. Photochemistry and Photobiology 2010; 86:1373-8.

[3] Kniebühler G, Pongratz T, Betz CS, Göke B, et al. Photodynamic therapy for cholangiocarcinoma using low dose mTHPC (Foscan®). Photodiagnosis and Photodynamic Therapy 2013.

[4] Moan J, Peng Q. An outline of the history of PDT. In: Patrice T, editor. Photodynamic Therapy 2003. p. 1-+.

[5] Raab O. Über die Wirkung fluoreszierender Stoffe auf Infusorien. Zeitschrift fur Biologie 1900; 39:524-46.

[6] von Tappeiner H. Über die Wirkung der photodymaischen (fluorescierenden) Stoffe auf Protozoen und Enzyme. Deutsches Archiv fur Klinische Medizin 1904; 80:427-87.

[7] von Tappeiner H, Jesionek H. Therapeutische Versuche mit fluoreszierenden Stoffen. Muenchener Medizinische Wochenschrift 1903; 47:2042-4.

[8] Triesscheijn M, Baas P, Schellens JHM, Stewart FA. Photodynamic therapy in oncology. Oncologist 2006; 11:1034-44.

[9] Zaak D, Kriegmair M, Stepp H, Stepp H, et al. Endoscopic detection of transitional cell carcinoma with 5-aminolevulinic acid: Results of 1012 fluorescence endoscopies. Urology 2001; 57:690-4.

[10] Stummer W, Novotny A, Stepp H, Goetz C, et al. Fluorescence-guided resection of glioblastoma multiforme by using 5-aminolevulinic acid-induced porphyrins: A prospective study in 52 consecutive patients. Journal of Neurosurgery 2000; 93:1003-13.

[11] Kreth FW, Berlis A, Spiropoulou V, Faist M, et al. The role of tumor resection in the treatment of glioblastoma multiforme in adults. Cancer 1999; 86:2117-23.

[12] Lacroix M, Abi-Said D, Fourney DR, Gokaslan ZL, et al. A multivariate analysis of 416 patients with glioblastoma multiforme: prognosis, extent of resection, and survival. Journal of Neurosurgery 2001; 95:190-8.

[13] Stummer W, Tonn J-C, Mehdorn HM, Nestler U, et al. Counterbalancing risks and gains from extended resections in malignant glioma surgery: A supplemental analysis from the randomized 5-aminolevulinic acid glioma resection study Clinical article. Journal of Neurosurgery 2011; 114:613-23.

[14] Stummer W, Pichlmeier U, Meinel T, Wiestler OD, et al. Fluorescence-guided surgery with 5-aminolevulinic acid for resection of malignant glioma: A randomised controlled multicentre phase III trial. Lancet Oncology 2006; 7:392-401.

[15] Dougherty TJ. An update on photodynamic therapy applications. Journal of Clinical Laser Medicine and Surgery 2002; 20:3-7.

[16] Kharkwal GB, Sharma SK, Huang YY, Dai TH, et al. Photodynamic therapy for infections: Clinical applications. Lasers in Surgery and Medicine 2011; 43:755-67.

[17] Smetana Z, Malik Z, Orenstein A, Mendelson E, et al. Treatment of viral infections with 5-aminolevulinic acid and light. Lasers in Surgery and Medicine 1997; 21:351-8.

[18] Henderson BW, Dougherty TJ. How does photodynamic therapy work. Photochemistry and Photobiology 1992; 55:145-57.

[19] O'Connor AE, Gallagher WM, Byrne AT. Porphyrin and nonporphyrin photosensitizers in oncology: Preclinical and clinical advances in photodynamic therapy. Photochemistry and Photobiology 2009; 85:1053-74.

[20] Allison RR, Downie GH, Cuenca R, Hu XH, et al. Photosensitizers in clinical PDT. Photodiagnosis and Photodynamic Therapy 2004; 1:27-42.

[21] Castano AP, Mroz P, Hamblin MR. Photodynamic therapy and anti-tumour immunity. Nature Reviews Cancer 2006; 6:535-45.

[22] Panzarini E, Inguscio V, Dini L. Immunogenic cell death: can it be exploited in PhotoDynamic Therapy for cancer? BioMed research international 2013; 2013:482160.

[23] Peng Q, Moan J, Nesland JM. Correlation of subcellular and intratumoral photosensitizer localization with ultrastructural features after photodynamic therapy. Ultrastructural Pathology 1996; 20:109-29.

[24] Beck TJ, Kreth FW, Beyer W, Mehrkens JH, et al. Interstitial photodynamic therapy of nonresectable malignant glioma recurrences using 5-aminolevulinic acid induced protoporphyrin IX. Lasers in Surgery and Medicine 2007; 39:386-93.

[25] Johansson A, Kreth F-W, Stummer W, Stepp H. Interstitial photodynamic therapy of brain tumors. IEEE Journal of Selected Topics in Quantum Electronics 2010; 16:841-53.

[26] Amelink A, Haringsma J, Sterenborg HJCM. Noninvasive measurement of oxygen saturation of the microvascular blood in Barrett's dysplasia by use of optical spectroscopy. Gastrointestinal Endoscopy 2009; 70:1-6.

[27] Morlet L, Vonarxcoinsmann V, Lenz P, Foultier MT, et al. Correlation between meta(tetrahydroxyphenyl)chlorin (m-THPC) biodistribution and photodynamic effects in mice. Journal of Photochemistry and Photobiology B: Biology 1995; 28:25-32.

[28] Ris HB, Altermatt HJ, Stewart CM, Schaffner T, et al. Photodynamic therapy with m-tetrahydroxyphenylchlorin in-vivo - Optimization of the therapeutic index. International Journal of Cancer 1993; 55:245-9.

[29] Triesscheijn M, Ruevekamp M, Antonini N, Neering H, et al. Optimizing meso-tetra-hydroxyphenyl-chlorin-mediated photodynamic therapy for basal cell carcinoma. Photochemistry and Photobiology 2006; 82:1686-90.

[30] Peng Q, Berg K, Moan J, Kongshaug M, et al. 5-aminolevulinic acid-based photodynamic therapy: Principles and experimental research. Photochemistry and Photobiology 1997; 65:235-51.

[31] Dailey HA, Smith A. Differential interaction of porphyrins used in photoradiation therapy with ferrochelatase. Biochemical Journal 1984; 223:441-5.

[32] Kondo M, Hirota N, Takaoka T, Kajiwara M. Heme-biosynthetic enzyme-activities and porphyrin accumulation in normal liver and hepatoma-cell lines of rat. Cell Biology and Toxicology 1993; 9:95-105.

[33] Leibovici L, Schoenfeld N, Yehoshua HA, Mamet R, et al. Activity of porphobilinogen deaminase in peripheral-blood mononuclear-cells of patients with metastatic cancer. Cancer 1988; 62:2297-300.

[34] Kennedy JC, Pottier RH. New trends in photobiology: Endogenous protoporphyrin IX, a clinically useful photosensitizer for photodynamic therapy. Journal of Photochemistry and Photobiology B: Biology 1992; 14:275-92.

[35] Peng Q, Moan J, Warloe T, Vladimir I, et al. Build-up of esterified aminolevulinic-acid-derivative-induced porphyrin fluorescence in normal mouse skin. Journal of Photochemistry and Photobiology B: Biology 1996; 34:95-6.

[36] Fotinos N, Campo MA, Popowycz F, Gurny R, et al. 5-Aminolevulinic acid derivatives in photomedicine: Characteristics, application and perspectives. Photochemistry and Photobiology 2006; 82:994-1015.

[37] Lehmann P. Methyl aminolaevulinate-photodynamic therapy: A review of clinical trials in the treatment of actinic keratoses and nonmelanoma skin cancer. British Journal of Dermatology 2007; 156:793-801.

[38] Rick K, Sroka R, Stepp H, Kriegmair M, et al. Pharmacokinetics of 5-aminolevulinic acid-induced protoporphyrin IX in skin and blood. Journal of Photochemistry and Photobiology B: Biology 1997; 40:313-9.

[39] Bader M, Zaak D, Stief C, Kriegmair M, et al. Photodynamic therapy of bladder cancer - A phase I study using hexyl-aminolevulinate. European Urology Supplements 2007; 6:172-.

[40] Bozzini G, Colin P, Betrouni N, Nevoux P, et al. Photodynamic therapy in urology: What can we do now and where are we heading? Photodiagnosis and Photodynamic Therapy 2012; 9:261-73.

[41] Zaak D, Sroka R, Khoder W, Adam C, et al. Photodynamic diagnosis of prostate cancer using 5-aminolevulinic acid - First clinical experiences. Urology 2008; 72:345-8.

[42] Ballabh P, Braun A, Nedergaard M. The blood-brain barrier: An overview - Structure, regulation, and clinical implications. Neurobiology of Disease 2004; 16:1-13.

[43] Valdes PA, Moses ZB, Kim A, Belden CJ, et al. Gadolinium- and 5-aminolevulinic acid-induced protoporphyrin IX levels in human gliomas: An ex vivo quantitative study to correlate protoporphyrin IX levels and blood-brain barrier breakdown. Journal of Neuropathology and Experimental Neurology 2012; 71:806-13.

[44] Sharman WM, Allen CM, van Lier JE. Photodynamic therapeutics: Basic principles and clinical applications. Drug Discovery Today 1999; 4:507-17.

[45] Kessel D, Woodburn K. Biodistribution of Photosensitizing Agents. International Journal of Biochemistry 1993; 25:1377-83.

[46] Ortner M-A. Photodynamic therapy for cholangiocarcinoma. Lasers in Surgery and Medicine 2011; 43:776-80.

[47] Mitra S, Foster TH. Photophysical parameters, photosensitizer retention and tissue optical properties completely account for the higher photodynamic efficacy of meso-tetra-hydroxyphenyl-chlorin vs Photofrin. Photochemistry and Photobiology 2005; 81:849-59.

[48] Bown SG, Rogowska AZ, Whitelaw DE, Lees WR, et al. Photodynamic therapy for cancer of the pancreas. Gut 2002; 50:549-57.

[49] Ortner MAEJ, Liebetruth J, Schreiber S, Hanft M, et al. Photodynamic therapy of nonresectable cholangiocarcinoma. Gastroenterology 1998; 114:536-42.

[50] Glanzmann T, Hadjur C, Zellweger M, Grosjean P, et al. Pharmacokinetics of tetra(m-hydroxyphenyl)chlorin in human plasma and individualized light dosimetry in photodynamic therapy. Photochemistry and Photobiology 1998; 67:596-602.

[51] Ronn AM, Nouri M, Lofgren LA, Steinberg BM, et al. Human tissue levels and plasma pharmacokinetics of temoporfin (Foscan®, mTHPC). Lasers in Medical Science 1996; 11:267-72.

[52] Braichotte D, Savary JF, Glanzmann T, Westermann P, et al. Clinical pharmacokinetic studies of tetra(meta-hydroxyphenyl)chlorin in squamous-cell carcinoma by fluorescence spectroscopy at 2 wavelengths. International Journal of Cancer 1995; 63:198-204.

[53] Jones HJ, Vernon DI, Brown SB. Photodynamic therapy effect of m-THPC (Foscan ®) in vivo: Correlation with pharmacokinetics. British Journal of Cancer 2003; 89:398-404.

[54] Pereira SP, Ayaru L, Rogowska A, Mosse A, et al. Photodynamic therapy of malignant biliary strictures using meso-tetrahydroxyphenylchlorin. European Journal of Gastroenterology and Hepatology 2007; 19:479-85.

[55] Betz CS, Rauschning W, Stranadko EP, Riabov MV, et al. Optimization of treatment parameters for Foscan ®-PDT of basal cell carcinomas. Lasers in Surgery and Medicine 2008; 40:300-11.

[56] Patterson MS, Wilson BC, Wyman DR. The propagation of optical radiation in tissue II. Optical properties of tissue and resulting fluence distributions. Lasers in Medical Science 1991; 6:379-90.

[57] Hull EL, Ediger MN, Unione AHT, Deemer EK, et al. Noninvasive, optical detection of diabetes: model studies with porcine skin. Optics Express 2004; 12:4496-510.

[58] Müller MG, Georgakoudi I, Zhang QG, Wu J, et al. Intrinsic fluorescence spectroscopy in turbid media: Disentangling effects of scattering and absorption. Applied Optics 2001; 40:4633-46.

[59] Wu J, Feld MS, Rava RP. Analytical model for extracting intrinsic fluorescence in turbid media. Applied Optics 1993; 32:3585-95.

[60] Diamond KR, Patterson MS, Farrell TJ. Quantification of fluorophore concentration in tissue-simulating media by fluorescence measurements with a single optical fiber. Applied Optics 2003; 42:2436-42.

[61] Stepp H, Beck T, Beyer W, Pfaller C, et al. Measurement of fluorophore concentration in turbid media by a single optical fiber. Medical Laser Application 2007; 22:23-34.

[62] Palte G, Johansson A, Hennig G, Beyer W, et al. Fluorescence and reflectance spectroscopy for protoporphyrin IX quantification in tissue-like media. Proceedings of SPIE 2011. p. 788340.

[63] Song LL, Hennink EJ, Young IT, Tanke HJ. Photobleaching kinetics of fluorescein in quantitative fluorescence microscopy. Biophysical Journal 1995; 68:2588-600.

[64] Wilson BC, Patterson MS, Lilge L. Implicit and explicit dosimetry in photodynamic therapy: A new paradigm. Lasers in Medical Science 1997; 12:182-99.

[65] Pogue BW, Sheng C, Benevides J, Forcione D, et al. Protoporphyrin IX fluorescence photobleaching increases with the use of fractionated irradiation in the esophagus. Journal of Biomedical Optics 2008; 13:034009/1-10.

[66] Jemal A, Bray F, Center MM, Ferlay J, et al. Global Cancer Statistics. Ca-a Cancer Journal for Clinicians 2011; 61:69-90.

[67] Kaatsch P, Spix C, Katalinic A, Hentschel S, et al. Krebs in Deutschland 2007/2008. 8. Ausgabe ed. Berlin: Robert Koch-Institut und die Gesellschaft der epidemiologischen Krebsregister in Deutschland e.V.; 2012.

[68] Goodenberger ML, Jenkins RB. Genetics of adult glioma. Cancer Genetics 2012; 205:613-21.

[69] Kros JM. Grading of gliomas: The road from eminence to evidence. Journal of Neuropathology and Experimental Neurology 2011; 70:101-9.

[70] Al-Okaili RN, Krejza J, Wang SM, Woo JH, et al. Advanced MR imaging techniques in the diagnosis of intraaxial brain tumors in adults. Radiographics 2006; 26:S173-U84.

[71] Friedman SN, Bambrough PJ, Kotsarini C, Khandanpour N, et al. Semi-automated and automated glioma grading using dynamic susceptibility-weighted contrast-enhanced perfusion MRI relative cerebral blood volume measurements. British Journal of Radiology 2012; 85:e1204-e11.

[72] Petrella JR, Provenzale JM. MR perfusion imaging of the brain: Techniques and applications. American Journal of Roentgenology 2000; 175:207-19.

[73] Dolecek TA, Propp JM, Stroup NE, Kruchko C. CBTRUS statistical report: primary brain and central nervous system tumors diagnosed in the united states in 2005-2009. Neuro-Oncology 2012; 14:v1-v49.

[74] Ohgaki H. Epidemiology of brain tumors. Methods in Molecular Biology 2009; 472:323-42.

[75] Stupp R, Hegi ME, Mason WP, van den Bent MJ, et al. Effects of radiotherapy with concomitant and adjuvant temozolomide versus radiotherapy alone on survival in glioblastoma in a randomised phase III study: 5-year analysis of the EORTC-NCIC trial. Lancet Oncology 2009; 10:459-66.

[76] Thon N, Kreth S, Kreth FW. Personalized treatment strategies in glioblastoma: MGMT promoter methylation status. Oncotargets And Therapy 2013; 6:1363-72.

[77] Göbel W, Brucker D, Kienast Y, Johansson A, et al. Optical needle endoscope for safe and precise stereotactically guided biopsy sampling in neurosurgery. Optics Express 2012; 20:26117-26.

[78] Stepp H, Beyer W, Brucker D, Ehrhardt A, et al. Fluorescence guidance during stereotactic biopsy. SPIE BiOS: International Society for Optics and Photonics; 2012. p. 82074H-H-9.

[79] Johansson A, Kreth F, Ardeshiri A, Stummer W, et al. Protoporphyrin IX for photodynamic therapy of brain tumours. SPIE Photonics Europe: International Society for Optics and Photonics; 2010. p. 77151M-M-8.

[80] Patel T. Worldwide trends in mortality from biliary tract malignancies. BMC Cancer 2002; 2.

[81] Tannapfel A, Wittekind C. Bile duct and gall bladder carcinoma: Biology and pathology. Internist 2004; 45:33-+.

[82] Kolligs FT, Zech CJ, Schonberg SO, Schirral J, et al. Interdisciplinary diagnosis of and therapy for cholangiocarcinoma. Zeitschrift fur Gastroenterologie 2008; 46:58-68.

[83] Zoepf T, Jakobs R, Arnold JC, Apel D, et al. Palliation of nonresectable bile duct cancer: Improved survival after photodynamic therapy. American Journal of Gastroenterology 2005; 100:2426-30.

[84] Wiedmann M, Caca K, Berr F, Schiefke I, et al. Neoadjuvant photodynamic therapy as a new approach to treating hilar cholangiocarcinoma. Cancer 2003; 97:2783-90.

[85] Rosen CB, Nagorney DM, Wiesner RH, Coffey RJ, et al. Cholangiocarcinoma complicating primary sclerosing cholangitis. Annals of Surgery 1991; 213:21-5.

[86] Jarnagin WR, Fong Y, DeMatteo RP, Gonen M, et al. Staging, resectability, and outcome in 225 patients with hilar cholangiocarcinoma. Annals of Surgery 2001; 234:507-17.

[87] Neuhaus P, Jonas S, Bechstein WO, Lohmann R, et al. Extended resections for hilar cholangiocarcinoma. Annals of Surgery 1999; 230:808-18.

[88] Bismuth H, Nakache R, Diamond T. Management strategies in resection for hilar cholangiocarcinoma. Annals of Surgery 1992; 215:31-8.

[89] Kiesslich T, Wolkersdorfer G, Neureiter D, Salmhofer H, et al. Photodynamic therapy for non-resectable perihilar cholangiocarcinoma. Photochemical & Photobiological Sciences 2009; 8:23-30.

[90] Bismuth H, Corlette MB. Intrahepatic Cholangioenteric Anastomosis in Carcinoma of Hilus of Liver. Surgery Gynecology & Obstetrics 1975; 140:170-8.

[91] Zervos EE, Osborne D, Goldin SB, Villadolid DV, et al. Stage does not predict survival after resection of hilar cholangiocarcinomas promoting an aggressive operative approach. American Journal of Surgery 2005; 190:810-5.

[92] Holzinger F, Baer HU, Schilling M, Stauffer EJ, et al. Congenital bile duct cyst: A premalignant lesion of the biliary tract associated with adenocarcinoma - A case report. Zeitschrift fur Gastroenterologie 1996; 34:382-5.

[93] Witzigmann H, Berr F, Ringel U, Caca K, et al. Surgical and palliative management and outcome in 184 patients with hilar cholangiocarcinoma - Palliative photodynamic therapy plus stenting is comparable to R1/R2 resection. Annals of Surgery 2006; 244:230-9.

[94] Leggett CL, Gorospe EC, Murad MH, Montori VM, et al. Photodynamic therapy for unresectable cholangiocarcinoma: A comparative effectiveness systematic review and meta-analyses. Photodiagnosis and Photodynamic Therapy 2012; 9:189-95.

2 Original manuscripts

5-Aminolevulinic acid-induced protoporphyrin IX levels in tissue of human malignant brain tumors

Ann Johansson, Gesa Palte, Oliver Schnell, Jörg-Christian Tonn, Jochen Herms and Herbert Stepp

Photochemistry and Photobiology 2010; 86:1373-8

Photochemistry and Photobiology, 2010, 86: 1373–1378

5-Aminolevulinic Acid-induced Protoporphyrin IX Levels in Tissue of Human Malignant Brain Tumors

Ann Johansson*[1], Gesa Palte[1], Oliver Schnell[2], Jörg-Christian Tonn[2], Jochen Herms[3] and Herbert Stepp[1]

[1]Laser-Forschungslabor, University Clinic Großhadern, Munich, Germany
[2]Department of Neurosurgery, University Clinic Großhadern, Munich, Germany
[3]Center for Neuropathology and Prion Research, University Clinic Großhadern, Munich, Germany

Received 25 June 2010, accepted 6 August 2010, DOI: 10.1111/j.1751-1097.2010.00799.x

ABSTRACT

Protoporphyrin IX (PpIX) produced from exogenous, orally administered 5-aminolevulinic acid (ALA) displays high tumor-selective uptake and is being successfully employed for fluorescence-guided resection (FGR) of human malignant gliomas. Furthermore, the phototoxicity of PpIX can be utilized for photodynamic therapy (PDT) of brain tumors, which has been shown previously. Here, the absolute PpIX concentration in human brain tissue was investigated following oral ALA administration (20 mg kg^{-1} b.w.). An extraction procedure was used to quantify PpIX in macroscopic tissue samples, weighing 0.013–0.214 g, obtained during FGR. The PpIX concentration was significantly higher in vital grade IV tumors (5.8 ± 4.8 μM, mean ± SD, range 0–28.2 μM, $n = 8$) as compared with grade III tumors (0.2 ± 0.4 μM, mean ± SD, range 0–0.9 μM, $n = 4$). There was also a large heterogeneity within grade IV tumors with PpIX displaying significantly lower levels in infiltration zones and necrotic regions as compared with vital tumor parts. The average PpIX concentration in vital grade IV tumor parts was in the range previously shown sufficient for PDT-induced tissue damage following irradiation. However, the feasibility of PDT for grade III brain tumors and for grade IV brain tumors displaying mainly necrotic tissue areas without solid tumor parts needs to be further investigated.

INTRODUCTION

Gliomas account for more than 70% of primary brain tumors (1). High-grade gliomas include WHO grade III tumors such as anaplastic astrocytoma (AA), anaplastic oligodendroglioma (AO), anaplastic oligoastrocytoma (AOA), anaplastic ganglioglioma (AG) and tumors of WHO grade IV such as glioblastoma multiforme (GBM) and gliosarcoma (GS). Conventional treatment options include surgery, radiation therapy and chemotherapy. These tumors always infiltrate the adjacent normal brain in a diffuse way (2,3), making it nearly impossible to visualize tumor borders and to surgically remove all vital tumor regions. Furthermore, glioma cells are at least partially resistant to radiation and chemotherapy (4). Hence, recurrences are unavoidable and median survival limited, *e.g.* 2-year survival rates of 43% and 3–8% for AA and GBM, respectively (1).

5-aminolevulinic acid (ALA) is a photosensitizer precursor that is converted into the actual photosensitizer, protoporphyrin IX (PpIX), as a part of the endogenous heme-cycle (5). PpIX generally displays a high tumor-selective uptake (in the range of 50:1 for the case of malignant brain tissue [6]), explained by differences in enzymatic activity in tumor cells as compared with normal tissue (7–9) plus a limited ability of ALA to penetrate an intact blood–brain barrier (10). The use of ALA for fluorescence-guided resection (FGR) has been demonstrated to be not only helpful for a better detection and delineation of vital tumor tissue from the infiltration zone and nonneoplastic brain, but has also improved the progression-free survival in patients with malignant gliomas as compared with surgery performed under white-light alone (65% *versus* 36% complete resection and 41% *versus* 21% 6-month progression-free survival) (11). In 2007, the use of ALA (Gliolan; medac GmbH, Wedel, Germany) at a dose of 20 mg kg^{-1} b.w. acquired clinical approval in the European Union for FGR of residual glioma. Recently, the potential of ALA-mediated FGR for visualizing anaplastic foci also in diffusely infiltrating gliomas without significant contrast enhancement on magnetic resonance has been shown (12).

PpIX also displays phototoxic effects, which are exploited for photodynamic therapy (PDT) in different organs, including brain tumors (13–16). Irradiation, *e.g.* at 635 nm, leads to excitation of PpIX and the subsequent formation of singlet oxygen and reactive oxygen species, which in turn causes cellular damage. Median survival following ALA-mediated brain-PDT of 15 months has been reported (13,17) and evidence exists for some intriguing long-term survivors (> 5 years) (18). Factors that might influence the treatment outcome are the patient-specific light (19,20) and photosensitizer distribution (6,21), the oxygenation status of the target tissue (22) as well as the synergistic effects of PDT and a treatment-induced immune response (23). For example, employing hematoporphyrin derivative (HpD) for PDT of GBM, higher photosensitizer uptake was associated with improved clinical outcome (21).

For FGR and brain-PDT, the PpIX uptake has mostly been investigated by means of its characteristic fluorescence (6,24). However, as fluorescence signals are inherently sensitive to the optical properties, *i.e.* the absorption and scattering coefficients, of the surrounding tissue, fluorescence spectroscopy

*Corresponding author email: ann.johansson@med.uni-muenchen.de (Ann Johansson)

alone makes it difficult to assess the absolute PpIX concentration. It is thus uncertain whether PpIX levels induced by the administration of 20 mg kg^{-1} b.w. ALA are sufficient for a successful PDT throughout the entire target volume.

Here, we investigate the absolute PpIX concentration within human brain tissue samples acquired during FGR. A procedure for the solubilization of tissue samples and the subsequent quantification of the PpIX concentration is employed for tissue samples including GBM, GS, AA, AO, AOA, AG and nonneoplastic tissue. The results are discussed with respect to tumor grade and the presence of tissue heterogeneities, such as necrotic regions.

MATERIALS AND METHODS

Patients and treatment procedure. Freshly prepared solution of ALA in normal drinking water (1500 mg ALA per 50 mL water at a dosage of 20 mg kg^{-1} b.w., Gliolan; medac GmbH, Wedel, Germany) was administered to the patients *ca* 3 h before induction of anesthesia. Resection in white light and fluorescence mode was performed employing a neurosurgical microscope (OPMI Pentero; Carl Zeiss Meditec, Jena, Germany) according to the institutional guidelines. During FGR, tissue resectates were collected, fixed in formalin, embedded in paraffin, sectioned and hematoxylin and eosin (H&E) stained for routine histopathological analysis. Diagnosis and tumor cell density (TCD) are listed in Table 1. At least one of the resected tissue pieces was excluded from the routine procedure, protected from further light exposure and stored on ice until further processing. A smaller part of this sample was fixed in formalin, embedded in paraffin and sectioned. Staining with H&E and MIB-1 for the Ki67 labeling index was performed for sample-specific diagnosis and for cell proliferation status, respectively. The remaining volume was employed for PpIX extraction as described below. This procedure did not interfere with the neuropathological workup for full and proper tissue diagnosis. The study was approved by the ethical committee of the University Clinic, Großhadern, Munich, and informed consent was obtained from all patients.

Extraction procedure. The tissue was cut into smaller pieces (<0.1 g) and weighed. Where heterogeneities were visible, such as dark-appearing necrotic regions, effort was made to analyze these separately. In adaptation to the protocol described earlier (25,26), each sample was immersed in 1 mL Solvable (Perkin Elmer LAS, Groningen, The Netherlands) and placed in a heated (45–50°C) ultrasound bath until the tissue was completely dissolved. Solvable is a product designed to solubilize the tissue and contains a mixture of dodecyl-dimethyl-aminoxide, secondary alcohol ethoxylate, sodium hydroxide and water. From this solution, three aliquots of 10–80 μL each were diluted in 1 mL Solvable and placed in the ultrasound bath for another 15 min. Care was taken to limit light exposure during the solubilization process. Seven hundred microliters of this solution was filled into a 2 mm optical pathlength quartz cuvette. Absorption spectra (λ = 350–750 nm, Lambda40; Perkin Elmer GmbH, Überlingen, Germany) were obtained and if necessary further dilution with Solvable was performed to ascertain an optical density below 0.1. Fluorescence spectroscopy (λ_{exc} = 400 nm, λ_{em} = 450–780 nm, Fluoromax-2; Instruments S.A. Inc., NJ) was employed to quantify the PpIX concentration, c_{PpIX}. Each fluorescence spectrum was analyzed by first subtracting a background fluorescence spectrum, obtained from pure Solvable. A Gaussian curve was fit to the data points in the wavelength intervals 500–600 and 750–780 nm, thus representing an interpolation of the autofluorescence from dissolved tissue. This component was subtracted and the resulting fluorescence intensity, in counts per second (cps) per g tissue, at 634 nm was used to quantify the PpIX concentration.

A calibration curve, relating the measured cps per g tissue to the true PpIX concentration was obtained by dissolving brain tumor tissue, obtained from a GBM where white-light resection had been performed without ALA administration, in Solvable according to the

Table 1. Patients' data, the resulting PpIX concentration (c_{PpIX}) and the corresponding Ki67 labeling index.

Patient	Age/sex	Diagnosis/TCD (routine H&E)	Sample site	m (g)	c_{PpIX} ± SD (μM)	Ki67 (%)
1	64/M	GBM/middle–high	Vital tumor	0.040	6.2 ± 0.2	–
2*	60/M	GBM/high	Vital tumor	0.049	3.8 ± 1.0	22
3*	25/F	GBM/high	Vital tumor	0.042	11.5 ± 6.8	32
4	54/F	GBM/high	Vital tumor	0.084	13.5 ± 10.7	40
5	45/M	GBM/middle	Vital tumor	0.032	0.5 ± 0.2	18
6*	31/M	GBM/high	Infiltr tumor	0.027	2.1 ± 0.4	30
7*	64/F	GBM/varying	a) Infiltr tumor	0.013	1.6 ± 0.1	17
			b) Nonneopl	0.087	0.0 ± 0.0	0
8	44/F	GBM	a) Vital tumor	0.006	1.3 ± 0.0	–
			b) Infiltr tumor	0.013	0.0 ± 0.0	1
9*	69/M	GBM	a) Vital tumor	0.0234	1.9 ± 0.0	20
			b) Necr	0.0912	0.3 ± 0.1	0
10	67/F	GBM	Necr	0.104	1.3 ± 1.3	0
11	59/F	GBM	Infiltr tumor	0.176	0.2 ± 0.1	6
12	48/M	GBM/high	Necr	0.022	0.0 ± 0.0	0
13*	69/F	GBM/high	Nonneopl	0.166	0.2 ± 0.2	0
14*	65/M	GBM	Nonneopl	0.018	0.0 ± 0.0	0
15	58/F	GBM	Nonneopl	0.013	0.1 ± 0.0	0
16	52/F	GS/high	Vital tumor	0.214	7.3 ± 3.0	21
17*	26/F	GS	Necr	0.040	0.3 ± 0.2	0
18	42/M	AO/high	Vital tumor	0.035	0.8 ± 0.1	23
19	45/M	AOA/middle	a) Vital tumor	0.053	0.0 ± 0.0	10
			b) Nonneopl	0.043	0.0 ± 0.0	0
20*	53/M	AA/middle	Vital tumor	0.071	0.0 ± 0.0	9
21	38/M	AA/middle–high	Vital tumor	0.064	0.1 ± 0.0	0
22	66/M	AG/middle	Nonneopl	0.036	0.0 ± 0.0	0

AA = anaplastic astrocytoma grade III; AG = anaplastic ganglioglioma grade III; AO = anaplastic oligodendroglioma grade III; AOA = anaplastic oligoastrocytoma grade III; GBM = glioblastoma multiforme grade IV; GS = gliosarcoma grade IV; nonneopl = nonneoplastic tissue; necr = necrosis, TCD = tumor cell density. *Primary tumor.

procedure described above. Known amounts of PpIX (Sigma Aldrich GmbH, Steinheim, Germany) from a Solvable-based stock solution with $c_{PpIX} = 10$ μM were added and the fluorescence intensity was analyzed as described above.

The nonparametric Mann–Whitney *U*-test was employed for testing statistical significance at the $P = 0.05$ level. The correlation coefficient was calculated as

$$r_{x,y} = \frac{\mathrm{cov}(x, y)}{\sigma_x \sigma_y}$$

where cov denotes the covariance and σ the standard deviation.

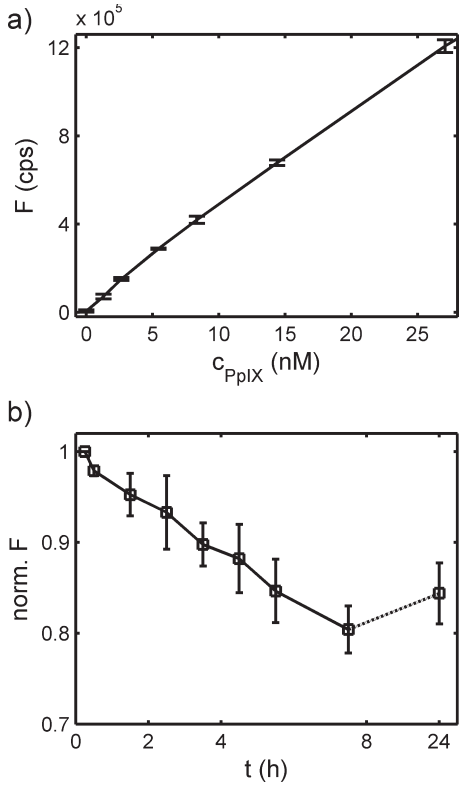

Figure 1. (a) Fluorescence intensity (cps) at 634 nm *versus* PpIX concentration resulting in an average $R^2 = 0.9974$. Error bars denote standard deviations resulting from three independent measurement series. (b) Fluorescence intensity as a function of immersion time in Solvable. Data have been normalized to the value at $t = 0$. Fluorescence data were acquired from a GBM with average $c_{PpIX} = 6.7$ μM.

RESULTS

Extraction procedure

Figure 1a shows the calibration curve relating fluorescence intensity, resulting from three independent measurements and expressed in cps, at 634 nm to absolute PpIX concentration. Figure 1b shows the PpIX fluorescence intensity as a function of the immersion time, postdilution, of GBM tissue in Solvable. Although the fluorescence intensity of PpIX in Solvable decreases with time, less than 5% variations were observed during the analysis procedure, *i.e.* within the first 2 h. The minimum detection limit for tissue samples weighing 0.02 g was *ca* 0.1 μM. Typically, the resulting c_{PpIX} varied by less than 10% between aliquots from the same tissue sample.

PpIX quantification

The average, sample-specific PpIX concentrations are listed in Table 1 and displayed in Fig. 2 as a bar plot. Each bar represents a separate tissue sample as obtained during the FGR procedure and numbers above the bars denote the number of subvolumes processed per tissue sample, *e.g.* as required to keep dissolved sample weight below 0.1 g or when separately analyzing heterogeneous structures. Error bars, indicating standard deviations, thus originate from spatial differences in PpIX accumulation but also to a minor part from variations between the three aliquots employed in the dilution procedure. The results indicate large intra- and interpatient variability of PpIX uptake. Particularly large is the intratumor heterogeneity for patients 3, 4, 10 and 16. As the extraction procedure requires relatively large tissue samples, the resulting PpIX concentration represents an average over a tissue volume possibly containing varying

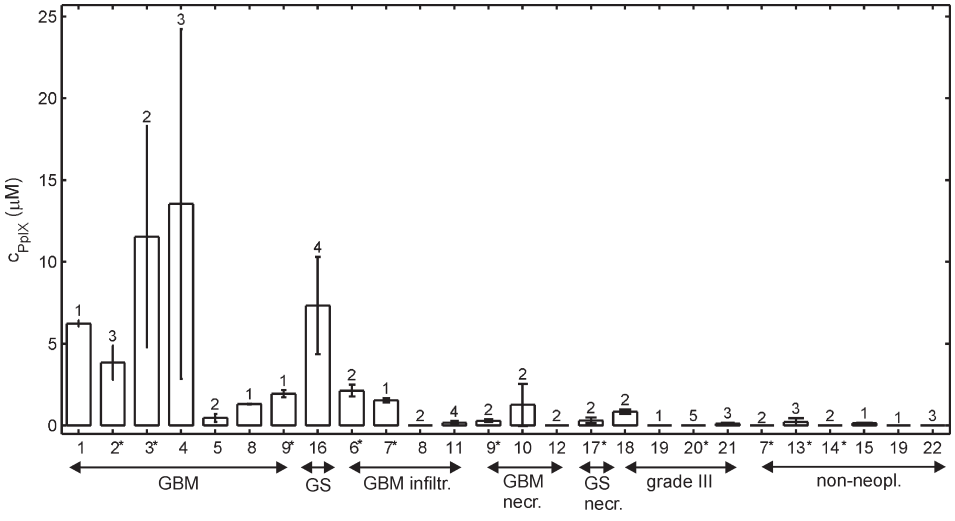

Figure 2. The absolute PpIX concentration for each patient. Primary tumors are indicated by *. Indicated are also the number of tissue samples analyzed and the corresponding standard deviations.

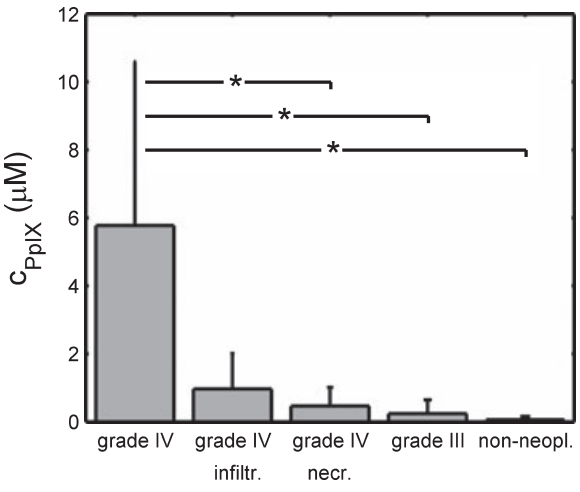

Figure 3. The PpIX concentration as averaged for each diagnosis. Error bars denote standard deviations and * indicates statistically significant differences in PpIX concentration at the $P = 0.05$ level.

TCD and cell viability. For patients where two samples were analyzed, *e.g.* patients 7, 8, 9 and 19, it is possible that no single sample represented only the one or the other tissue type, thus explaining the lower uptake in the malignant samples for these patients. For vital grade III and IV tumors a higher PpIX accumulation was observed for high TCD as compared with samples presenting lower TCD, infiltrating tumor cells or necrotic regions. From this study one cannot conclude what is the cell-to-cell variation of PpIX uptake and whether it is cancer cell specific. PpIX levels in nonneoplastic samples were undetectable with the exception of patients 13 and 15. For these patients, the presence of PpIX might be due to smaller regions with GBM tissue not present in the subvolumes investigated by H&E staining. The correlation coefficient between c_{PpIX} and the Ki67 labeling index was 0.78.

Water-soluble porphyrins, such as uro- and coproporphyrin, were observed *via* fluorescence between 610 and 620 nm for patients 5, 9, 17 and 20. The presence of these fluorescence components was also associated with relatively low PpIX uptake.

The diagnosis-specific PpIX concentration is shown in Fig. 3. The PpIX concentration was 5.8 ± 4.8 μM (mean ± SD, range: 0–28.2 μM) for vital grade IV tumors, *i.e.* GBM and GS with high TCD, 1.0 ± 1.0 μM (mean ± SD, range: 0–2.5 μM) for infiltrating grade IV tumors, 0.5 ± 0.5 μM (mean ± SD, range: 0–2.3 μM) for grade IV tumors with necrotic parts and 0.2 ± 0.4 μM (mean ± SD, range: 0–0.9 μM) for grade III tumors, *i.e.* AA, AO, AOA and AG. The median PpIX uptake was below the actual detection limit for nonneoplastic tissue. Hence, the PpIX uptake seems to correlate with tissue malignancy. The Mann–Whitney *U*-test indicated significant differences between vital grade IV tumors and grade III tumors, necrotic parts of grade IV tumors as well as nonneoplastic brain tissue. No statistically significant differences could be observed between primary and recurrent GBM or GS.

DISCUSSION

ALA-induced PpIX has been successfully employed for FGR of human malignant gliomas, resulting in improved treatment outcome as compared with surgery performed under white light alone (11). Furthermore, ALA-mediated brain-PDT is currently being investigated and initial clinical trials have shown promising results in terms of survival (13,17,18). Here, we have investigated the absolute PpIX concentration in brain tissues following oral ALA administration at 20 mg kg^{-1} b.w. with the motivation to elucidate whether ALA-induced PpIX levels are sufficient for an effective PDT.

The Solvable-based solubilization process was easily implemented and was characterized by low cost, good accuracy and high reproducibility. Evidence of chemical bleaching could be observed as the immersion time in Solvable was increased, in agreement with a previous report (26). However, for the time period relevant for the solubilization process the PpIX fluorescence displayed less than 5% variations. In agreement with the results published for meso-tetra(hydroxyphenyl)chlorin (mTHPC) quantification in rat liver tissue (26), the use of 100% Solvable during the entire solubilization process and proper subtraction of the autofluorescence component were necessary for obtaining sufficient accuracy and reproducibility. The light levels employed during FGR have been shown to induce only moderate photobleaching (27) and hence we did not consider any decrease in PpIX levels due to the FGR procedure. The assumption of no pronounced photobleaching was supported by the absence of photoproduct fluorescence around 670 nm both in dissolved tissue and within intact tissue as measured *via* fiber-based fluorescence spectroscopy (data not shown).

The absolute PpIX concentration was found to range between 0 and 28.2 μM in the human brain tissue samples investigated. Large variations were observed within tumors as well as with respect to individual patients and diagnoses. This variability is expected due to the natural heterogeneity in malignant tissue with neighboring vital, necrotic and infiltrating tumor parts. In this study, significantly higher PpIX levels were observed in vital grade IV tumors as compared with grade III tumors. Moreover, within grade IV tumors, PpIX levels varied significantly between different tumor areas; the highest PpIX concentrations were observed within vital tumor parts, followed by infiltration zones adjacent to normal brain tissue and necrotic areas. The PpIX fluorescence has previously been observed to increase with tumor grade as well as with TCD (27,28). In agreement with these publications, our study also indicated lower average PpIX concentration within infiltrating tumor tissue as compared with vital grade IV tumors. However, the differences were not statistically significant as might be explained by the heterogeneity of the tissue. Provided that PpIX uptake is tumor cell selective, the varying TCD in infiltration zones makes the PpIX distribution very patchy on a microscopic scale. The extraction procedure allowed characterization of the PpIX concentration only on a macroscopic scale and hence these cell-to-cell variations remain unknown.

Undetectable or only very low PpIX levels were found in nonneoplastic brain tissue, an observation in agreement with previous fluorescence spectroscopy studies (29). Others have detected PpIX fluorescence from outside tumor tissue for recurrent malignant gliomas and metastatic brain tumors, where also edema, inflammatory cells and infiltrating astrocytes could be observed (28). That study unfortunately did not provide any information on the absolute PpIX concentration

and hence it is difficult to put these observations in relation to the minimum detection limit of our extraction protocol. The low but detectable PpIX levels for Patients 13 and 15, both diagnosed as GBM on the routine histopathological analysis but showing nonneoplastic tissue in the sample site, might possibly be due to edema-induced leakage of PpIX from tumor into surrounding tissue as previously proposed (28,30). Furthermore, sampling error cannot be ruled out completely due to the tissue acquisition and analysis procedure.

Our results also show that the low PpIX fluorescence typically observed *in vivo* from dark-appearing, necrotic tissue is to a great extent due to true concentration variations. This observation is in agreement with previous reports, where, *e.g.* no PpIX fluorescence could be observed from necrotic tumor regions during FGR of GBM (29). A correlation between PpIX fluorescence and tissue proliferation status, as indicated by the MIB-1 labeling index, has been reported (24), indicating the importance of cell proliferation activity for ALA-to-PpIX conversion. This observation was confirmed in our study by the significant correlation between the absolute PpIX concentration and the Ki67 labeling index. Interestingly, the presence of fluorescence peaks between 610 and 620 nm was associated with low PpIX uptake in our study. Reduced mitochondrial viability has been reported to lead to the induction of water-soluble porphyrins *in vivo* following ALA administration (31), possibly indicating reduced cell viability within the tissue samples of patients 5, 9, 17 and 20.

Taken together, investigations of the PpIX uptake in relation to local TCD and cell viability on the microscopic scale are warranted. Only by such studies the possibility of sensitizing individual tumor cells that infiltrate normal, surrounding tissue as well as the risk of unintentionally sensitizing normal, surrounding brain tissue can be judged.

Reports on absolute PpIX concentration in relation to the resulting PDT effect in human tissues are rare. For various human skin malignancies, topical application of ALA has been reported to result in c_{PpIX} = 1–2 μM (32). As that study employed the same ALA administration procedure as used conventionally (4–6 h application times of 20% ALA in ointment) for ALA-mediated skin-PDT (33), PpIX levels in this range seem sufficient for PDT of superficial skin malignancies when irradiated at 75 J cm^{-2}. Similarly, oral ALA administration (30–50 mg kg^{-1} b.w.) has been reported to induce c_{PpIX} = 2–9 μM in human Barrett's esophagus (34). The subsequent irradiation with 100–200 J cm^{-2} at 635 nm has been employed for efficient PDT (35). Studies in various animal tumor models contain more comparative data on absolute PpIX levels and subsequent PDT efficacy. For example, in the 9L gliosarcoma rat brain tumor model, repetitive ALA administration was shown to induce PpIX levels in the 2–5 μM range, a photosensitizer concentration that also led to pronounced tissue damage following interstitial irradiation with 50 J (36). PpIX concentrations between 10 and 20 μM have been observed in rat stomach (37), where PDT at 50 J was also shown to induce significant PDT damage (38). PpIX levels in murine and rat tumor models in the range of 1–10 μM are generally sufficient for inducing phototoxic effects (see *e.g.* 39–41).

The PpIX levels observed within vital grade IV malignancies in this study are thus in the range previously shown sufficient for PDT-induced tissue damage. Of course, one needs to be careful in extrapolating the results from human skin and Barrett's esophagus and from various animal tumor models to human malignant gliomas. For an effective PDT, it is also crucial to ascertain a sufficient light dose and oxygen supply. In this respect, hypoxic regions, areas of spontaneous necrosis and tumor infiltration zones might require special consideration. The varying PpIX levels observed between patients and within tumor samples indicate that PDT dosimetry based solely on the administered light and drug doses is insufficient for predicting and/or controlling the therapeutic outcome. Although the bulk average PpIX concentration of infiltrating tumor tissue seems to be insufficient for PDT, it remains to be elucidated whether the uptake in individual infiltrating tumor cells is enough to selectively target the malignant cells within the infiltration zones.

In summary, large intertumoral variations of PpIX uptake following oral ALA administration were evident as well as large differences between solid, necrotic and infiltrating tumor parts. For vital grade IV tumors, the PpIX concentrations as averaged over the bulk of the tissue sample were in the range previously shown sufficient for PDT-induced tissue damage following irradiation. Grade III, nonneoplastic samples as well as grade IV tumors with mainly necrotic parts exhibited significantly lower PpIX uptake. It remains to be elucidated whether PpIX levels in lower-grade brain tumors, infiltrating tumor tissue and higher-grade tumors with significant necrotic volumes are sufficient for an effective PDT.

Acknowledgements—This work was financially supported by the Alexander von Humboldt Foundation, the German Ministry of Education and Research (project Neurotax, grant 13N10172) and by means of the local organizational framework of the German Glioma Network (GGN). A. Henn is gratefully acknowledged for her support in preparing samples for the histological analysis.

REFERENCES

1. Ohgaki, H. (2009) Epidemiology of brain tumors. *Methods Mol. Biol.* **472**, 323–342.
2. Claes, A., A. J. Idema and P. Wesseling (2007) Diffuse glioma growth: A guerilla war. *Acta Neuropathol.* **114**, 443–458.
3. Drappatz, J., A. D. Norden and P. Y. Wen (2009) Therapeutic strategies for inhibiting invasion in glioblastoma. *Expert. Rev. Neurother.* **9**, 519–534.
4. Omay, S. B. and M. A. Vogelbaum (2009) Current concepts and newer developments in the treatment of malignant gliomas. *Indian J. Cancer* **46**, 88–95.
5. Peng, Q., K. Berg, J. Moan, M. Kongshaug and J. M. Nesland (1997) 5-Aminolevulinic acid-based photodynamic therapy: Principles and experimental research. *Photochem. Photobiol.* **65**, 235–251.
6. Stepp, H., T. Beck, T. Pongratz, T. Meinel, F. W. Kreth, J. C. Tonn and W. Stummer (2007) ALA and malignant glioma: Fluorescence-guided resection and photodynamic treatment. *J. Environ. Pathol. Toxicol. Oncol.* **26**, 157–164.
7. El-Sharabasy, M. M., A. M. El-Waseef, M. M. Hafez and S. A. Salim (1992) Porphyrin metabolism in some malignant diseases. *Br. J. Cancer* **65**, 409–412.
8. Kaneko, S. (2009) Photodynamic medicine in malignant gliomas: Focus on PpIX accumulation in malignant glioma tissues. In *Photodynamic Therapy: Back to the Future* (Edited by D. Kessel). Proceedings of SPIE, SPIE, Bellingham, WA.
9. Collaud, S., A. Juzeniene, J. Moan and N. Lange (2004) On the selectivity of 5-aminolevulinic acid-induced protoporphyrin IX formation. *Curr. Med. Chem. Anticancer Agents* **4**, 301–316.
10. Ennis, S. R., A. Novotny, J. Xiang, P. Shakui, T. Masada, W. Stummer, D. E. Smith and R. F. Keep (2003) Transport of

5-aminolevulinic acid between blood and brain. *Brain Res.* **959**, 226–234.
11. Stummer, W., U. Pichlmeier, T. Meinel, O. D. Wiestler, F. Zanella and H. J. Reulen (2006) Fluorescence-guided surgery with 5-aminolevulinic acid for resection of malignant glioma: A randomised controlled multicentre phase III trial. *Lancet Oncol.* **7**, 392–401.
12. Widhalm, G., S. Wolfsberger, G. Minchev, A. Woehrer, M. Krssak, T. Czech, D. Prayer, S. Asenbaum, J. A. Hainfellner and E. Knosp (2010) 5-Aminolevulinic acid is a promising marker for detection of anaplastic foci in diffusely infiltrating gliomas with nonsignificant contrast enhancement. *Cancer* **116**, 1545–1552.
13. Beck, T. J., F. W. Kreth, W. Beyer, J. H. Mehrkens, A. Obermeier, H. Stepp, W. Stummer and R. Baumgartner (2007) Interstitial photodynamic therapy of nonresectable malignant glioma recurrences using 5-aminolevulinic acid induced protoporphyrin IX. *Lasers Surg. Med.* **39**, 386–393.
14. Kostron, H. (2010) Photodynamic diagnosis and therapy and the brain. In *Photodynamic Therapy; Methods and Protocols* (Edited by C. J. Gomer), pp. 261–280. Humana Press, New York.
15. Stepp, H., T. Beck, W. Beyer, T. Pongratz, R. Sroka, R. Baumgartner, W. Stummer, B. Olzowy, J. Mehrkens, J. C. Tonn and H. J. Reulen (2005) Fluorescence-guided resections and photodynamic therapy for malignant gliomas using 5-aminolevulinic acid. In *Photonic Therapeutics and Diagnostics*, Vol. 5686 (Edited by K. E. Bartels, L. S. Bass, W. T. W. de Riese, K. W. Gregory, H. Hirschberg, A. Katzir, N. Kollias, S. J. Madsen, R. S. Malek, K. M. McNally-Heintzelman, L. P. Tate, Jr., E. A. Trowers and B. J.-F. Wong), pp. 547–557. Proceedings of SPIE, SPIE, Bellingham, WA.
16. Eljamel, M. S., C. Goodman and H. Moseley (2008) ALA and Photofrin fluorescence-guided resection and repetitive PDT in glioblastoma multiforme: A single centre Phase III randomised controlled trial. *Lasers Med. Sci.* **23**, 361–367.
17. Johansson, A., F. W. Kreth, W. Stummer and H. Stepp (2009) Interstitial photodynamic therapy of brain tumours. *IEEE JSTQE* **16**(4), 841–853.
18. Stummer, W., T. Beck, W. Beyer, J. H. Mehrkens, A. Obermeier, N. Etminan, H. Stepp, J. C. Tonn, R. Baumgartner, J. Herms and F. W. Kreth (2008) Long-sustaining response in a patient with non-resectable, distant recurrence of glioblastoma multiforme treated by interstitial photodynamic therapy using 5-ALA: Case report. *J. Neurooncol.* **87**, 103–109.
19. Beck, T. J., W. Beyer, T. Pongratz, W. Stummer, R. Waidelich, H. Stepp, S. Wagner and R. Baumgartner (2003) Clinical determination of tissue optical properties *in vivo* by spatially resolved reflectance measurements. In *Photon Migration and Diffuse-Light Imaging*, Vol. 5138 (Edited by David A. Boas), pp. 96–105. Proceedings of SPIE, SPIE, Bellingham, WA.
20. Muller, P. J. and B. C. Wilson (1986) An update on the penetration depth of 630 nm light in normal and malignant human brain tissue *in vivo*. *Phys. Med. Biol.* **31**, 1295–1297.
21. Stylli, S. S., M. Howes, L. MacGregor, P. Rajendra and A. H. Kaye (2004) Photodynamic therapy of brain tumours: Evaluation of porphyrin uptake versus clinical outcome. *J. Clin. Neurosci.* **11**, 584–596.
22. Laubach, H. J., S. K. Chang, S. Lee, I. Rizvi, D. Zurakowski, S. J. Davis, C. R. Taylor and T. Hasan (2008) In-vivo singlet oxygen dosimetry of clinical 5-aminolevulinic acid photodynamic therapy. *J. Biomed. Opt.* **13**, 050504.
23. Castano, A. P., P. Mroz and M. R. Hamblin (2006) Photodynamic therapy and anti-tumour immunity. *Nat. Rev. Cancer* **6**, 535–545.
24. Ishihara, R., Y. Katayama, T. Watanabe, A. Yoshino, T. Fukushima and K. Sakatani (2007) Quantitative spectroscopic analysis of 5-aminolevulinic acid-induced protoporphyrin IX fluorescence intensity in diffusely infiltrating astrocytomas. *Neurol. Med Chir. (Tokyo)* **47**, 53–57.
25. Lilge, L., C. O'Carroll and B. C. Wilson (1997) A solubilization technique for photosensitizer quantification in ex vivo tissue samples. *J. Photochem. Photobiol. B, Biol.* **39**, 229–235.
26. Kascakova, S., B. Kruijt, H. S. de Bruijn, A. van der Ploeg-van den Heuvel, D. J. Robinson, H. J. Sterenborg and A. Amelink (2008) Ex vivo quantification of mTHPC concentration in tissue: Influence of chemical extraction on the optical properties. *J. Photochem. Photobiol. B, Biol.* **91**, 99–107.
27. Stummer, W., S. Stocker, S. Wagner, H. Stepp, C. Fritsch, C. Goetz, A. E. Goetz, R. Kiefmann and H. J. Reulen (1998) Intraoperative detection of malignant gliomas by 5-aminolevulinic acid-induced porphyrin fluorescence. *Neurosurgery* **42**, 518–526.
28. Utsuki, S., H. Oka, S. Sato, S. Shimizu, S. Suzuki, Y. Tanizaki, K. Kondo, Y. Miyajima and K. Fujii (2007) Histological examination of false positive tissue resection using 5-aminolevulinic acid-induced fluorescence guidance. *Neurol. Med. Chir. (Tokyo)* **47**, 210–213.
29. Stummer, W., A. Novotny, H. Stepp, C. Goetz, K. Bise and H. J. Reulen (2000) Fluorescence-guided resection of glioblastoma multiforme by using 5-aminolevulinic acid-induced porphyrins: A prospective study in 52 consecutive patients. *J. Neurosurg.* **93**, 1003–1013.
30. Madsen, S. J., E. Angell-Petersen, S. Spetalen, S. W. Carper, S. A. Ziegler and H. Hirschberg (2006) Photodynamic therapy of newly implanted glioma cells in the rat brain. *Lasers Surg. Med.* **38**, 540–548.
31. Dietel, W., C. Fritsch, R. H. Pottier and R. Wendenburg (1997) 5-Aminolaevulinic-acid-induced formation of different porphyrins and the photomodifications. *Lasers Med. Sci.* **12**, 226–236.
32. Fritsch, C., P. Lehmann, W. Stahl, K. W. Schulte, E. Blohm, K. Lang, H. Sies and T. Ruzicka (1999) Optimum porphyrin accumulation in epithelial skin tumours and psoriatic lesions after topical application of delta-aminolaevulinic acid. *Br. J. Cancer* **79**, 1603–1608.
33. Peng, Q., T. Warloe, K. Berg, J. Moan, M. Kongshaug, K. E. Giercksky and J. M. Nesland (1997) 5-Aminolevulinic acid-based photodynamic therapy. Clinical research and future challenges. *Cancer* **79**, 2282–2308.
34. Ackroyd, R., N. Brown, D. Vernon, D. Roberts, T. Stephenson, S. Marcus, C. Stoddard and M. Reed (1999) 5-Aminolevulinic acid photosensitization of dysplastic Barrett's esophagus: A pharmacokinetic study. *Photochem. Photobiol.* **70**, 656–662.
35. Claydon, P. E. and R. Ackroyd (2004) 5-Aminolaevulinic acid-induced photodynamic therapy and photodetection in Barrett's esophagus. *Dis. Esophagus* **17**, 205–212.
36. Bisland, S. K., L. Lilge, A. Lin, R. Rusnov and B. C. Wilson (2004) Metronomic photodynamic therapy as a new paradigm for photodynamic therapy: Rationale and preclinical evaluation of technical feasibility for treating malignant brain tumors. *Photochem. Photobiol.* **80**, 22–30.
37. Loh, C. S., D. Vernon, A. J. MacRobert, J. Bedwell, S. G. Bown and S. B. Brown (1993) Endogenous porphyrin distribution induced by 5-aminolaevulinic acid in the tissue layers of the gastrointestinal tract. *J. Photochem. Photobiol. B* **20**, 47–54.
38. Loh, C. S., J. Bedwell, A. J. MacRobert, N. Krasner, D. Phillips and S. G. Bown (1992) Photodynamic therapy of the normal rat stomach: A comparative study between di-sulphonated aluminium phthalocyanine and 5-aminolaevulinic acid. *Br. J. Cancer* **66**, 452–462.
39. Peng, Q., J. Moan, T. Warloe, J. M. Nesland and C. Rimington (1992) Distribution and photosensitizing efficiency of porphyrins induced by application of exogenous 5-aminolevulinic acid in mice bearing mammary carcinoma. *Int. J. Cancer* **52**, 433–443.
40. Hua, Z., S. L. Gibson, T. H. Foster and R. Hilf (1995) Effectiveness of delta-aminolevulinic acid-induced protoporphyrin as a photosensitizer for photodynamic therapy in vivo. *Cancer Res.* **55**, 1723–1731.
41. Van Hillegersberg, R., J. M. Hekking-Weijma, J. H. Wilson, A. Edixhoven-Bosdijk and W. J. Kort (1995) Adjuvant intraoperative photodynamic therapy diminishes the rate of local recurrence in a rat mammary tumour model. *Br. J. Cancer* **71**, 733–737.

Protoporphyrin IX fluorescence and photobleaching during interstitial photodynamic therapy of malignant gliomas for early treatment prognosis

Ann Johansson, Florian Faber, Gesa Kniebühler, Herbert Stepp, Ronald Sroka, Rupert Egensperger, Wolfgang Beyer, Friedrich-Wilhelm Kreth

Lasers in Surgery and Medicine 2013

Protoporphyrin IX Fluorescence and Photobleaching During Interstitial Photodynamic Therapy of Malignant Gliomas for Early Treatment Prognosis

Ann Johansson, PhD,[1†] Florian Faber, MD,[2†] Gesa Kniebühler, Dipl.-Phys.,[1] Herbert Stepp, PhD,[1] Ronald Sroka, PhD,[1] Rupert Egensperger, MD,[3] Wolfgang Beyer, PhD,[1*] and Friedrich-Wilhelm Kreth, MD[2*]

[1]*Laser-Forschungslabor, University Hospital of Munich, Marchioninistraße 23, 81377 Munich, Germany*

[2]*Department of Neurosurgery, University Hospital of Munich, Marchioninistraße 15, 81377 Munich, Germany*

[3]*Center of Neuropathology and Prion Research, University Hospital of Munich, Feodor-Lynen-Straße 23, 81377 Munich, Germany*

Background and Objective: Interstitial photodynamic therapy (iPDT) of non-resectable recurrent glioblastoma using 5-aminolevulinic acid (ALA)-induced protoporphyrin IX (PpIX) has shown a promising outcome. It remained unclear, however, to what extent inter- and intra-tumoural differences of PpIX concentrations influence the efficacy of iPDT. In the current pilot study, we analysed PpIX concentrations quantitatively and assessed PpIX induced fluorescence and photobleaching intraoperatively.

Materials and Methods: Five patients harbouring non-resectable glioblastomas were included. ALA (20 or 30 mg/kg body weight) was given 5–8 hours before treatment. Stereotactic biopsies were taken throughout the tumour volume for both histological analysis and determination of PpIX concentrations, which were measured by chemical extraction. Cylindrical light diffusors were stereotactically implanted. Prior to and after irradiation, fluorescence measurements were performed. Outcome measurement was based on clinical and neuro-radiological follow up.

Results: In three patients, a strong PpIX fluorescence was seen before treatment, which was completely photobleached after iPDT. High concentrations of PpIX could be detected in viable tumour parts of these patients (mean PpIX uptake per tumour: 1.4–3.0 μM). In the other two patients, however, no or only low PpIX uptake (0–0.6 μM) could be detected. The patients with strong PpIX uptake showed treatment response and long-term clinical stabilisation (no progression in 29, 30 and 36 months), early treatment failure was seen in the remaining two patients (death after 3 and 9 months).

Conclusions: Intra-tumoural PpIX concentrations exhibited pronounced inter- and intra-tumoural variations in glioblastoma, which are directly linked to variable degrees of fluorescence intensity. High intra-tumoural PpIX concentrations with strong fluorescence intensity and complete photobleaching after iPDT seem to be associated with favourable outcome. Real-time monitoring of PpIX fluorescence intensity and photobleaching turned out to be feasible and safe and might be employed for early treatment prognosis of iPDT. Lasers Surg. Med.

Key words: 5-aminolevulinic acid (ALA); absolute protoporphyrin IX concentration; fluorescence spectroscopy; photobleaching; glioblastoma

[†]These authors contributed equally to this work.

Authors' Contribution: Ann Johansson—former physicist in the Laser-Forschungslabor, designed and developed the methods for measuring PpIX concentration as well as fluorescence and bleaching, performed measurement and primary evaluation of spectra, wrote first manuscript versions. Florian Faber—resident in neurosurgery, medical assistant in operating theatre and in stereotactic treatment planning, collected and evaluated the clinical data, and was involved in manuscript writing. Gesa Kniebühler—physicist in the Laser-Forschungslabor, performed measurements of the absolute concentrations of PpIX in biopsies. Herbert Stepp—physicist in the Laser-Forschungslabor, contributed to the treatment concept and manuscript writing. Ronald Sroka—head of the Laser-Forschungslabor, contributed to the treatment concept and manuscript writing. Rupert Egensperger—resident in neuropathology, was responsible for histopathological analysis of biopsy samples. Wolfgang Beyer—physicist in the Laser-Forschungslabor, performed light dosimetry and irradiation, evaluation of spectral measurements, and contributed to manuscript writing. Friedrich-Wilhelm Kreth—leader of the stereotactic section of the neurosurgical department, was the leading medical doctor performing patient acquirement, stereotactic treatment planning, fibre placement, and contributed to manuscript writing.

Conflict of Interest Disclosures: All authors have completed and submitted the ICMJE Form for Disclosure of Potential Conflicts of Interest and have disclosed the following: [Ann Johansson was sponsored by the Alexander von Humboldt-Foundation.].

Contract grant sponsor: German Ministry of Education and Research (project Neurotax); Contract grant number: 13N10172; Contract grant sponsor: Photonamic GmbH (Wedel, Germany).

*Corresponding to: Dr. Wolfgang Beyer, Laser-Forschungslabor, University Hospital of Munich, Marchioninistraße 23, 81377 Munich, Germany.
E-mail: wolfgang.beyer@med.uni-muenchen.de
and Prof. Dr. Friedrich-Wilhelm Kreth, Department of Neurosurgery, Ludwig-Maximilians-University, Klinikum Großhadern, Marchioninistraße 15, 81377 Munich, Germany.
E-mail: friedrich-wilhelm.kreth@med.uni-muenchen.de

Accepted 15 February 2013
Published online in Wiley Online Library (wileyonlinelibrary.com).
DOI 10.1002/lsm.22126

INTRODUCTION

Glioblastoma multiforme (GBM) is the most malignant human brain tumour. Modern standard treatment, which includes surgery in combination with external beam radiation plus concomitant and adjuvant temozolomide chemotherapy, has significantly improved survival time (median: 15 months). Moreover, silencing of the DNA repair enzyme *O*(6)-methylguanine-DNA methyltransferase (*MGMT*) has been shown to be associated with an additional approximately twofold median survival advantage after radiochemotherapy. Overall, however, the prognosis for patients with GBM is still dismal. Even though glioblastomas are tumours, which widely infiltrate the surrounding brain parenchyma, localised treatment strategies such as open tumour resection have been shown to be beneficial for selected patients [1]. Given the fact that not all patients are suitable for open tumour resection because of an unfavourable (risky) tumour location and/or significant co-morbidity, alternative treatments, such as stereotactic radiotherapy or interstitial laser-thermotherapy might be employed. Stereotactic iPDT has shown initial promising results [2], tempting us to further develop and improve this alternative method for selected cases.

PDT relies on the light-induced activation of a photosensitiser and the subsequent formation of different reactive radicals and oxygen species, which in turn cause cellular damage. Since its clinical introduction in 1980 for the treatment of human brain malignancies, hematoporphyrin derivative (HpD) and its purified versions photofrin and photosan, also referred to as first generation photosensitisers, have been the most commonly employed photosensitisers for brain-PDT [3–5]. Whereas the therapeutic irradiation is most often applied within the surgical cavity following resection [5,6], interstitial PDT (iPDT) relies on thin optical fibres being inserted into the tumour mass [3,5,7–9].

In an effort to circumvent the risks associated with the use of the first generation photosensitisers, studies employing 5-aminolevulinic acid (ALA) for iPDT have been carried out at the University Hospital of Munich. ALA is a pre-cursor that is converted into the actual photosensitiser, protoporphyrin IX (PpIX), as a part of the endogenous heme-synthesis [10]. Oral ALA administration leads to high tumour-selective PpIX accumulation [11] and shorter time periods of general photosensitisation as compared to HpD and photofrin. Generally, the selectivity is explained by a decreased ferrochelatase activity within cancer cells, thus limiting the conversion efficiency of PpIX to heme [12] and an increased activity of the rate limiting enzyme porphobilinogen deaminase (PBGD) in tumour tissue [13]. The limited ability of ALA to penetrate the intact blood brain barrier (BBB) also contributes to the tumour-selective PpIX uptake [14]. In a feasibility study, 10 patients suffering from recurrent GBM were treated by means of ALA-mediated iPDT [2]. In that study, we aimed at administering a light dose exceeding the pre-determined threshold dose to the entire target volume without considering variations in light distribution, initial PpIX concentration and oxygen availability during iPDT. Such a dosimetry model might be justifiable, if the photosensitiser displays good tumour selectivity as discussed in Ref. 15 and if photosensitiser and oxygen concentrations pose no limitation. The patients treated with iPDT in that study had a median survival of 15 months. Four patients lived longer than 24 months, two of them longer than 48 months [2] and one of them [16] was still alive at the last follow-up at 7 years. However, a third of the patients did suffer early progression. Partly, this may be attributed to the fact that the current dosimetry models of iPDT rely only on the delivered light and photosensitiser, but patient-specific, spatially- and time-dependent variations of light, photosensitiser and oxygen distributions are not considered [15]. Further reasons for the large heterogeneity in treatment response, including the occurrence of long-term survivors as well as early treatment failures, might be the variability of light distribution, differences in photosensitiser accumulation [8,17] and different synergism between iPDT and the immune response [18]. Further, iPDT could induce changes in tissue oxygenation and blood flow [19].

Hence, increasing effort has been undertaken to implement real-time treatment monitoring during iPDT. In the explicit dosimetry model one aims at separately monitoring the light, photosensitiser and tissue oxygenation levels [20–22]. In contrast to this, the implicit dosimetry model aims at tracking one single parameter, such as the photosensitiser photobleaching kinetics, that implicitly contains information on the total PDT dose [23]. This model relies on the assumption that PDT-induced singlet oxygen causes tissue damage as well as photodegradation of the photosensitiser. The usefulness of an implicit dosimetry model has been confirmed in pre-clinical models [24,25] as well as for human skin-PDT [26,27] where a rapid photobleaching has been shown to correlate with improved treatment outcome. Speculatively, the PpIX-specific photobleaching kinetics might be employed for early treatment prognosis and to assure the application of a sufficient light dose in order to improve treatment efficacy [28].

With the aim to investigate possible reasons for the observed variability in treatment response to brain-iPDT, we analysed patient-specific photosensitiser accumulation and photobleaching. Here, we present a clinical procedure for iPDT with parallel, minimally invasive spectroscopic monitoring of both, PpIX fluorescence intensity and photobleaching efficiency. The PpIX-specific fluorescence measured *in vivo* is compared to the absolute PpIX concentration as quantified in tissue biopsies obtained prior to iPDT. The patient-specific PpIX uptake and photobleaching are put in relation to the patient-specific histopathology and to the iPDT-induced changes on early magnetic resonance imaging (MRI) data. We further linked these findings to the clinical outcome of the investigated patients. Finally, we speculate on the use of *in vivo*, real-time spectroscopic monitoring as a tool for early treatment prognosis along the lines of an implicit dosimetry model.

PATIENTS AND METHODS

Patient Selection

Adult patients with a circumscribed glioblastoma with a maximum diameter of 3 cm as defined by gadolinium enhanced T1 weighted MRI and a Karnofsky Performance Status (KPS) of at least 70 were considered eligible for the study. A confirmatory stereotactic biopsy was performed for all patients as detailed below. All patients gave written informed consent. The prospective study protocol allowing spectroscopic and molecular-genetic analyses of tissue samples, which were collected by stereotactic biopsy before iPDT, was reviewed and approved by the institutional review board of the Ludwig-Maximilians-University, Munich, Germany (AZ 216/14).

Stereotactic Treatment Planning

Treatment planning was based on multi-modal imaging data. Image fusion of the stereotactically localised computerised tomography (CT; contrast enhanced scans, 2 mm slices), with additional MRIincluding gadolinium enhanced T1-(1 mm slices) and T2-weighted scans (2 mm slices), and *O*-(2-[^{18}F]fluoroethyl)-1-tyrosine (^{18}FET)-Positron Emission Tomography (PET) scans were acquired for optimal visualisation of the tumour and to define the treatment volume (Image Fusion Software, BrainLAB AG, Heimstetten, Germany). Irradiation planning was performed with the @target 1.19 software (BrainLAB AG). The positions of the therapeutic light sources were determined by manually optimising overlap between tumour and treatment volumes while at the same time guaranteeing a minimum source separation of 8 mm. Here, treatment volume was defined as the iso-dose curve at 1,870 J/cm^2 (assuming absorption, μ_a, and reduced scattering, μ_s', coefficients of 0.2 and 20 cm^{-1}, respectively). Further details on the treatment planning procedure can be found in [2].

Molecular Stereotactic Biopsy Technique

The intended drug dose was 30 mg/kg body weight ALA (medac GmbH, Wedel, Germany) dissolved in 100 ml water and applied orally. The dose used for fluorescence guided open resection of glioblastomas is 20 mg/kg which has been shown to be well tolerated by the patients [11]. Other groups, however, have used higher ALA doses (in the range of 40–60 mg/kg) for PDT treatments of tumours of the urinary bladder [29] and oesophagus [30,31]. In the current study we decided to use a dose in between these extremes. For safety reasons this dose was further reduced to 20 mg/kg for Patent 1 as he had a small tumour with little necrosis, see further Table 2. All patients were treated under general anaesthesia. Intraoperatively, the oxygen saturation was set to 100% in order to prevent a possible lack of cellular oxygen due to oxygen consumption during the treatment. It has been shown that oxygen ventilation can significantly increase cerebral oxygen tension by approx. 60% in an animal model [32]. Glioblastomas exhibit significantly less oxygen tension than normal human brain [33]. According to these data it can be expected that ventilation with 100% O_2 also increases the local pO_2 within the GBM tissues. However, this assumption needs further elucidation. Immediately prior to iPDT a molecular serial stereotactic biopsy was performed as described previously [34]. In brief, co-registration of CT, MRI and FET–PET imaging (as described above) served for 3D visualisation of the tumour and simulation of the optimal trajectory. Serial biopsies were taken along this trajectory in 1 mm steps. Using microforceps, the maximum amount of tissue per biopsy specimen was 1 mm^3. The tissue sampling procedure was guided by intra-operative smear preparations, routinely performed by the attending neuropathologist, and guaranteed sampling of both the solid and necrotic tumour volumes. Tissue probes were employed for histopathological examination, including the tumour cell density (TCD), the tumour proliferation status (via the Ki67 labelling index), for molecular-genetic analyses such as the determination of *O*(6)-methylguanine-DNA methyltransferase (*MGMT*) promoter methylation status (Table 1) and for PpIX extraction and quantification as described below.

TABLE 1. Patient Data

Patient	Age/sex	Diagnosis	Treatment history	TCD/Ki67(%)/*MGMT*	Tumour volume (cm^3)
1	42/M	prim. GBM	—	Medium/10/negative	1.5
2	48/M	rec. GBM	res, RCT, temozolomide	Low-medium/5/positive	10.0
3	50/M	rec. GBM	res, temozolomide, RCT, temozolomide	High/1/positive	1.7
4	76/M	rec. GBM	RCT	Medium/1/partially positive	7.0
5	50/F	rec. GBM	res + RT, res + RIT, temozolomide, seed implantation, temozolomide, seed implantation, Avastin-PC-chemotherapy	Medium/50/positive	9.4

Tumour volume was determined based on the fused MR (T1-weighted gadolinium-enhanced and T2-weighted) and CT images prePDT.

MGMT, methyl guanine methyl transferase; RCT, radiotherapy plus concomitant and adjuvant temozolomide; res, resection; RIT, radio-immuno therapy; RT, radiotherapy; TCD, tumour cell density.

TABLE 2. Treatment Details

Patient	Number biopsies PpIX/H&E	ALA (mg/kg b.w)	DLI (hours)	Number fibres	Light dose (J)	Source strength (mW/cm)	Source length (cm)
1	10/11*	20	8	4	5,760	200	2
2	6/6	30	5	6	12,960	150	2
3	3/5	30	5&6†	4	5,760	200	2
4	5/3	30	5	4	5,760	200	3
5	5/6	30	6	5	10,800	200	3

DLI, drug-light interval.
*Biopsies were obtained 1 day prior to PDT.
†Irradiation was performed in two consecutive sessions with two fibres active at a time.

Stereotactic Interstitial Photodynamic Therapy (iPDT)

The fibres for therapeutic light delivery consisted of four to six 600-μm diameter cylindrical diffusers (Fig. 1; Light Guide Optics, Rheinbach, Germany) with 20 or 30 mm length, see further Table 2. Diffusor length was at least equal to the tumour extension along the insertion trajectory. These fibres were inserted via a stereotactic approach, employing a modified Riechert-Mundinger stereotactic frame, and fibre positions were controlled via X-ray markers on the cylinders and an orthogonal C-arm. A multi-port laser system (≤4 ports, 635 nm, 2 W maximum output power per port, Ceralas PDT Diode Laser, biolitec AG, Jena, Germany) was used as the light source. For patients 2 and 5, the addition of a custom-made beam splitter unit allowed the use of six and five source fibres, respectively. Therapeutic irradiation was performed with a constant power of 150 or 200 mW/cm to a total delivered light dose of 720 J/cm per fibre. Due to different expenditure of time for stereotactic treatment planning and fibre placement, the irradiation occurred 5–8 hours after ALA administration. The PDT was supplemented with *in situ* spectroscopic measurements pre- and post-PDT as detailed below.

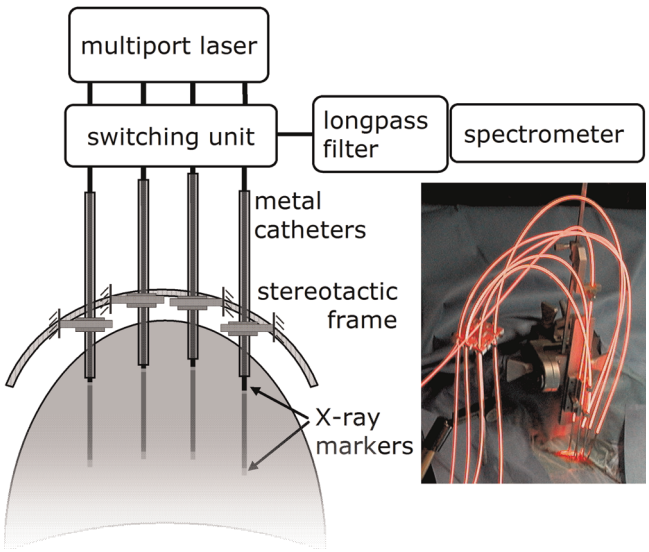

Fig. 1. Principal setup for iPDT of brain tumours with real-time spectroscopic monitoring. The switching unit controlled which fibre was employed as a detector fibre. Inset is a photograph of the clinical setting during iPDT where optical fibres, metal catheters and the fixation device onto the stereotactic frame can be seen.

Extraction Procedure

The biopsies collected for PpIX quantification were weighed, immersed in 1–2 ml solvable (Perkin Elmer LAS, Groningen, The Netherlands) and placed in a heated (45–50°) ultrasound bath until the tissue was completely dissolved. Care was taken to limit light exposure during the solubilisation process. Seven hundred microlitre of this solution were filled into a 2-mm optical path length quartz cuvette. Absorption spectra (λ = 350–750 nm, Lambda40, Perkin Elmer GmbH, Überlingen, Germany) were obtained and if necessary further dilution with solvable was performed to ascertain an optical density below 0.1. Fluorescence spectra were obtained from pure solvable and from dissolved tissue (λ_{exc} = 400 nm, λ_{em} = 450–780 nm, Fluoromax-2, Instruments S.A., Inc., Edison, NJ). Fluorescence from solvable and the autofluorescence of dissolved tissue was subtracted and the resulting fluorescence intensity, in counts per second (cps)/g tissue, at 632 nm was used to quantify the PpIX concentration, cPpIX. A calibration curve was obtained by adding known amounts of PpIX to dissolved GBM brain tissue obtained from a patient where white-light resection had been performed without ALA administration. The procedure is detailed in Ref. 8.

In Vivo Spectroscopy

In situ spectroscopic measurements of the light transmission between therapeutic fibres were performed prior to and post-iPDT via the setup illustrated in Figure 1. Sequentially, each fibre was set to emit 200 mW/cm at 635 nm and each of the remaining fibres was employed to detect the light transmission between 630 and 800 nm. An optical switch (MPM-2000, Mikropack, Ostfildern, Germany) controlled, which fibre was used for detection. The detection unit consisted of a long pass filter (RG645, Schott Glas, Mainz, Germany) and a miniature

spectrometer (S2000 alternatively USB2000+, Mikropack). By properly choosing cut-on wavelength and thickness of the longpass filter, simultaneous detection of the light transmission at 635 nm and fluorescence between 670 and 800 nm was possible. Hence, minimally invasive *in situ* measurements could be performed without the need for additional fibre probes. The 635-nm light transmission was assessed as the maximum signal between 630 and 640 nm. In order to avoid absolute fluorescence measurements, the PpIX fluorescence F at 700 nm was determined relative to the autofluorescence background according to Equation (1)

$$F = \frac{I_{700\,\mathrm{nm}} - kI_{750\,\mathrm{nm}}}{kI_{750\,\mathrm{nm}}} \quad (1)$$

$I_{700\ \mathrm{nm}}$ is the signal at 700 nm, and the term $kI_{750\ \mathrm{nm}}$ is an estimate of the autofluorescence contribution at 700 nm, which has to be subtracted from $I_{700\ \mathrm{nm}}$ in order to assess the PpIX-specific fluorescence component. At 750 nm no PpIX fluorescence is expected. The k-value was determined by the analysis of spectra exhibiting exclusively autofluorescence. For this purpose, only those post-iPDT spectra were considered, which had no evident PpIX-component even before iPDT. From these pure autofluorescence spectra, a mean ratio of $I_{700\ \mathrm{nm}}/I_{750\ \mathrm{nm}} = 2$ was determined and accordingly, k was set equal to 2. In order to reduce the signal-to-noise ratio, only fibre pairs with source-detector separations (cylinder centre-to-centre distances) smaller than 15 mm were included in the data analysis. The minimum distance was 8 mm.

Patient Evaluation After iPDT

All patients received dexamethasone in the first 3 days after the PDT. The first post-operative MRI investigation (gadolinium enhanced T1 weighted and T2 weighted scans) was done at day 1 after surgery for assessment of early treatment effects. The PDT effect was judged based on the changes in MRI contrast agent uptake as visually observed (Faber and Kreth). Further clinical and neuroradiological follow-up was performed 1 month post-operatively and thereafter at 3-month intervals at the outpatient clinic.

RESULTS

The real-time PpIX fluorescence monitoring during stereotactically guided iPDT is feasible. It was intuitively integrated into the serial stereotactic biopsy approach. Prior to the placement of light application fibres for iPDT, 8–15 tissue samples were taken along one of the planned treatment trajectories. Three to eight samples were used for histopathological evaluation and molecular genetic analysis, another 3–10 samples were collected to study PpIX concentration. The diagnosis of glioblastoma was confirmed for all patients (Table 1).

The PpIX concentration measurements performed on tissue biopsies and the intra-operative measurements of fluorescence intensities were analysed (Fig. 2). All patients that showed high pre-irradiation PpIX fluorescence (patients 1, 3 and 4), also showed a high PpIX concentration in the extracted tissue, at least in parts of the tumour. The mean values of the PpIX concentrations measured along the biopsy trajectories ranged from 1.4 to 3.0 μM for these patients (Fig. 2, columns 1 and 2). The strongest PpIX fluorescence intensity was found for patient 1, corresponding well with the PpIX extraction values, which were also among the highest of all patients. Little PpIX-fluorescence was found for patient 2, although one tissue sample showed a high PpIX concentration. This tumour was characterised by extensive necrosis. Some samples taken adjacent to biopsy proven vital tumour showed no PpIX. Patient 5 showed even less PpIX fluorescence. In this case, none of the extraction measurements showed PpIX either. The analyses of spectral measurements performed pre- and post-iPDT for patients 1, 3 and 4 showed high pre-irradiation PpIX fluorescence and very low post-irradiation PpIX-fluorescence, indicative of substantial photobleaching. For patient 2, a photobleaching of the low average PpIX fluorescence could not be detected.

Furthermore, we compared the pre- and post-operative contrast enhanced MRI images at representative positions of the tumours (Fig. 2, columns 3 and 4). The largest differences in contrast uptake between pre- and post-operative imaging were observed for patients 1, 3 and 4, the ones with the highest PpIX-signals. Patient 2 showed reduced contrast uptake only in parts of the tumour, for patient 5, contrast uptake was still visible in the post-operative MRI.

Figure 3 shows examples of the fluorescence spectra measured with irradiation fibres. A distinct PpIX fluorescence peak around 700 nm can be seen in the pre-PDT data for patient 1 and this characteristic fluorescence was photobleached during therapy. The spectrum from patient 2, on the other hand, displayed unspecific fluorescence between 650 and 750 nm that was not characteristic of PpIX but was also partly photobleached during PDT.

Intra-operatively determined PpIX concentration and fluorescence levels were correlated with clinical outcome data and neuro-radiological follow up (Table 3). The reduction of contrast uptake observed post-operatively in MRI analyses of patients 1, 3 and 4 was associated with a favourable clinical outcome (responders), no progression was observed for 29–36 months. In contrast, patients 2 and 5 with no intra-operatively detectable PpIX concentration and fluorescence showed no change in MRI contrast agent uptake and incurred clinical progress at 3 and 9 months, respectively (non-responders). Beyond these findings, there was no clear evidence for a correlation between TCD, proliferation index or *MGMT*-status with the clinical outcome (Tables 1 and 3).

DISCUSSION

iPDT is being investigated as a treatment option for brain malignancies. Oral administration of ALA and

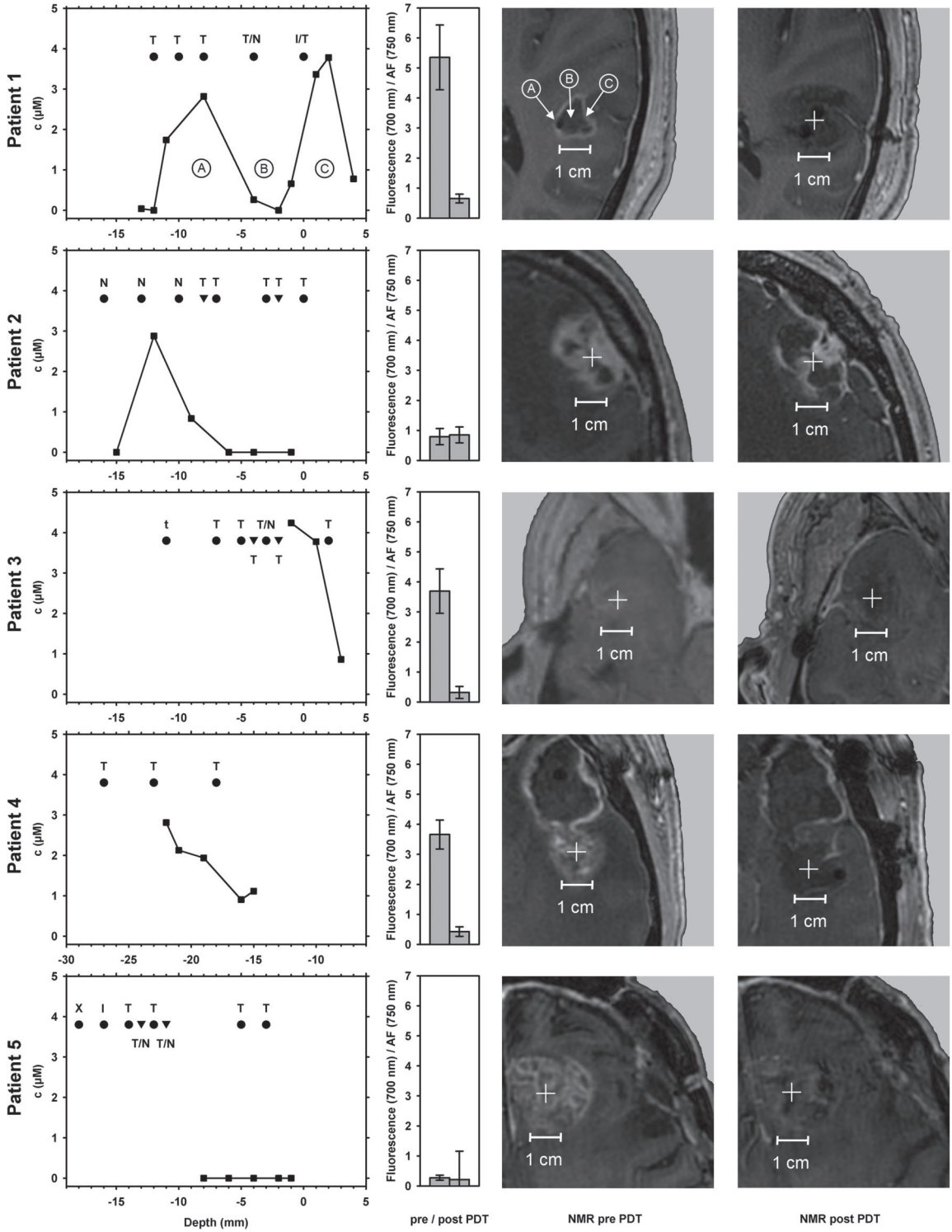

Fig. 2. The curves in the 1st column show the absolute PpIX concentrations determined by chemical extraction along the biopsy trajectories prior to PDT for all patients. The tumour depth 0 mm corresponds with the distal tumour point along the trajectory. Areas of vital tumour (T), necrosis (N), cortex (X) and infiltrating tumour (I) as determined from the H&E stained biopsies (filled circles) and smear preparations (triangles) are also indicated. The 2nd column shows the mean fluorescence signals F relative to the autofluorescence measured between irradiation fibres before and after each treatment session. Error bars denote standard deviations resulting from averaging over all source and detector fibre pairs with distances <15 mm. The 3rd and 4th column show NMR images pre- and post-PDT. The cross indicates the centre of the irradiated volume. The letters A, B and C in the 1st and 3rd column for the 1st patient exemplarily mark corresponding positions.

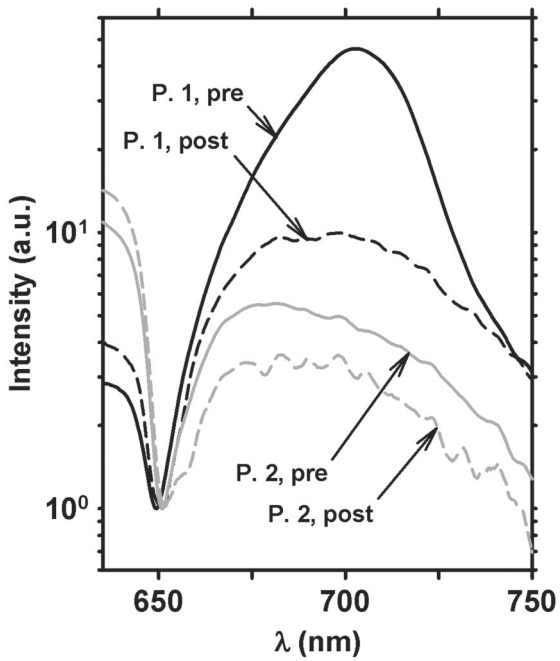

Fig. 3. Measured spectra, normalised at 650 nm showing transmission signal at 635 nm suppressed by a longpass filter and PpIX fluorescence centred around 700 nm with autofluorescence background, pre- and post-PDT for patients 1 and 2. Source-detector separation was 10 and 11 mm for patients 1 and 2, respectively.

subsequent irradiation at 635 nm has been shown to result in median survival of 15 months [2]. The clinical procedures employed by our group and other groups [2,15] have so far involved only standardised light and ALA doses. The observation of some intriguing long-term survivors leads to the speculation that some individuals might present conditions that are particularly beneficial for PDT. Such conditions might include high PpIX uptake, absence of hypoxic and necrotic tumour regions, as well as good oxygen supply. In the current pilot study the feasibility and safety of iPDT was tested and the relation of PpIX build-up and photobleaching to outcome measurement was investigated.

The absolute PpIX concentrations observed were in the range 0–4.2 μM for the five patients included in this report. As reviewed in Ref. 8, the induction of efficient photodynamic effects in human and animal tissues is possible with PpIX levels in the range of 1–10 μM. The three responders among the five patients indeed showed an average PpIX concentration in this range. Furthermore, the observed range, and uptake, are in agreement with previously observed photosensitiser levels within brain tissue samples acquired during ALA-mediated fluorescence-guided resection (FGR) [8,17,35]. This variability is expected, due to the heterogeneous composition of the tumour volume, consisting of neighbouring vital, hypoxic and necrotic parts: Viable tumour tissue was characterised by the highest PpIX concentrations and fluorescence as shown in patients 1, 3 and 4. On the other hand, tumours with extended central necrosis surrounded by extremely thin layers of viable tumour tissue were characterised by lower mean PpIX uptake, see for example in patient 2. In patient 5 exhibiting no PpIX uptake and fluorescence, an exceptionally undifferentiated histopathological phenotype was found; This patient had previously been subjected to extensive multi-modal treatment. Although one might expect an even increased PpIX-accumulation capacity in highly undifferentiated and strongly proliferating (Ki67 was 50%, Table 1) tumours, our results indicate that extensive dedifferentiation of tumour cells after previously performing multi-modal treatment might hamper PpIX biosynthesis.

The applied dosimetry feedback model of this study includes real-time monitoring of the PpIX fluorescence intensity and photobleaching. Such a model can be useful for both the optimal adjustment of irradiation parameters to achieve complete photobleaching of the treatment volume without employing unnecessarily long treatment times and early prognostic evaluation [36]. The chosen approach is in accordance with the implicit dosimetry model as proposed by Wilson et al. [23], who have assumed that the same process(es) induce(s) both tissue damage and photosensitiser consumption, thereby avoiding the need to separately monitor light fluence rate, photosensitiser concentration and tissue oxygenation. The implicit dosimetry model holds the advantage that it is relatively uncomplicated, technically easy and cheap. Our measurement configuration utilised the same fibres and light

TABLE 3. PpIX Concentrations in Biopsies, MRI Data and Follow-Up

Patient	cPpIX (μM)	MR imaging changes	Follow-up status
1	1.4 ± 1.4 (0–3.8)	sign. regr.	No progr. 36 months
2	0.6 ± 1.2 (0–2.9)	No change	Progr., deceased after 3 months
3	3.0 ± 1.8 (0.9–4.2)	sign. regr.	No progr. 30 months
4	1.8 ± 0.8 (0.9–2.8)	sign. regr.	No progr. 29 months
5	0 ± 0	No change	Progr., deceased after 9 months

Average ± standard deviation (range) of PpIX concentrations in biopsies (cPpIX), MRI data 1 day post-PDT and the patient status at time of writing.
sign. regr., significant regression; progr., progression.

source as employed for therapeutic light delivery for *in vivo* PpIX fluorescence monitoring, thereby avoiding the use of additional measurement fibres.

In our opinion, essential requirements for a potentially successful iPDT are, the proof of a sufficiently high PpIX-concentration in vital malignant tissue in combination with the application of a sufficiently high light fluence to all critical parts of the tumour. If the initial PpIX concentration is too low, photobleaching will destroy the photosensitiser before a lethal amount of intra-cellular reactive oxygen species could be produced [15]. The low PpIX-accumulation outside the tumour helps to avoid normal brain injury [15]. In other words, there are relatively few safety concerns regarding the application of high light doses. In contrast any increase of the drug dose should be performed extremely cautiously. In order to avoid thermally induced side effects of iPDT in case of reduced inter-fibre distances, additional temperature measurements are indicated.

The varying PpIX levels observed in this study indicate that an iPDT dosimetry based solely on the administered light and drug doses is insufficient for predicting and/or controlling the therapeutic outcome. The standardised irradiation time of 3,600 seconds employed in our clinical work is based on patient-averaged values for target tissue optical properties and photobleaching kinetics [2,15,37]. Numerous groups are investigating different approaches towards real-time treatment supervision relying on the different, patient-individualised PDT dosimetry models, for example for prostate-PDT [20–22] and PDT in intraperitoneal tissues [38]. Recently, Yang et al. [39] reported on a setup and initial data employing combined fluorescence imaging and non-contact point spectroscopy during intraoperative, photofrin-mediated brain-PDT. The authors speculate on the use of the system for individualised PDT by identifying and targeting fluorescent tissue remaining post-FGR and/or to employ photobleaching kinetics along the concept of an implicit dosimetry model [23]. The true potential of treatment supervision and feedback to individualise therapy is, however, still relatively unexploited for brain-PDT. However, even with establishing individualised treatment protocols, hypoxic regions and areas of spontaneous necrosis probably need special consideration due to their lower PpIX uptake [8], limited light penetration [40] as well as poor oxygen availability. A complete phototoxic eradication of all tumour cells may thus be improbable. To obtain long term survival one may have to rely on secondary effects, such as shut down of tumour vasculature or induction of an efficient immune response. A shut down of tumour vasculature might be caused by the development of a local edema within a around the treatment volume. Initial research on ALA-PDT induced immune responses has already indicated, for example an increased expression of heat shock proteins [41,42]. Similar responses, especially a direct phototoxic action on the tumour vasculature might also be initiated by other photosensitisers, such as temoporfin, photofrin, or Tookad soluble, which are in clinical use or clinical studies. However, in the current study 5-ALA was preferred because of its high tumour selectivity.

As a result of the first pre- and post-iPDT intra-operative fluorescence measurements, we observed an association between initial PpIX concentration, fluorescence levels, photobleaching and clinical outcome data: patients with high intra-operative PpIX intensity, high fluorescence levels and pronounced photobleaching experienced remarkably reduced MRI contrast agent uptake after iPDT and favourable outcome with long term survival. As there were no cases with high initial PpIX intensity and no photobleaching after irradiation in the series, we could not elucidate, whether pronounced photobleaching correlates with treatment response and favourable outcome. The absence of photobleaching, however, might indicate insufficient irradiation as a consequence of high tissue absorption or large interfibre distances. Patients with both no or little intra-operatively detectable PpIX concentration and low fluorescence levels before iPDT experienced early progress. Hence, one might consider applying PpIX fluorescence measurements as early as the stereotactic biopsy procedure, to select patients suitable for iPDT [43,44]. In this session, PpIX concentration should be measured quantitatively, either by applying quantitative fluorescence spectroscopy as suggested by several groups (see for example [45–48]) or by chemical extraction from biopsies.

CONCLUSION

Treatment monitoring by detecting PpIX fluorescence during iPDT of glioblastoma is feasible and safe. Intratumoural PpIX concentrations exhibited pronounced inter- and intra-tumoural variations. Initial intra-operative fluorescence is directly linked with the mean intra-tumoural PpIX concentrations and the clinical outcome. This could be used within an implicit dosimetry model for optimising treatment parameters and for an early treatment prognosis as well as for selection of patients suitable for iPDT. The observation of longterm survival for all cases of strong fluorescence is encouraging and deserves further investigation. Prospective clinical trials with higher patient numbers are highly warranted.

ACKNOWLEDGMENTS

In memoriam: Dr. Ann Johansson had finished most of this manuscript when she died in an accident during mountain climbing in 2011 at the age of 32. The coauthors want to express their reverence to Ann for her invaluable contribution to Photodynamics.

The Alexander von Humboldt Foundation is gratefully acknowledged for its financial support of Ann Johansson, and Sabine Sandner for technical support.

REFERENCES

1. Stummer W, Reulen HJ, Meinel T, Pichlmeier U, Schumacher W, Tonn JC, Rohde V, Oppel F, Turowski B, Woiciechowsky C, Franz K, Pietsch T. Extent of resection and survival in glioblastoma multiforme: Identification of and adjustment for bias. Neurosurgery 2008;62(3):564–576.

2. Beck TJ, Kreth FW, Beyer W, Mehrkens JH, Obermeier A, Stepp H, Stummer W, Baumgartner R. Interstitial photodynamic therapy of nonresectable malignant glioma recurrences using 5-aminolevulinic acid induced protoporphyrin IX. Lasers Surg Med 2007;39(5):386–393.
3. Kostron H, Obwegeser A, Jakober R. Photodynamic therapy in neurosurgery: A review. J Photochem Photobiol B 1996; 36(2):157–168.
4. Stylli SS, Kaye AH. Photodynamic therapy of cerebral glioma—A review. Part II—Clinical studies. J Clin Neurosci 2006;13(7):709–717.
5. Muller PJ, Wilson BC. Photodynamic therapy of brain tumors—A work in progress. Lasers Surg Med 2006;38(5): 384–389.
6. Kaye AH, Morstyn G, Brownbill D. Adjuvant high-dose photoradiation therapy in the treatment of cerebral glioma: A phase1–2 study. J Neurosurg 1987;67(4):500–505.
7. Powers SK, Cush SS, Walstad DL, Kwock L. Stereotactic intratumoral photodynamic therapy for recurrent malignant brain tumors. Neurosurgery 1991;29(5):688–695.
8. Johansson A, Palte G, Schnell O, Tonn JC, Herms J, Stepp H. 5-aminolaevulinic acid-induced protoporphyrin IX levels in tissue of human malignant brain tumours. Photochem Photobiol 2010;86(6):1373–1378.
9. Zaak D, Sroka R, Höppner M, Khoder W, Reich O, Tritschler S, Muschter R, Knüchel R, Hofstetter A. Photodynamic therapy by means of 5-ALA induced PPIX in human prostate cancer—Preliminary results. Med Laser Appl 2003;18(1):91–95.
10. Peng Q, Berg K, Moan J, Kongshaug M, Nesland JM. 5-Aminolevulinic acid-based photodynamic therapy: Principles and experimental research. Photochem Photobiol 1997;65(2): 235–251.
11. Stummer W, Pichlmeier U, Meinel T, Wiestler OD, Zanella F, Reulen HJ. Fluorescence-guided surgery with 5-aminolevulinic acid for resection of malignant glioma: A randomised controlled multicentre phase III trial. Lancet Oncol 2006; 7(5):392–401.
12. El-Sharabasy MM, El-Waseef AM, Hafez MM, Salim SA. Porphyrin metabolism in some malignant diseases. Br J Cancer 1992;65(3):409–412.
13. Collaud S, Juzeniene A, Moan J, Lange N. On the selectivity of 5-aminolevulinic acid-induced protoporphyrin IX formation. Curr Med Chem Anti-Canc Agents 2004;4(3):301–316.
14. Ennis SR, Novotny A, Xiang J, Shakui P, Masada T, Stummer W, Smith DE, Keep RF. Transport of 5-aminolevulinic acid between blood and brain. Brain Res 2003;959(2): 226–234.
15. Johansson A, Kreth FW, Stummer W, Stepp H. Interstitial photodynamic therapy of brain tumors. IEEE J Selected Topics Quantum Electron 2010;16(4):841–853.
16. Stummer W, Beck T, Beyer W, Mehrkens JH, Obermeier A, Etminan N, Stepp H, Tonn JC, Baumgartner R, Herms J, Kreth FW. Long-sustaining response in a patient with nonresectable, distant recurrence of glioblastoma multiforme treated by interstitial photodynamic therapy using 5-ALA: Case report. J Neurooncol 2008;87(1):103–109.
17. Eleouet S, Rousset N, Carre J, Vonarx V, Vilatte C, Louet C, Lajat Y, Patrice T. Heterogeneity of delta-aminolevulinic acid-induced protoporphyrin IX fluorescence in human glioma cells and leukemic lymphocytes. Neurol Res 2000; 22(4):361–368.
18. Castano AP, Mroz P, Hamblin MR. Photodynamic therapy and anti-tumour immunity. Nat Rev Cancer 2006;6(7):535–545.
19. Fingar VH. Vascular effects of photodynamic therapy. J Clin Laser Med Surg 1996;14(5):323–328.
20. Zhu TC, Finlay JC, Hahn SM. Determination of the distribution of light, optical properties, drug concentration, and tissue oxygenation in-vivo in human prostate during motexafin lutetium-mediated photodynamic therapy. J Photochem Photobiol B 2005;79(3):231–241.
21. Weersink RA, Bogaards A, Gertner M, Davidson SR, Zhang K, Netchev G, Trachtenberg J, Wilson BC. Techniques for delivery and monitoring of TOOKAD (WST09)-mediated photodynamic therapy of the prostate: Clinical experience and practicalities. J Photochem Photobiol B 2005;79(3):211–222.
22. Johansson A, Axelsson J, Andersson-Engels S, Swartling J. Realtime light dosimetry software tools for interstitial photodynamic therapy of the human prostate. Med Phys 2007; 34(11):4309–4321.
23. Wilson BC, Patterson MS, Lilge L. Implicit and explicit dosimetry in photodynamic therapy. Lasers Med Sci 1997;12:182–199.
24. Dysart JS, Singh G, Patterson MS. Calculation of singlet oxygen dose from photosensitizer fluorescence and photobleaching during mTHPC photodynamic therapy of MLL cells. Photochem Photobiol 2005;81(1):196–205.
25. Sheng C, Hoopes PJ, Hasan T, Pogue BW. Photobleaching-based dosimetry predicts deposited dose in ALA-PpIX PDT of rodent esophagus. Photochem Photobiol 2007;83(3):738–748.
26. Ericson MB, Sandberg C, Stenquist B, Gudmundson F, Karlsson M, Ros AM, Rosen A, Larko O, Wennberg AM, Rosdahl I. Photodynamic therapy of actinic keratosis at varying fluence rates: Assessment of photobleaching, pain and primary clinical outcome. Br J Dermatol 2004;151(6): 1204–1212.
27. Cottrell WJ, Paquette AD, Keymel KR, Foster TH, Oseroff AR. Irradiance-dependent photobleaching and pain in delta-aminolevulinic acid-photodynamic therapy of superficial basal cell carcinomas. Clin Cancer Res 2008;14(14):4475–4483.
28. Pogue BW, Sheng C, Benevides J, Forcione D, Puricelli B, Nishioka N, Hasan T. Protoporphyrin IX fluorescence photobleaching increases with the use of fractionated irradiation in the esophagus. J Biomed Opt 2008;13(3):034009.
29. Waidelich R, Stepp H, Baumgartner R, Weninger E, Hofstetter A, Kriegmair M. Clinical experience with 5-aminolevulinic acid and photodynamic therapy for refractory superficial bladder cancer. J Urol 2001;165(6):1904–1907.
30. Mackenzie GD, Jamieson NF, Novelli MR, Mosse CA, Clark BR, Thorpe SM, Bown SG, Lovat LB. How light dosimetry influences the efficacy of photodynamic therapy with 5-aminolaevulinic acid for ablation of high-grade dysplasia in Barrett's esophagus. Lasers Med Sci 2008;23(2):203–210.
31. Pech O, Gossner L, May A, Rabenstein T, Vieth M, Stolte M, Berres M, Ell C. Long-term results of photodynamic therapy with 5-aminolevulinic acid for superficial Barrett's cancer and high-grade intraepithelial neoplasia. Gastrointest Endosc 2005;62(1):24–30.
32. Rossi S, Longhi L, Balestreri M, Spagnoli D, deLeo A, Stocchetti N. Brain oxygen tension during hyperoxia in a swine model of cerebral ischaemia. In: Mendelow AD, Baethmann A, Czernick Z, Hoff JT, Ito U, James HE, Kuroiwa T, Marmarou A, Marshall LF, Reulen HJ, editors. Acta Neurochir Suppl. 2000; 76, 243–245.
33. Vaupel P. Blood-flow and metabolic microenvironment of brain-tumors. J Neuro-Oncol 1994;22(3):261–267.
34. Kreth FW, Muacevic A, Medele R, Bise K, Meyer T, Reulen HJ. The risk of haemorrhage after image guided stereotactic biopsy of intra-axial brain tumours—A prospective study. Acta Neurochir (Wien) 2001;143(6):539–545.
35. Stummer W, Novotny A, Stepp H, Goetz C, Bise K, Reulen HJ. Fluorescence-guided resection of glioblastoma multiforme by using 5-aminolevulinic acid-induced porphyrins: A prospective study in 52 consecutive patients. J Neurosurg 2000;93(6):1003–1013.
36. Hennig G, Stepp H, Johansson A. Photobleaching-based method to individualize irradiation time during interstitial 5-aminolevulinic acid photodynamic therapy. Photodiagnosis Photodyn Ther 2011;8(3):275–281.
37. Stepp H, Beck T, Pongratz T, Meinel T, Kreth FW, Tonn JC, Stummer W. ALA and malignant glioma: Fluorescence-guided resection and photodynamic treatment. J Environ Pathol Toxicol Oncol 2007;26(2):157–164.
38. Wang HW, Zhu TC, Putt ME, Solonenko M, Metz J, Dimofte A, Miles J, Fraker DL, Glatstein E, Hahn SM, Yodh AG. Broadband reflectance measurements of light penetration, blood oxygenation, hemoglobin concentration, and drug concentration in human intraperitoneal tissues before and after photodynamic therapy. J Biomed Opt 2005;10(1):14004.

39. Yang VX, Muller PJ, Herman P, Wilson BC. A multispectral fluorescence imaging system: Design and initial clinical tests in intra-operative Photofrin-photodynamic therapy of brain tumors. Lasers Surg Med 2003;32(3):224–232.
40. Mitra S, Foster TH. Carbogen breathing significantly enhances the penetration of red light in murine tumours in vivo. Phys Med Biol 2004;49(10):1891–1904.
41. Etminan N, Peters C, Lakbir D, Bunemann E, Borger V, Sabel MC, Hanggi D, Steiger HJ, Stummer W, Sorg RV. Heat-shock protein 70-dependent dendritic cell activation by 5-aminolevulinic acid-mediated photodynamic treatment of human glioblastoma spheroids in vitro. Br J Cancer 2011; 105(7):961–969.
42. Kammerer R, Buchner A, Palluch P, Pongratz T, Oboukhovskij K, Beyer W, Johansson A, Stepp H, Baumgartner R, Zimmermann W. Induction of immune mediators in glioma and prostate cancer cells by non-lethal photodynamic therapy. PLoS ONE 2011;6(6):e21834.1–e21834.14.
43. Widhalm G, Wolfsberger S, Minchev G, Woehrer A, Krssak M, Czech T, Prayer D, Asenbaum S, Hainfellner JA, Knosp E. 5-Aminolevulinic acid is a promising marker for detection of anaplastic foci in diffusely infiltrating gliomas with nonsignificant contrast enhancement. Cancer 2010;116(6):1545–1552.
44. Göbel W, Brucker D, Kienast Y, Johansson A, Kniebühler G, Rühm A, Eigenbrod S, Fischer S, Goetz M, Kreth FW, Ehrhardt A, Stepp H, Irion KM, Herms J. Optical needle endoscope for safe and precise stereotactically guided biopsy sampling in neurosurgery. Opt Express 2012;22(24):26117–26126.
45. Amelink A, Kruijt B, Robinson DJ, Sterenborg HJ. Quantitative fluorescence spectroscopy in turbid media using fluorescence differential path length spectroscopy. J Biomed Opt 2008;13(5):054051.
46. Kanick SC, Robinson DJ, Sterenborg HJCM, Amelink A. Semi-empirical model of the effect of scattering on single fiber fluorescence intensity measured on a turbid medium. Biomedical Optics Express 2012;3(1):137–152.
47. Valdes PA, Kim A, Leblond F, Conde OM, Harris BT, Paulsen KD, Wilson BC, Roberts DW. Combined fluorescence and reflectance spectroscopy for in vivo quantification of cancer biomarkers in low- and high-grade glioma surgery. J Biomed Opt 2011;16(11):116007.
48. Stepp H, Beck T, Beyer W, Pfaller C, Schuppler M, Sroka R, Baumgartner R. Measurement of fluorophore concentration in turbid media by a single optical fiber. Med Laser Appl 2007;22(1):23–34.

Photodynamic therapy for cholangiocarcinoma using low dose mTHPC (Foscan®)

Gesa Kniebühler, Thomas Pongratz, Christian S. Betz, Burkhard Göke, Ronald Sroka, Herbert Stepp, Jörg Schirra

Photodiagnosis and Photodynamic Therapy 2013

Photodiagnosis and Photodynamic Therapy (2013) xxx, xxx–xxx

Available online at www.sciencedirect.com

SciVerse ScienceDirect

journal homepage: www.elsevier.com/locate/pdpdt

Photodynamic therapy for cholangiocarcinoma using low dose mTHPC (Foscan®)☆

Gesa Kniebühler[a], Thomas Pongratz[a], Christian S. Betz[b], Burkhard Göke[c], Ronald Sroka[a], Herbert Stepp[a], Jörg Schirra[c,*]

[a] *Laser-Forschungslabor, LIFE Center, University Hospital of Munich, Campus Großhadern, Marchioninistraße 23, 81377 Munich, Germany*
[b] *Department of Otorhinolaryngology, University Hospital of Munich, Campus Großhadern, Marchioninistraße 15, 81377 Munich, Germany*
[c] *Assistant Professor of Gastroenterology, Department of Internal Medicine II, University Hospital of Munich, Campus Großhadern, Marchioninistraße 15, 81377 Munich, Germany*

KEYWORDS
Cholangiocarcinoma;
mTHPC;
Foscan® PDT;
Fluorescence kinetics

Summary
Background: Photodynamic therapy (PDT) combined with stenting is an effective treatment modality for palliation of nonresectable cholangiocarcinoma (CC). A drawback of standard PDT using Photofrin® as photosensitizer is the long lasting skin photosensitivity of up to 3 months. The aim of this study was to show the outcome of PDT of CC, potential side effects and to determine the best drug light interval (DLI) using mTHPC (Foscan®) at a low dose.
Methods: 13 patients with nonresectable CC were treated with stenting and PDT (3 mg Foscan® per treatment, 0.032–0.063 mg/kg body weight, 652 nm, 50 J/cm). Fluorescence measurements were performed with a single bare fiber for 5/13 patients prior to PDT at the tumor site to determine the fluorescence contrast. For another 7/13 patients, long-term fluorescence-kinetics were measured on the oral mucosa to determine the time of maximal relative fluorescence intensity.
Results: The results so far indicate a median survival time of 13 months. Side effects such as perforations or skin phototoxicity could not be observed. Foscan® fluorescence within the tumor site was clearly detectable but a significant fluorescence contrast of tumor to adjacent healthy tissue could not be found. The fluorescence kinetics measured in the oral mucosa showed a maximum at 3.85 days (median) after drug administration.

☆ This manuscript is part of the inaugural thesis of Gesa Kniebühler to be submitted at the Medical Faculty of the Ludwig-Maximilians-University of Munich.

* Corresponding author. Tel.: +49 89 7095 3031; fax: +49 89 7095 5299.
E-mail addresses: gesa.kniebuehler@med.uni-muenchen.de (G. Kniebühler), thomas.pongratz@med.uni-muenchen.de (T. Pongratz), christian.betz@med.uni-muenchen.de (C.S. Betz), burkhard.goeke@med.uni-muenchen.de (B. Göke), ronald.sroka@med.uni-muenchen.de (R. Sroka), herbert.stepp@med.uni-muenchen.de (H. Stepp), joerg.schirra@med.uni-muenchen.de (J. Schirra).

1572-1000/$ – see front matter
http://dx.doi.org/10.1016/j.pdpdt.2012.12.005

Please cite this article in press as: Kniebühler G, et al. Photodynamic therapy for cholangiocarcinoma using low dose mTHPC (Foscan®). Photodiagnosis and Photodynamic Therapy (2013), http://dx.doi.org/10.1016/j.pdpdt.2012.12.005

Conclusion: Combined stenting and PDT performed with a low Foscan® dose results in equal and potentially longer survival times compared to standard Photofrin® PDT, while lowering the risk of side effects strongly. Thus it may improve the quality of life.

Introduction

The incidence rate of cholangiocarcinoma (CC) varies strongly throughout the world [1]. The yearly incidence in Western Europe amounts to about 3—5 per 100,000 with an increasing trend [2]. The only curative therapy is the complete resection or liver transplantation. However at diagnosis the tumor is mostly at such an advanced state that resection is no longer possible [3]. For palliative treatment commonly stents are inserted. Nevertheless the prognosis for patients with nonresectable CC is still fairly poor. While the mean survival time for patients treated with stents alone is about 6 months, stenting combined with photodynamic therapy (PDT), commonly performed with Photofrin® or Photosan®, has been shown to be a promising alternative palliative treatment form [4,5]. In addition to a reduction of cholestasis and an improvement in quality of life, a meta-analysis showed an increase of the mean survival time by 265 days [6]. Thus this combined treatment modality is comparable to incomplete R1 and R2 resections [4].

For PDT, a photosensitizer is applied to the patient and activated by light of an appropriate wavelength. Depending on the type of photosensitizer employed, activation results in the build-up of different radicals and reactive oxygen species, such as singlet oxygen, which in turn cause cellular damage [7]. PDT is primarily a local treatment restricted to the illuminated tissue. However, the immune system could be stimulated by local PDT, which might result in the additional treatment of distant metastases, as demonstrated in animal models [8,9]. Another advantage of PDT is that very little photosensitizer accumulates in the nuclei [10], whereby the DNA remains comparably unaffected [11]. Furthermore, a dose accumulation as in radiotherapy does not occur. In view of the given aspects and the minor side effects, mainly skin photosensitization, PDT can thus be performed repetitively. The type of photosensitizer, its dosage and the drug light interval (DLI) are selected in dependence of the treatment site and stage of the tumor. Until now, PDT for CC is commonly performed with the first generation photosensitizer Photofrin®. A great drawback using Photofrin® is the patients' long lasting skin photosensitivity requiring shielding from intense sunlight for up to 3 months. Additionally the therapeutic penetration depth for Photofrin®-based PDT is limited to approximately 4—6 mm [5]. Another photosensitizer is Protoporphyrin IX (PPIX), the direct precursor of heme, which accumulates after exogenous administration of 5-aminolevulinic acid (5-ALA). PPIX shows a low systemic toxicity and a short period of skin photosensitivity of 24—48 h [12]. However, PDT with 5-ALA for the cholangiocarcinoma was stated to be unsuitable because of its therapeutic penetration depth of less than 2 mm [13] and the resulting insufficient reduction of bile duct stenoses [14]. Thus the need for a better photosensitizer is evident.

A promising photosensitizer for PDT of cholangiocarcinoma is meso-tetrahydroxyphenylchlorin (mTHPC, Foscan®). Compared to Photofrin® it has a high quantum yield for PDT reactions, an activation at longer wavelengths which results in a deeper therapeutic penetration and a reduced period of photosensitivity. Foscan® was approved in 2001 in the EU for the palliative treatment of head and neck cancer with a maximal dose of 0.15 mg/kg body weight, a fluence of 20 J/cm^2 and a DLI of 96 h [15]. With a dose of 0.15 mg/kg b.w. and excitation light at 652 nm the therapeutic penetration depth is expected to be about 9 mm [16]. Though in general desirable, such a deep therapeutic penetration can also result in complications such as perforations, when treating hollow organs [17,18]. By reducing the Foscan® dose, these risks might be lowered. In addition, the skin phototoxicity lasting about 2—4 weeks after the full dose may be reduced further by using lower Foscan® doses [19]. In a study performed by Betz et al. [20], patients with basal cell carcinomas (BCCs) were treated with reduced Foscan® doses of 0.03—0.15 mg/kg b.w. with correspondingly adjusted fluences and DLIs. For the complete dose range they could report on complete remissions of BCCS in 96.7% of the cases, whereas side effects such as pain and phototoxic reactions were reported to be more common in patients treated with a high drug dose (0.06—0.15 mg/kg). In line with these results, PDT of cholangiocarcinoma was performed in the present study with Foscan® at 3 mg per treatment, which resulted in a mean dose of 0.044 ± 0.007 mg/kg b.w. (mean $\pm$ SD) and a range of 0.032—0.063 mg/kg b.w. The necessary fluence was assumed to be 50 J/cm^2 instead of the standard 20 J/cm^2 to compensate for the reduction of the drug dose.

A patient oriented DLI-determination for low dose Foscan® treatment of cholangiocarcinoma is missing so far. Different ways to determine the DLI for PDT are discussed in the literature, as the optimal DLI may vary for different PDT approaches. For example the optimal time point for light irradiation may be either the peak drug concentration in plasma [21], the time with the maximum fluorescence contrast of cancerous to normal tissue [22] or the peak drug concentration in the target tissue [22,23].

It was the aim of the present study to investigate the DLI and the PDT-response applying a reduced dose of Foscan® in individual treatment attempts for PDT of cholangiocarcinoma. The reduced drug dose was chosen with the main intent to reduce the risk of perforations and the side effects, especially the skin photosensitivity.

Materials and methods

Foscan® was used in individual treatment attempts as off-label use for PDT of cholangiocarcinoma. The patients were informed about the off-label use of Foscan®, and written informed consent was obtained from each patient. The study was approved by the Munich Institutional Review Board of the Ludwig-Maximilians-University.

Please cite this article in press as: Kniebühler G, et al. Photodynamic therapy for cholangiocarcinoma using low dose mTHPC (Foscan®). Photodiagnosis and Photodynamic Therapy (2013), http://dx.doi.org/10.1016/j.pdpdt.2012.12.005

Table 1 Details of patients, bismuth types, PDT parameters and fluorescence measurements.

Patient	Treatment	Sex	Age	Bismuth type	DLI [h]	Foscan® dose [mg/kg b.w.]	Fluorescence contrast measurements	Fluorescence kinetics measurements
1	1	Female	55	IV	20	0.045	Yes	No
2	2	Male	67	IIIb	20	0.046	Yes	No
3	3	Male	76	IV	20	0.043	Yes	No
4	4	Male	72	IIIb	20	0.042	Yes	No
5	5	Male	86	IV	20	0.054	Yes	(Yes)
6-1	6	Female	71	IV	20	0.041	No	No
7	7	Male	68	IIIb	20	0.041	No	No
8	8	Male	66	IIIb	20	0.046	No	No
9	9	Female	81	II	20	0.063	No	(Yes)
10	10	Male	83	I	70	0.035	No	(Yes)
11	11	Male	62	IIIb	70	0.038	No	Yes
6-2	12	Female	71	IV	72	0.041	No	Yes
12	13	Male	60	I	67	0.032	No	Yes
13	14	Male	83	IIIa	67	0.043	No	Yes

(Yes): fluorescence measurements without standardization.

In total, 13 non-selected consecutive patients, 3 females and 10 males, with advanced nonresectable cholangiocarcinoma and clinically significant bile duct stenoses were investigated over a period of 25 months from May 2010 onwards. The mean age was 72 years, ranging from 55 to 86 years. For 1 of the 13 patients, PDT was performed a second time one year after the first treatment, resulting in a total of 14 PDT treatments investigated in the present study (Table 1). According to the Bismuth-Corlette classification [24], 4 patients were categorized as Bismuth type IV, 6 as type III, 1 as type II, and 2 as type I. The diagnosis was confirmed by histopathology in 9 patients. For the remaining 4 patients, histology showed inflammation but no malignant cells. For these patients diagnosis was based on typical endoscopic and radiologic findings (hilar strictures and hilar tumor mass in CT/MRI). No patient had distant metastases at the time of PDT, but 1 patient had local peritoneal carcinosis without ascites. All patients underwent endoscopic retrograde cholangiopancreatography (ERCP) combined with PDT for endoscopic drainage of bile duct stenoses. In patients typed Bismuth II—IV, 2 or 3 biliary drainages (double-pigtail catheters) were placed and changed by ERCP every 2—3 months during follow up. ERCP procedures were accompanied by antibiotic therapy.

For 5 of the 13 patients fluorescence was measured during ERCP and prior to PDT-irradiation in the tumor stenosis and the adjacent healthy bile duct. In these patients, the fluorescence probe was brought into gentle contact with the mucosa under direct visualization by through-the-scope cholangioscopy (SpyGlass®, Boston Scientific, Natick, MA) and documented by video. For another 7 of the 13 patients, fluorescence-kinetics measurements were performed in the oral mucosa after Foscan®-administration.

Protocol for PDT

While in head and neck PDT-treatment protocols patients receive Foscan® at a dose of 0.15 mg/kg b.w., all 13 patients included in the present study were given Foscan® (Biolitec pharma Ltd., United Drug House, Magna Drive, Dublin 24, Ireland) at a fixed dose of 3 mg for practical reasons. With patients body weights ranging from 47.9 to 92.4 kg this resulted in a dose range of 0.032—0.063 mg/kg b.w. and a mean dose of 0.044 ± 0.007 mg/kg b.w. (mean $\pm$ SD). The lipophilic Foscan® was slowly applied via a central venous catheter during approximately 5 min with simultaneous infusion of a common lipid solution to avoid photosensitization of a peripheral vein. The first 9 treatments were performed after a DLI of 20 h. According to the results of the fluorescence kinetics performed during treatment 5 and 9, DLIs of 67—72 h were chosen for the following 5 treatments, as shown in Table 1.

PDT was performed with laser light at 652 nm (Ceralas, Biolitec, Jena, Germany). The stenoses were irradiated by means of a cylindrical light diffuser of 4 cm length (Light Guide Optics GmbH, Rheinbach, Germany). By repositioning the diffuser, the complete lengths of the stenoses were irradiated, applying a fluence of 50 J/cm at a fluence rate of 200 mW/cm. The choice of this fluence is based on the assumption that the bile duct has a diameter of approximately 3 mm and the consideration that a cylinder with a diameter of 3 mm has a surface of 1 cm^2 per 1 cm length. Multiple backscatter in the cylindrical organ was not accounted for, potentially increasing the expectable treatment depth. For stenoses of the hilar bifurcation, parts of the common bile ducts were irradiated twice, so that the light dose at the overlapping sites (2—3 cm) added up to 100 J/cm.

During the first six days after Foscan® administration, daylight exposure was not allowed and the patients' room was illuminated with yellow light below 200 Lux. Patients had to cover their skin and wear dark sunglasses when leaving their rooms. Typically on the sixth day, the lights were changed to common white lights and after seven to eight days the patients were discharged from hospital. Patients were advised to shield from direct sunlight and strong

Please cite this article in press as: Kniebühler G, et al. Photodynamic therapy for cholangiocarcinoma using low dose mTHPC (Foscan®). Photodiagnosis and Photodynamic Therapy (2013), http://dx.doi.org/10.1016/j.pdpdt.2012.12.005

artificial light sources for approximately another week, according to the standard patient information leaflet.

For analysis of the PDT outcome side effects and survival time were evaluated as efficacy parameters of this study. Survival time was analyzed by Kaplan–Meier analysis.

Fluorescence measurements

In the initial 5 of the 13 patients fluorescence measurements were performed within the tumor region and adjacent healthy bile duct tissue prior to PDT to determine the contrast of the relative fluorescence intensity between these tissues.

Fluorescence kinetics in the oral mucosa were measured for 3 patients without standardization, as indicated in Table 1. In an additional 4 patients, standardized measurements were performed. Measurements were performed directly before drug administration and thereafter once or twice a day until the patients were discharged from hospital, which was commonly on day 7 or 8. For 1 patient, fluorescence kinetics could be measured for 48 days, since he underwent additional treatment in the same hospital. For 3 of the 4 patients also the fluorescence kinetics of the skin were measured.

For comparison purposes fluorescence kinetics in one single patient of the head and neck department suffering from a pharyngeal squamous cell carcinoma (SCC) and receiving standard Foscan® PDT (0.15 mg/kg b.w.) could be measured. The relative fluorescence intensity could be measured for days 1–13 on healthy tissue of the oral mucosa.

The fluorescence measurements were performed by means of a fiber based probe. Excitation light of a violet laser diode module (Flexpoint® Lasermodule, Laser Components, Olching, Germany) emitting at 405 nm was coupled into a 50% arm of a fiber based 50/50 beam splitter (multimode coupler, ATI optique, Courcouronnes, France) with 400 μm core diameter. For the contrast measurements a single bare fiber with a core diameter of 400 μm was connected to the 100% arm as sensor, which was pushed through the working channel of a cholangioscope and pressed gently onto the tissue. The power of the excitation light emitted at the fiber tip was measured to be 350 μW. The fluorescence emitted from the tissue was collected by the same single fiber and was transmitted through the second 50% arm of the beam splitter, in which a long pass filter (435 nm, colored glass filter, Schott AG, Mainz, Germany) was integrated to block the excitation light. Fluorescence spectra were detected by a miniature spectrometer in the spectral range from 339 to 1029 nm (Oceans Optics USB2000+, Mikropack, Ostfildern, Germany) which was connected to the beam splitter. At each site 1–13 single spectra were recorded after slight repositioning.

For the fluorescence measurements in the oral cavity the same set-up was used, only using a different fiber with a core diameter of 375 μm as sensor. The fiber was hand-held and its tip pressed gently onto the oral mucosa of the cheek. On each cheek, 9 measurements were performed, trying to measure 3 times in the same region but repositioning the fiber slightly each time to prevent bleaching effects. For the same reason the integration time was minimized.

Spectra evaluation

In order to account for possible day to day variations of the laser light intensity, a solid fluorescence standard was measured before each session. Data was processed using MATLAB® (The MathWorks, Inc., Natick, MA). When processing the data, first, all detected spectra were normalized to the integration time, the dark background intensity determined and subsequently subtracted from each raw spectrum. The autofluorescence background was considered by fitting and subtracting an exponential decay. From these spectra the maxima of the fluorescence peaks at 652 nm were extracted.

For treatments 11–14, fluorescence kinetics after Foscan® administration were measured in the oral mucosae. For each measurement session the mean of the maxima of the 18 measurements and the standard deviation were calculated. For calibration purposes the mean values and standard deviations were divided by the peak intensity of the fluorescence standard. To determine the normalized maxima intensities and the time points at which they occur, all kinetics were curve fitted by Eq. (1), which was derived by considering the Foscan® administration as a bolus injection. If so, Foscan® pharmacokinetics can be satisfactorily described by a simple two compartment model [25], the first compartment being the vasculature with rate constants for losses by excretion and transport into the second compartment, the cells of the tissue to be measured. The second compartment has losses for efflux of Foscan® also accounted for by a rate constant. Considering both compartments results in a function of the following form (Eq. (1)) where a, b and c can be determined by the initial drug concentration and the rate constants:

$$f(t) = a \cdot (1 - \exp(b \cdot t)) \cdot \exp(-c \cdot t). \quad (1)$$

Results

Fluorescence contrast

For 5 of the 13 patients, the Foscan® fluorescence was measured prior to PDT by means of ERCP as to determine the contrast of malignant to healthy bile duct tissue. For comparison, the relative fluorescence was also measured in the oral mucosa. Fig. 1 shows the resulting relative intensities normalized for each patient to the mean of the fluorescence intensity measured at the site of the tumor. Unfortunately, the measurements for patient 2 in the healthy bile duct could not be evaluated due to technical reasons. For the other measurements the fluorescence varies strongly, even for the same tissue sites, so that a significant selectivity of Foscan® in malignant versus healthy tissue could not be demonstrated for the bile duct. Still, it could be demonstrated that Foscan® does accumulate in the malignant tissue. Nonetheless, fluorescence measurements in the bile duct were not proceeded. They prolonged the ERCP and therefore treatment resulted to be more stressful for the patients, while gaining additional knowledge could not be expected. However the relative fluorescence measured for patients 3, 4 and 5 in oral mucosa lies within one standard deviation of the fluorescence measured in the tumor,

Please cite this article in press as: Kniebühler G, et al. Photodynamic therapy for cholangiocarcinoma using low dose mTHPC (Foscan®). Photodiagnosis and Photodynamic Therapy (2013), http://dx.doi.org/10.1016/j.pdpdt.2012.12.005

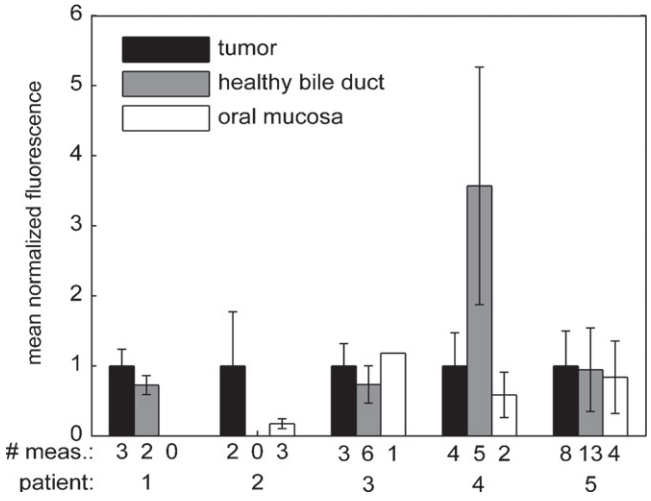

Figure 1 Normalized mean fluorescence and standard deviation measured by means of endoscopic cholangioscopy prior to PDT treatment for malignant tissue, healthy tissue of the bile duct and oral mucosa (for patient 2 fluorescence was measured at the tongue instead of the cheek). Foscan® peak intensities are normalized to the mean tumor fluorescence intensity of each patient. The numbers at the bottom of each bar represent the number of measurements included.

justifying measurements in the oral mucosa as indicator for the fluorescence in the tumor.

Fluorescence kinetics

In Fig. 2 the results of the fluorescence kinetics measurements are shown. Fig. 2a shows the long term kinetics for patient 11 and the least squares curve fit based on Eq. (1). Fig. 2b shows the standardized fluorescence kinetics measurements of all 4 patients until day 9. To evaluate the variation of these kinetics a boxplot diagram of the extracted maximum fluorescence intensity values after curve fitting is shown in Fig. 3a. For 3 of these 4 patients, fluorescence kinetics were also measured at the skin. The kinetics curves are not shown but the fluorescence intensities of the maxima are plotted in the boxplot diagram in Fig. 3a. Also the maxima of the fluorescence intensities measured in the oral mucosa and skin measured in the head and neck patient administered 0.15 mg/kg b.w. Foscan® are included for comparison (marked by +). From Fig. 3a it could be derived that according to the curve fits after normalization to the standard the median of the normalized maxima is 0.029 and the mean value 0.031. The relative intensities measured at the skin are lower, with a median of 0.0032 and a mean of 0.004. The ratio of the mean values of oral mucosa and skin is 7.75. For the head and neck patient the normalized maximum is 0.069 for oral mucosa and 0.012 for skin. The ratio of oral mucosa to skin is 5.75 and is thus in the same range as the ratio of the low dose patients. For the ratio of normal and low dose a factor of 2.2 results for oral mucosa and a factor of 3 for skin.

In Fig. 3b a boxplot diagram of the times to maximal intensity is shown. For oral mucosa the time to maximum intensity equals 3.85 days (median) and the mean 3.95 days. For comparison, the time to maximum in oral mucosa for

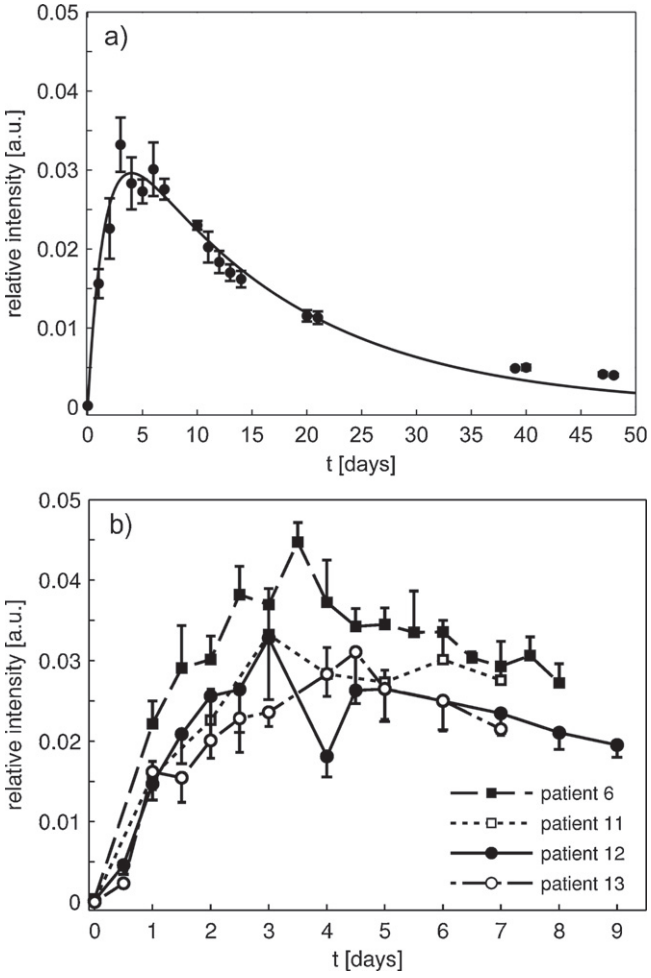

Figure 2 Fluorescence kinetics measured on oral mucosa after administration of 3 mg (0.032—0.063 mg/kg b.w.) Foscan®: (a) for patient 11 measured over a period of 48 days, (b) for 4 patients measured up to 9 days, for clarity standard deviations are plotted only in one direction.

the head and neck patient occurring at 3.08 days is indicated as well. For the fluorescence kinetics of the skin for all patients, the variation of the data points were very large and the slope of the kinetics between day 2 and 5 was close to zero so that times to maximum intensity could not be derived reliably from the curve fit.

PDT outcome

The overall survival times were analyzed by Kaplan—Meier analysis with 95% confidence intervals, as shown in Fig. 4. PDT was performed 3 months (median) after diagnosis. As can be seen in the Kaplan—Meier survival curve, 5 of the 13 patients died 6, 7, 8, 9 and 13 months after diagnosis. All deceased patients were categorized with Bismuth III or IV. The patient who died 6 months after diagnosis developed metastases in lung and bones, which was diagnosed 1 month after PDT and might have been present at PDT already. The patient, who died 7 months after diagnosis had liver abscesses, which were detected during PDT-ERCP. A subsequent CT showed local peritoneal carcinosis, in addition.

Please cite this article in press as: Kniebühler G, et al. Photodynamic therapy for cholangiocarcinoma using low dose mTHPC (Foscan®). Photodiagnosis and Photodynamic Therapy (2013), http://dx.doi.org/10.1016/j.pdpdt.2012.12.005

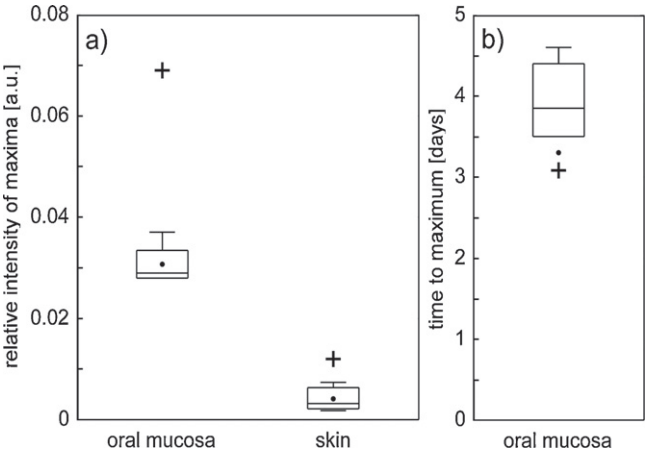

Figure 3 Fluorescence kinetics measured on oral mucosa and skin after administration of 3 mg (0.032—0.063 mg/kg b.w.) Foscan®: (a) box plot diagram of the intensity maxima derived from the two compartment curve fit for all 4 patients of oral mucosa measurements and for 3 of the 4 patients for skin measurements, (b) box plot diagram of the time to maximal intensity for oral mucosa kinetics as derived from the curve fit, • indicates mean values, + indicates the intensity maxima as well as the time to the maxima after administration of 0.15 mg/kg Foscan®.

Even with the 4 early deceases — the censored 8 patients are still in the follow up — the median survival time results to 13 months. When only regarding patients with Bismuth types III and IV the median results to 11 months.

For 10 of the 13 patients, temporary ailment in the upper abdomen during the first 48 h (median) followed the treatment. This could have been evoked either by PDT or by the accompanying ERCP. Nausea was reported by 7 patients. All ailments were easily treated by analgetics and antiemetics. Apart from this, the first patient developed an acute self-limiting edematous pancreatitis, and endoscopy revealed a local ulcer at the papilla. This was likely caused by long local irradiation with the endoscopic xenon light during a long lasting cholangioscopy. As a consequence, the endoscopic light was turned off in the subsequent procedures if a stable endoscopic position had been achieved. No other local complications and, especially, no perforation occurred. None of the patients experienced skin irritations during their hospital stay, nor did any of the patients report on skin irritations later on.

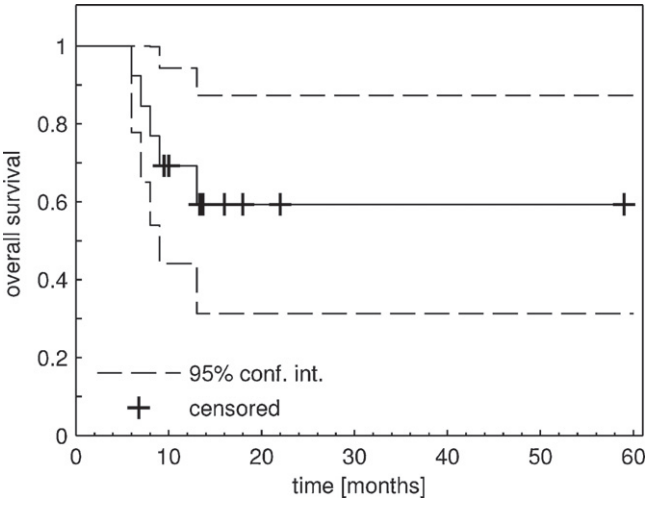

Figure 4 Kaplan—Meier diagram of 13 treated patients for overall survival after diagnosis. Patients deceased 6, 7, 8, 9 and 13 months after diagnosis. The other 8 patients are still in the follow up.

Discussion

PDT using Photofrin® as photosensitizer is effective for treatment of nonresectable hilar cholangiocarcinoma. Disadvantages of Photofrin® include a long period of general phototoxicity and a limited penetration depth at the tumor site. In contrast, the light penetration depth is greater with Foscan® and the duration of general phototoxicity is much shorter. In the present study, Foscan® was introduced at a low dose as photosensitizer for PDT of cholangiocarcinoma. The main findings were as follows: (1) a significant Foscan® fluorescence was detectable at the tumor site already 20 h after administration. (2) Foscan® did not accumulate at the tumor site compared to the adjacent healthy tissue. (3) The optimal drug-light interval was three to four days. (4) PDT using Foscan® was effective in terms of survival. (5) No severe side effects could be observed.

Fluorescence contrast

In the present study, a Foscan® dose of 3 mg per treatment resulting in 0.032—0.063 mg/kg b.w. and DLIs of 20 and 67—72 h were used for PDT treatment in contrast to the approved 0.15 mg/kg b.w. at a DLI of 96 h for head and neck cancer. The choice of a short DLI and a low Foscan® dose was based on the publications of Triescheijn et al. [21], who found a DLI of 24 h to be best for treating basal cell carcinomas (BCCs) with 0.1 mg/kg bodyweight Foscan®, and of Betz et al., describing treatment outcomes of patients with BCCs with administered doses ranging from 0.03 to 0.15 mg/kg b.w. and DLIs ranging from 1 to 96 h [20]. For patients treated with 0.05 mg/kg b.w., a fluence of 50 J/cm^2 and a DLI of 48 h, complete remission was reported in 100% of the cases and reducing the photosensitizer dose to 0.04 mg/kg b.w. with shortening the DLI to 24 h yielded an only slightly lower remission rate. The good remission rates with short DLIs might be explained by the study of Braichotte et al. [26], who found the highest contrast between squamous cell carcinomas and normal tissue as early as 2—4 h after drug administration (high dose regime), which may represent a rapid distribution within the vascular system followed by a rapid decrease.

For the determination of the optimal DLI, however, both the contrast versus healthy tissue and the absolute concentration in the tumor tissue have to be considered. As the highest accumulation occurs later than the highest contrast [26—28], the decision on the DLI is a compromise. In this study with a reduced drug dose, attention was paid to maintain a sufficient drug accumulation in the tumor tissue. Therefore, for the sake of efficacy, the focus was on the drug concentration rather than on the maximum contrast.

Please cite this article in press as: Kniebühler G, et al. Photodynamic therapy for cholangiocarcinoma using low dose mTHPC (Foscan®). Photodiagnosis and Photodynamic Therapy (2013), http://dx.doi.org/10.1016/j.pdpdt.2012.12.005

As the drug accumulation is usually a broad peak, a DLI of 20 h seemed to be a reasonable compromise for the present study. Measurements of Foscan® fluorescence intensities in the bile duct and on oral mucosa were intended to quantify the contrast in CC patients. By using a single bare fiber with a small core diameter for the fluorescence measurements, the optical tissue properties do not influence the fluorescence measurements strongly [29,30]. Therefore it is a reasonable approach to compare the measured fluorescence in different tissues to each other. When interpreting the fluorescence measurements within the tumor stenoses prior to PDT, however, it has to be kept in mind that positioning the fiber within a bile duct stenosis is difficult even with guidance by direct cholangioscopy. A vertical positioning of the fiber onto the tissue cannot always be assured. It proved unexpectedly time consuming to capture reliable spectra. After having investigated 5 patients, it was decided to discontinue these measurements to avoid undue stress to the patients.

Moreover, bile duct stenoses due to CC usually consist of a mixture of tumor tissue, inflammation, and necrosis, and even forceps biopsies from tumor stenoses have a sensitivity of only 43—88% [3]. Therefore, the measurements might not vary only because of concentration differences but also due to difficulties in positioning the fiber reproducibly in smooth contact with the tissue and because of the nature of the tissue itself. Nevertheless, although the measured relative fluorescence intensities in malignant tissue are not significantly different from the Foscan® levels within the surrounding healthy tissue, the fluorescence measurements indicate that 20 h after administration, there is a significant Foscan® accumulation in malignant tissue. Any further conclusion about absolute Foscan® concentration or tumor selectivity cannot be made due to the high variations in signal intensity for both tissue types, the low number of measurements and the impossibility to measure pharmacokinetics in the bile duct. However, the small and inconsistent differences in the fluorescence contrast between the tumor and the normal tissue of the bile duct led to the conclusion that the short DLI of 20 h needs to be questioned. Instead it was intended to find the time point of maximum accumulation of Foscan® by measurements of fluorescence kinetics at a better accessible site.

Fluorescence kinetics

Apart from the practicability, measuring fluorescence in the oral cavity to gain information of the photosensitizer present in the bile duct was triggered by Glanzmann et al. [28]. They measured the relative fluorescence with fluorescence spectroscopy in 21 patients prior to PDT in the bronchia, the esophagus and the oral cavity, finding a linear correlation between the relative fluorescence of the esophagus and the oral cavity. This suggests that information of the relative fluorescence in the bile duct may also be gained by measuring the relative fluorescence in the oral mucosa, though of course the kinetics might differ. The fluorescence kinetics measured in the present study show a maximum at day 3.85 (92 h, median) after Foscan® administration. This is in good agreement with the fluorescence kinetics measured in the oral mucosa for high dose (0.3 mg/kg b.w.) published by Braichotte et al. [26], who also showed that the maximum relative fluorescence intensity in tumor tissue occurs earlier, varying with the tumor type, by approximately 20—30 h. As the kinetics measured in the present study for low dose are similar to those of high dose, a DLI of 68—72 h was chosen for the last four patients. In addition, this DLI choice allows to delay the treatment by a day without endangering the treatment efficiency.

PDT outcome

Although a low Foscan® dose was used in this study, the median survival time after diagnosis is 13 months. This is in the range found in previous retrospective studies using the photosensitzer Photofrin® or Photosan-3® for PDT of non-resectable cholangiocarcinoma [4,31—34]. Keeping in mind that 8 out of 13 patients are still in the follow up, PDT with a low dose of Foscan® seems to be a promising treatment modality.

Pereira et al. were first to treat CCs with a dose of 0.15 mg/kg b.w. Foscan®. They included 4 patients with hilar CCs in their study. PDT combined with stenting resulted in survival times of 1—12 months [18]. However, they also reported on 2 severe complications, assumed to be related to PDT with high Foscan® doses, one with post-mortem evidence of a perforated gallbladder, and 2 patients had hand erythema during the first 2 weeks. They concluded that combined stenting and PDT prolongs life compared to stenting alone and can increase quality of life, but a significant risk of complications has to be accepted. Wolkersdörfer et al. reported on the treatment of 11 patients with hilar bile duct cancer using also a Foscan® dose of 0.15 mg/kg b.w. [17]. They focussed on the therapeutic depth and found it doubled compared to PDT performed with Photofrin® while a similar rate of infectious complications and skin phototoxicity occurred. They also had to report on one case of bile duct wall perforation. In the same study four patients showed phototoxic skin reactions, one severe (grade III) and three grade I or II.

To our knowledge this study is the first reporting on PDT of CCs performed with a low dose of 0.03 mg/kg b.w. Foscan®. A great advantage using Foscan® at a low dose is the, based on the outcome of the present study, expected decrease in side effects during treatment as well as during the follow up. In the present study, neither serious complications due to PDT nor any other side effects apart from temporary ailment in the upper abdomen or nausea could be registered.

A major reason for the low phototoxicity of a low dose of Foscan® may be the reduced amount of Foscan® present in healthy tissue, such as the skin, as shown in the hamster cheek pouch model [35]. The comparison of the relative fluorescence measured in the head and neck patient administered 0.15 mg/kg b.w. Foscan® confirms this, though it is only one data point measured. With this restriction, the peak intensities found in oral mucosa after low dose Foscan were lower by a factor of 2.2, those in skin were lower by a factor of 3. As a consequence, the risk of developing skin edema, erythema or sun burns when exposed to sunlight or intense room light is reduced compared to the standard drug dose. Assuming a similar pharmacokinetics for high and low drug doses, as suggested by the present results, skin

Please cite this article in press as: Kniebühler G, et al. Photodynamic therapy for cholangiocarcinoma using low dose mTHPC (Foscan®). Photodiagnosis and Photodynamic Therapy (2013), http://dx.doi.org/10.1016/j.pdpdt.2012.12.005

photosensitivity can also be expected to be considerably shortened. This is in good agreement with the lack of symptoms caused by skin photosensitization observed in the present study.

As all 5 deceased patients had high Bismuth types (III and IV), one might conclude a limited benefit for these more advanced cases. However, the median survival regarding only high Bismuth type patients is still 11 months, with 5 of these patients still alive. It may therefore be too early to finally conclude that low dose Foscan® PDT is inferior to PDT using Photofrin® or Photosan-3® for this group of patients. In addition, individual factors such as local complications, comorbidity, and the presence of distant metastases as shown in our cases would be of greater importance for survival than the Bismuth stage irrespective of the kind of photosensitizer used. In view of the low side effect profile observed so far, the quality of the survival time appears to be in favour of low dose Foscan® and may further argue for using low dose Foscan®. Especially, since for palliative treatments of cholangiocarcinoma in patients with a limited prognosis, the according benefit with regard to quality of life is very important. Moreover, it may allow for repeated PDT treatments [31] and may also qualify PDT as a neoadjuvant therapy before surgery of resectable cholangiocarcinoma [36].

Conclusion

The results of this study suggest that nonresectable CC can be treated with a low dose of Foscan® at 3 mg resulting in 0.032—0.063 mg/kg b.w., a light dose of 50—100 J/cm at 652 nm applied by radial diffusers and DLIs of 67—72 h. The outcome seems to be comparable to standard PDT using Photofrin®. No local side effects occurred, and compared with both Photofrin® and Foscan® in the high dose regime, skin photosensitivity is expected to be considerably reduced in severity and duration. In addition, when using a low dose of Foscan®, the treatment is more cost-effective. The usefulness of low dose Foscan®-PDT for cholangiocarcinoma should be investigated in further controlled studies.

References

[1] Shaib Y, El-Serag HB. The epidemiology of cholangiocarcinoma. Seminars in Liver Disease 2004;24:115—25.
[2] Patel T. Worldwide trends in mortality from biliary tract malignancies. BMC Cancer 2002:2.
[3] Kolligs FT, Zech CJ, Schönberg SO, et al. Interdisciplinary diagnosis of and therapy for cholangiocarcinoma. Zeitschrift fur Gastroenterologie 2008;46(58):68.
[4] Witzigmann H, Berr F, Ringel U, et al. Surgical and palliative management and outcome in 184 patients with hilar cholangiocarcinoma — palliative photodynamic therapy plus stenting is comparable to r1/r2 resection. Annals of Surgery 2006;244:230—9.
[5] Ortner MAEJ, Liebetruth J, Schreiber S, et al. Photodynamic therapy of nonresectable cholangiocarcinoma. Gastroenterology 1998;114:536—42.
[6] Leggett CL, Gorospe EC, Murad MH, Montori VM, Baron TH, Wang KK. Photodynamic therapy for unresectable cholangiocarcinoma: a comparative effectiveness systematic review and meta-analyses. Photodiagnostics and Photodynamics 2012.
[7] Agostinis P, Berg K, Cengel KA, et al. Photodynamic therapy of cancer: an update. CA — Cancer Journal for Clinicians 2011;61:250—81.
[8] Castano AP, Mroz P, Hamblin MR. Photodynamic therapy and anti-tumour immunity. Nature Reviews Cancer 2006;6:535—45.
[9] Korbelik M. Cancer vaccines generated by photodynamic therapy. Photochemistry and Photobiology Science 2011;10:664—9.
[10] Peng Q, Moan J, Nesland JM. Correlation of subcellular and intratumoral photosensitizer localization with ultrastructural features after photodynamic therapy. Ultrastructural Pathology 1996;20:109—29.
[11] Dougherty TJ, Gomer CJ, Henderson BW, et al. Photodynamic therapy. Journal of the National Cancer Institute 1998;90:889—905.
[12] Webber J, Kessel D, Fromm D. Plasma levels of protoporphyrin ix in humans after oral administration of 5-aminolevulinic acid. Journal of Photochemistry and Photobiology B — Biology 1997;37:151—3.
[13] Ortner M-A. Photodynamic therapy for cholangiocarcinoma. Lasers in Surgery and Medicine 2011;43:776—80.
[14] Zoepf T, Jakobs R, Rosenbaum A, Apel D, Arnold JC, Riemann JF. Photodynamic therapy with 5-aminolevulinic acid is not effective in bile duct cancer. Gastrointestinal Endoscopy 2001;54:763—6.
[15] European Medicines Agency. Foscan: Epar — product information; 2009. www.ema.europa.eu [12.12.2011].
[16] Bown SG, Rogowska AZ, Whitelaw DE, et al. Photodynamic therapy for cancer of the pancreas. Gut 2002;50:549—57.
[17] Wolkersdoerfer G, Emmanuel K, Denzer U, et al. Temoporfin improves tumoricidal efficacy of photodynamic therapy (pdt) for bile duct cancer. Annals of Oncology 2008;19:176—7.
[18] Pereira SP, Ayaru L, Rogowska A, Mosse A, Hatfield ARW, Bown SG. Photodynamic therapy of malignant biliary strictures using meso-tetrahydroxyphenylchlorin. European Journal of Gastroenterology and Hepatology 2007;19:479—85.
[19] Wagnieres G, Hadjur C, Grosjean P, et al. Clinical evaluation of the cutaneous phototoxicity of 5,10,15,20-tetra(m-hydroxyphenyl)chlorin. Photochemistry and Photobiology 1998;68:382—7.
[20] Betz CS, Rauschning W, Stranadko EP, et al. Optimization of treatment parameters for foscan (r)-pdt of basal cell carcinomas. Lasers in Surgery and Medicine 2008;40:300—11.
[21] Triesscheijn M, Ruevekamp M, Antonini N, Neering H, Stewart FA, Baas P. Optimizing meso-tetra-hydroxyphenyl-chlorin-mediated photodynamic therapy for basal cell carcinoma. Photochemistry and Photobiology 2006;82:1686—90.
[22] Morlet L, Vonarxcoinsmann V, Lenz P, et al. Correlation between meta(tetrahydroxyphenyl)chlorin (m-thpc) biodistribution and photodynamic effects in mice. Journal of Photochemistry and Photobiology B — Biology 1995;28:25—32.
[23] Ris HB, Altermatt HJ, Stewart CM, et al. Photodynamic therapy with m-tetrahydroxyphenylchlorin in-vivo — optimization of the therapeutic index. International Journal of Cancer 1993;55:245—9.
[24] Bismuth H, Corlette MB. Intrahepatic cholangioenteric anastomosis in carcinoma of hilus of liver. Surgery, Gynecology and Obstetrics 1975;140:170—8.
[25] Sroka R, Beyer W, Gossner L, Sassy T, Stocker S, Baumgartner R. Pharmacokinetics of 5-aminolevulinic-acid-induced porphyrins in tumour-bearing mice. Journal of Photochemistry and Photobiology B — Biology 1996;34:13—9.
[26] Braichotte D, Savary JF, Glanzmann T, et al. Clinical pharmacokinetic studies of tetra(meta-hydroxyphenyl)chlorin in squamous-cell carcinoma by fluorescence spectroscopy at 2 wavelength. International Journal of Cancer 1995;63:198—204.
[27] Cramers P, Ruevekamp M, Oppelaar H, Dalesio O, Baas P, Stewart FA. Foscan (r) uptake and tissue distribution in

Please cite this article in press as: Kniebühler G, et al. Photodynamic therapy for cholangiocarcinoma using low dose mTHPC (Foscan®). Photodiagnosis and Photodynamic Therapy (2013), http://dx.doi.org/10.1016/j.pdpdt.2012.12.005

relation to photodynamic efficacy. British Journal of Cancer 2003;88:283—90.
[28] Glanzmann T, Hadjur C, Zellweger M, et al. Pharmacokinetics of tetra(m-hydroxyphenyl)chlorin in human plasma and individualized light dosimetry in photodynamic therapy. Photochemistry and Photobiology 1998;67:596—602.
[29] Stepp HTB, Beyer B, et al. Measurement of fluorophore concentration in turbid media by a single optical fiber. Medical Laser Application 2007;22:23—34.
[30] Diamond KR, Patterson MS, Farrell TJ. Quantification of fluorophore concentration in tissue-simulating media by fluorescence measurements with a single optical fiber. Applied Optics 2003;42:2436—42.
[31] Berr F, Wiedmann M, Tannapfel A, et al. Photodynamic therapy for advanced bile duct cancer: evidence for improved palliation and extended survival. Hepatology 2000;31:291—8.
[32] Ortner MEJ, Caca K, Berr F, et al. Successful photodynamic therapy for nonresectable cholangiocarcinoma: a randomized prospective study. Gastroenterology 2003;125:1355—63.
[33] Wiedmann M, Berr F, Schiefke I, et al. Photodynamic therapy in patients with non-resectable hilar cholangiocarcinoma: 5-year follow-up of a prospective phase ii study. Gastrointestinal Endoscopy 2004;60:68—75.
[34] Zoepf T, Jakobs R, Arnold JC, Apel D, Riemann JF. Palliation of nonresectable bile duct cancer: improved survival after photodynamic therapy. American Journal of Gastroenterology 2005;100:2426—30.
[35] Glanzmann T, Forrer M, Blant SA, et al. Pharmacokinetics and pharmacodynamics of tetra(m-hydroxyphenyl)chlorin in the hamster cheek pouch tumor model: comparison with clinical measurements. Journal of Photochemistry and Photobiology B — Biology 2000;57:22—32.
[36] Wiedmann M, Caca K, Berr F, et al. Neoadjuvant photodynamic therapy as a new approach to treating hilar cholangiocarcinoma. Cancer 2003;97:2783—90.

Please cite this article in press as: Kniebühler G, et al. Photodynamic therapy for cholangiocarcinoma using low dose mTHPC (Foscan®). Photodiagnosis and Photodynamic Therapy (2013), http://dx.doi.org/10.1016/j.pdpdt.2012.12.005

In memoriam Dr. Ann Johansson

Ann was a great physicist and an even greater colleague and friend.

Ann, it was great to know you
and I would have wished to do so for a longer time.

Acknowledgments

Hereby I want to thank

- Prof. Dr. Jochen Herms, for supervising this thesis and encouraging me throughout the whole time.
- Dr. Reinhold Baumgartner and Dr. Ronald Sroka for letting me work at the Laser-Forschungslabor, for many interesting discussions and warning me of the hazardous corner in the LFL building.
- Dr. Herbert Stepp, for an interesting topic to work on, scientific support and an awful lot of proof reading.
- Dr. Wolfgang Beyer, for always being addressable for questions, but especially for being a reliable cafeteria goer and organizing a lot of ice cream.
- Dipl. Ing. Thomas Pongratz, for helping out whenever there was something critical to build and for many age related discussions.
- Dr. Adrian Rühm, for his sense of humor and helpful discussions.
- Georg Hennig, for helping out whenever necessary, even when I had to measure on a weekend. But even more I want to thank him for many fun times discussing the world's biggest problems or navigating on a map through Africa and North America.
- Katharina Thomsen, for helping out whenever necessary and knowing where to find what, which saved an awful lot of time.
- Michael Heide, for reminding us to keep the lab clean and thus "workable", for appreciating my taste in watches.
- Sabine Sandner, for great support in the lab and for many good talks.
- Dr. Michael Fedorov, for Chinese food and Leberkas.
- Kornelia Eberle, for the great support regarding administrative questions.
- Dr. Sibylle Freitag, for helping me with the language. I did not give her a lot of time though, so all remaining mistakes are my fault.

Working in projects I also want to thank all authors of the manuscripts, especially

- Prof. Dr. Jörg Schirra, for conducting the Foscan® study and encouraging a publication
- Dr. Oliver Schnell and Dr. Valerie Albrecht, for thinking of us whenever tissue biopsies were taken.
- Dr. Werner Göbel, Dr. André Ehrhardt (Karl Storz) and MRC Systems for a great teamwork.

Finally I owe special thanks to my family,

- to my parents Käthe and Manfred for supporting me all my life, not just financially. Keep up doing a great job!
- to my brothers Bodo and Hanno and his wife Stephanie, because I am grateful for such a fun family.
- to my family in law for adopting me.
- last but not least to my husband Roland. Thank you for your support during the whole time and special thanks for staying with me during the final period of writing it.

Eidesstattliche Versicherung

Name, Vorname

Ich erkläre hiermit an Eides statt,

dass ich die vorliegende Dissertation mit dem Thema

selbständig verfasst, mich außer der angegebenen keiner weiteren Hilfsmittel bedient und alle Erkenntnisse, die aus dem Schrifttum ganz oder annähernd übernommen sind, als solche kenntlich gemacht und nach ihrer Herkunft unter Bezeichnung der Fundstelle einzeln nachgewiesen habe.

Ich erkläre des Weiteren, dass die hier vorgelegte Dissertation nicht in gleicher oder in ähnlicher Form bei einer anderen Stelle zur Erlangung eines akademischen Grades eingereicht wurde.

Ort, Datum

Unterschrift Doktorandin/Doktorand